Natural Resources Canada | Ressources naturelles Canada

ᓄᓇᙳᐊᓕᕆᓂᕐᒧᑦ ᖃᐅᔨᓴᖅᑏᑦ ᑲᓇᑕᒥ

ᑲᓇᑕᒥ ᓄᓇᓂᑦ ᖃᐅᔨᓴᓂᕐᒧᑦ ᓄᓇᙳᐊᖅ 257S

ᓄᓇᕗᑦᓗ ᐅᔭᖅᑲᓂᑦ ᖃᐅᔨᓴᖅᑏᑦ ᑎᑎᕋᕐᕕᖓ

ᒪᑐᐃᖓᔪᖅ ᓄᓇᖑᐊᖅ 2016-14S

ᓄᓇᓂ ᖃᐅᔨᓴᕐᓂᖅ

CLEARWATER FIORD (NORTH)

ᕿᑭᖅᑖᓗᒃ, ᓄᓇᕗᑦ

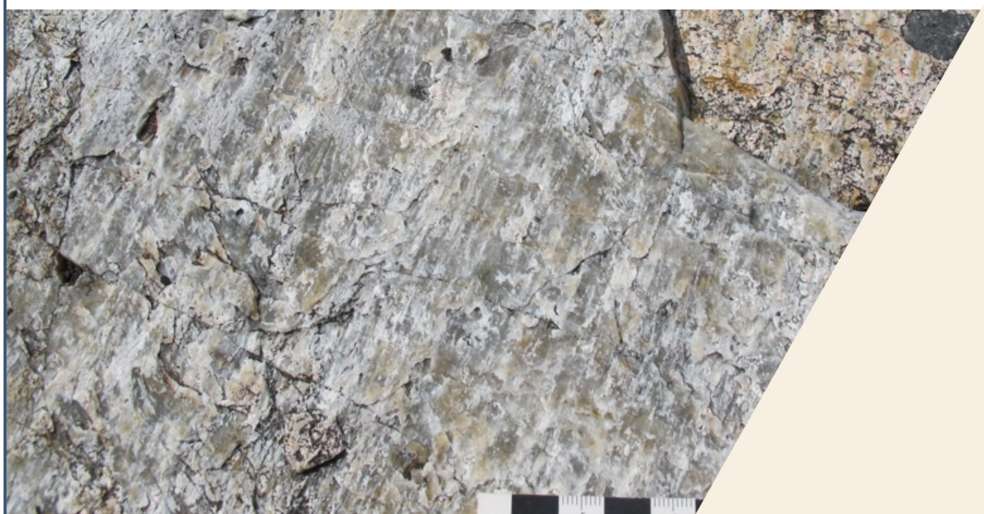

ᓄᓇᓐᖑᐊᑦ
ᑭᓱᓕᕆᓂᖕᒥᓂᒃ
ᑎᑎᖅᑲᖕᒥ

ᐱᒋᐊᕐᓂᖓ

ᓄᓇᙳᐊᓕᕆᓂᕐᒧᑦ ᖃᐅᔨᓴᖅᑏᑦ ᑲᓇᑕᒥ
ᑲᓇᑕᒥ ᐅᔭᖅᑲᓂᑦ ᖃᐅᔨᓴᓂᕐᒧᑦ ᓄᓇᖑᐊᑦ

2016

Canada

ᓴᖅᑭᖅᑎᑕᐅᔪᑦ

CANADA-NUNAVUT GEOSCIENCE OFFICE
ᑲᓇᑕᐅᑉ-ᓄᓇᕗᑦᒧ ᐅᔭᖅᑲᓂᒃ ᖃᐅᔨᓴᖅᑏᑦ
BUREAU GÉOSCIENTIFIQUE CANADA-NUNAVUT
KANATAMI-NUNAVUMI GEOSCIENCE TITIGAKVIIT

ᓄᓇᒃᑯᐊᑉ ᓈᓴᐅᑎᖓ

ᓄᓇᒥᐅᑕᓕᕆᔨᒃᑯᑦ ᑲᓇᑕᒥ, ᓄᓇᖑᐊᓕᕆᓂᕐᒧᑦ ᖃᐅᔨᓴᖅᑏᑦ ᑲᓇᑕᒥ
ᑲᓇᑕᒥ ᓄᓇᓂᑦ ᖃᐅᔨᓴᓂᕐᒧᑦ ᓄᓇᖑᐊᖅ 257S (ᐱᒋᐊᕐᓂᖓ),
ᑲᓇᑕ ᓄᓇᕗᑦᒧ ᐅᔭᖅᑲᓂᑦ ᖃᐅᔨᓴᖅᑏᑦ ᑎᑎᕋᕐᕕᖓ
ᒪᑐᐃᖓᔪᖅ ᓄᓇᖑᐊᖅ 2016-14S

ᐊᑎᖓ

ᓄᓇᓂ ᖃᐅᔨᓴᕐᓂᖅ, Clearwater Fiord (north), ᕿᑭᖅᑖᓗᒃ, ᓄᓇᕗᑦ

ᐊᖏᓂᖓ

1:100 000

ᑎᑎᕋᖅᓯᒪᔪᑦ ᑐᑭᓯᐊᕈᑎᖏᑦ

ᑎᑎᕋᖅᓯᒪᔪᑦ ᓈᓴᐅᑎᖓ. M183-1/257-2016S-PDF
ISBN 978-0-660-05094-2
doi:10.4095/298760

ᐊᔪᓕᑦᑕᐅᔭᓕᐊᖅᑲᖏᑦᑐᑦ

ᐊᑐᓕᕐᑯᔭᐅᔪᑦ ᐅᕐᑲᖅᑕᐅᓯᒪᔪᑦ ᖃᐅᔨᒋᐊᕐᕚᓘᓐᓃᑦ

St-Onge, M.R., Weller, O.M., Dyck, B.J., Rayner, N.M., Chadwick T., ᐊ ᒻᒪ Liikane, D., 2016. ᓄᓇᓂ ᖃᐅᔨᓴᕐᓂᖅ, Clearwater Fiord (north), ᕿᑭᖅᑖᓗᒃ, ᓄᓇᕗᑦ; ᓄᓇᙳᐊᓕᐊᓂᕐᒧᑦ ᖃᐅᔨᓴᖅᑏᑦ ᑲᓇᑕᒥ, ᑲᓇᑕᒥ ᓄᓇᓂᑦ ᖃᐅᔨᓴᓂᕐᒧᑦ ᓄᓇᙳᐊᖅ 257S (ᐱᒋᐊᕐᓂᖓ); ᓄᓇᕗᓪᓗ ᐅᔭᖅᑲᓂᑦ ᖃᐅᔨᓴᖅᑏᑦ ᑎᑎᕋᕐᕕᖓ, ᒪᑐᐃᖓᔪᖅ ᓄᓇᖑᐊᖅ 2016-14S, ᐊᖏᓂᖓ 1:100 000. doi:10.4095/298760

ABSTRACT

This map summarizes the field observations for the Clearwater Fiord (north) map area following eight weeks of regional and targeted bedrock mapping on western Hall Peninsula. The 2015 field campaign completes a two-decade mission to update map coverage for the whole of Baffin Island south of latitude 70°N. The bedrock is dominated by a Paleoproterozoic metaplutonic suite, ranging in composition from gabbro to syenogranite, with crosscutting relations indicating a progression from mafic to silicic magmatism. Prevailing upper amphibolite to lower granulite facies metamorphic conditions overlap the stability limits of magnetite and orthopyroxene, which is consistent with equilibrium phase diagrams and regional aeromagnetic data. Metasedimentary rocks, including quartzite, pelite, marble, and metagreywacke, are present as screens and enclaves between and within plutonic bodies. An examination of the 'ghost' stratigraphy suggests that the metasedimentary rocks can be correlated with the middle Paleoproterozoic Lake Harbour Group in the south and Piling Group in the north. Two basaltic dyke swarms and shallowly dipping Ordovician limestone respectively crosscut and overly the Paleoproterozoic units.

ᐃᓱᒪᒋᔭᐅᔪᑦ

ᑖᓐᓇ ᓄᓇᖑᐊᖅ ᓇᓗᓇᐃᔭᐃᔪᖅ ᖃᐅᔨᓴᖅᑎᓪᓗᒋᑦ ᖃᐅᔨᔭᐅᔪᑦ Clearwater Fiord (north) ᓄᓇᖑᐊᖅ 8-ᓂᑦ ᐱᓇᓱᐊᕈᓯᕐᓂᑦ ᐊᕕᑦᑐᖅᓯᒪᔪᒥᑦ ᐊᒻᒪ ᖃᐅᔨᓴᕐᓂᕐᑲᓗᐊᓚᐅᖅᑐᑦ ᕐᑯᐊᖑᐃᓐᓇᖅᑐᒥᑦ ᓄᓇᙳᐊᓕᐅᓂᕐᒥᑦᐱᖓᓐᓇᖓᓂ ᓴᐅᒥᒻᒥᑦ. 2015-ᒥ ᖃᐅᔨᓴᕐᓂᐅᔪᖅ ᐱᔮᖅᓯᓚᐅᖅᑐᖅ ᐊᕿᒍᓂᑦ ᐊᕙᑎᓂᑦ ᐱᓕᕆᐊᖑᔪᖅ ᐅᓪᓗᒥᒨᖓᓕᖅᑎᑕᐅᓪᓗᑎ ᓄᓇᖑᐊᑦᕿᑭᖅᑖᓗᒻᒥ ᓂᒋᓕᒫᖓᓂᑦ 70°N. ᕐᑯᐊᖑᐃᓐᓇᖅᑐᖅ ᐃᓗᓕᕐᑲᕐᓂᕆᔭᖓ Paleoproterozoic metaplutonic suite, ᐊᔾᔨᒋᖏᓐᓂᕐᑲᖅᑐᑦ ᐃᓗᓕᖏᑦ ᐱᒋᐊᖅᑐᓂ gabbro ᑎᑭᑦᑐᒍ syenogranite, ᕐᑯᓕᕘᕆᕐᑲᑦᑕᐅᑎᓪᓗᑎ ᖃᓄᐃᓘᕐᑲᑦᑕᐅᑎᓂᖏᑦᓇᓗᓇᐃᖅᓯᔪᖅ ᐱᕙᓪᓕᐊᓂᖓ mafic ᑎᑭᑦᑐᒍ silicic magmatism. ᒫᓐᓇᐅᔪᒥᑦ ᑕᑯᔅᓴᐅᔪᖅ ᕐᑯᑦᑎᓂᖅᓴᖓᒍ amphibolite ᐊᑎᓐᓂᖓᓄᑦ granulite facies metamorphic ᖃᓄᐃᓐᓂᓕᔭᖏᑦ ᕐᑯᓕᕆᕐᑲᑦᑕᐅᑎᔪᑦ ᒪᑭᑕᑦᑎᐊᕈᓇᕐᓂᖓ ᑭᓪᓕᖅᑲᖅᑎᑦᑎᔪᖅ magnetite ᐊᒻᒪ orthopyroxene, ᒪᓕᓐᓂᕐᑲᖅᑐᖅ ᓇᓕᒧᑦᑎᑦᑎᓂᕐᒦᑦᑐᓂᑦ ᐊᔾᔨᙳᐊᑦ ᐊᒻᒪ ᐊᕕᑦᑐᖅᓯᒪᔪᒥᑦᑲᖓᑕᓲᒃᑯᑦ ᓂᐱᖅᑲᕐᓇᕐᑲᕐᓂᖓᓄᑦ ᑐᑭᓯᒋᐊᕈᑏᑦ. Metasedimentary ᐅᔭᖅᑲᐃᑦ, ᐱᕐᑲᓯᐅᑎᓪᓗᑎ quartzite, pelite, ᑐᓐᓅᔭᖅ, ᐊᒻᒪ ᐊᕕᑦᑐᖅ metagreywacke, ᑕᑯᔅᓴᐅᑎᑕᐅᔪᑦ ᐊᒻᒪ ᐊᕕᑦᑐᖅᓯᒪᔪᓂᑦ

ᐊᑯᓐᓂᖏᓐᓂ ᐃᓗᐊᓂᓗ plutonic ᐃᓗᓕᓖᑦ. ᖃᐅᔨᓴᖅᑕᐅᓂᕆᔭᖓ 'ᑖᕋᐃᑦᑐᖅ' ᓄᓇᓕᕆᓂᕐᒧᑦ ᓇᓗᓇᐃᖅᓯᔪᖅ metasedimentary ᐅᔭᖅᑲᐃᑦ ᑲᑎᙵᓂᖃᕈᓇᖅᑐᑦ ᕿᑎᖓᓃᑦᑐᓂ Paleoproterozoic ᑭᒥᕈᒥ ᐱᓕᕆᔪᑦ ᓂᒋᖓᓂ ᐊᒻᒪ ᐳᑑᕆᕝᑦᐅᐊᓐᓇᖓᓂ. ᒪᕿᒃ basaltic ᐅᔭᖅᑲᐃᑦ ᐊᒥᓲᑦ ᐊᒻᒪᐃᒃᑲᑦᑐᒨᖓᔪᑦ Ordovician limestone ᖁᓕᕇᖅᑲᑦᑕᐅᑎᔪᑦ ᐊᒻᒪ ᖁᓛᒧᑦ Paleoproterozoic ᑲᑎᓐᖓᔪᓂᑦ.

ᓄᓇᙳᐊᑉ ᒥᓭᓄᑦ

ᑐᑭᓯᒋᐊᕈᑎᓪᓗᐊᑕᐃᑦ

ᑎᑎᕋᖅᑐᑦ: M.R. St-Onge, O.M. Weller, B.J. Dyck, N.M. Rayner, T. Chadwick, ᐊ ᒻᒪ D. Liikane

ᓄᓇᓂ ᖃᐅᔨᓴᖅᑎ M.R. St-Onge, O.M. Weller, B.J. Dyck, N.M. Rayner, T. Chadwick, ᐊᒻᒪ D. Liikane, ᓄᓇᙳᐊᓕᕆᓂᕐᒧᑦ ᖃᐅᔨᓴᖅᑏᑦ ᑲᓇᑕᒥ; S. Noble-Nowdluk, T. Milton, ᐊᒻᒪ T. Rowe, ᓄᓇᕗᑦ ᒐᕙᒪᒃᑯᑦ, 2015

ᓄᓇᒥ ᖃᐅᔨᓴᕐᓂᕐᒧ ᓇᓗᓇᐃᔭᐃᔪᖅ M.R. St-Onge ᐊᒻᒪ ᑎᑎᕋᖅᑕᐅᒃᑲᓐᓂᖅᑐᑦ ᐆᒧᖓ M.R. St-Onge ᐊᒻᒪ O.M. Weller, 2015

ᓄᓇᒥ ᖃᐅᔨᓴᓂᕐᒧᑦ ᒪᓕᓐᓂᐊᖅᑐᖅ ᐱᓕᕆᐊᒧᑦ ᖁᐊᙳᐃᓐᓇᖅᑐᓂᑦ ᑐᑭᓯᒋᐊᕈᑎᓂᑦ, ᕿᓯᖓ 2.6

ᓄᓇᙳᐊᓕᐊᖅᑏᑦ A. Morin, A. Ford, C. Gilbert, L. Robertson, G. Buller, ᐊ ᒻᒪ R. Buenviaje

ᓄᓇᙳᐊᓕᕆᔪᖅ N. Côté

ᑐᑭᓕᐅᕆᔭᐅᔪᖅ ᖃᓪᓗᓈᑎᑐ ᐃᓄᒃᑎᑐᒧᑦ Wintranslation; ᑐᑭᓕᐅᕆᓯᒪᔪᖅ ᓯᓚ ᓈᒻᒪᒃᑲᓗᐊᕆᐊᒃᓴᖅ ᐅᖃᐅᓯᐅᓯᒪᙱᑦᑐᖅ.

ᐅᓇ ᓄᓇᙳᐊᖅ ᐃᓚᒋᔭᖓ ᓄᓇᐅᑉ ᖃᓄᐃᓕᖓᓂᖓᓂᑦ ᓄᓇᙳᐊᓕᐅᕐᓂᕐᒧᑦ ᐅᑯᓄᖓ ᐆᒪᕐᑯᑎᓕᕆᔾᑯᑦ ᐊᒻᒪ ᐅᔭᕋᐅᔭᓕᕆᔾᑯᓄᑦ (GEM) ᐱᓕᕆᐊᖑᔪᒥᑦ ᕿᑭᖅᑖᓗᒥ ᑐᑭᒧᐊᖅᑎᑕᐅᓪᓗᓂ ᓄᓇᙳᐊᓕᕆᓂᕐᒧᑦ ᖃᐅᔨᓴᖅᑏᑦ ᑲᓇᑕᒥ (GSC) ᐱᓕᕆᖃᑎᖃᖅᖢᑎᑦ ᑲᓇᑕᒥ ᓄᓇᕗᓪᓗ ᓄᓇᐅᑉ ᖄᖓᓃᑦᑐᓂ ᖃᐅᔨᓴᖅᑐᓕᕆᔾᑯᑦ ᑎᑎᕋᕖᖓᓂ (CNGO), ᓄᓇᕗᒻᒥ ᓯᓚᑦᑐᖅᓴᕐᕖᒃ, ᑲᐅᔨᑕᓐ ᓯᓚᑦᑐᖅᓴᕐᕖᒃᔪᐊᖅ, ᓯᓚᑦᑐᖅᓴᕐᕖᒃᔪᐊᖓ ᐋᒃᕙᑦ, ᐊᒻᒪᓗ ᓄᓇᕗᑦ ᒐᕙᒪᒃᑯᑦ.

ᐃᖅᑲᓇᐃᔭᖅᑐᓕᕆᓂᕐᒧᑦ ᐃᑲᔪᖅᑐᑦ ᓯᓚᕐᔪᐊᒥ ᐅᑭᐅᑕᖅᑐᖓᓂ ᐱᓕᕆᐊᖅ ᐃᓚᒋᓪᓗᓂᐅᒃ ᑐᕋᖓᒋᓐᓂᑦ ᓴᖅᑮᔭᖅᑎᑎᒃᑲᓂᕐᓗᑎᑦ ᖃᐅᔨᓴᓂᕐᒧᑦ ᖃᐅᔨᓴᖅᑎᓄᑦ ᑲᓇᑕᐅᑉ ᐅᑭᐅᑕᖅᑐᖓᓂ. PCSP 05615

ᓄᓇᙳᐊᖅ ᖃᓄᐃᓕᖓᓂᖓᓄᑦ Universal Transverse Mercator, ᐊᕕᒃᑐᖅᓯᒪᓂᒃᑯᑦ 19. North American Datum 1983

ᓄᓇᙳᐊᑉ ᐆᒃᑐᕋᖅᑕᐅᓯᒪᓂᖓᒍᑦ 1:250 000 ᓄᓇᒥᐅᑕᓕᕆᔾᒃᑯᓐᓂᑦ ᑲᓇᑕᒥ, ᐋᖅᑭᒋᐊᖅᑕᐅᓯᒪᓪᓗᑎᑦ.
ᖁᕝᕙᓯᓐᓂᖓ ᒦᑕᓂᑦ ᖁᑖᒍᑦ ᑐᑭᖄᖅᑐᖅ ᐃᒪᐅᑉ ᓇᐅᒃᑰᕐᓂᖓᑕ ᖁᕝᕙᓯᖕᓂᖓ

ᑐᑭᑲᖅᑐᖅ ᓂᐱᓐᓇᖅᑐᖃᕐᓂᖓᑕ ᒥᑭᒡᓕᕙᓪᓕᐊᓂᖓ 2016, 31°52'W, ᒥᒃᓵᕙᓪᓕᐊᓪᓗᓂ 29.2' ᐊᕐᕌᒍᑕᒫᑦ.
ᓇᓃᓐᓂᖏᓐᓄᑦ ᖃᐅᔾᓇᓱᖕᓂᖅ ᐊᔾᔨᒌᖏᑦᑐᑦ ᐅᕙᙵ 31°26'W ᐱᖓᖕᓇᖅ ᐅᕙᓂ ᓂᒋᐊᑕ ᐱᖓᖕᓇᖅᐸᓯᐊᓂ ᑎᓇᖅᑯᐊᓂᑦ ᐅᕗᖓ 32°15'W ᐱᖓᖕᓇᖅ ᐅᕙᓂ ᐅᐊᖕᓇᖓᑕ ᑲᓇᖕᓇᖅᐸᓯᐊᑕ ᑎᓇᖅᑯᐊᓂ ᓄᓇᙳᐊᕐᒥᑦ.

ᐅᓇ ᓄᓇᙳᐊᖅ ᐊᑐᖅᑕᐅᔭᓇᐊᖃᙱᑦᑐᖅ ᑕᒪᓈᒃᑯᑎᐅᓗᓂ ᓄᓇᖁᖅᑐᓂᑦ.

ᐊᔾᔨᓐᖑᐊᖅ ᐊᑎᖓ: ᐊᓴᓇᓯᒪᑎᐊᖅᑐᖅ, ᐊᒻᒎᐊᖓᔪᖅ, ᓴᓐᓂᖓᔪᑦ ᐃᑳᖓᔪᑦ ᐅᐊᓐᓇᒎᑦ ᑐᔅᓯᕋᐅᑕᐅᓂᐊᖅᑐᒥᑦ ᕿᑭᖅᑖᓗᒻᒥ ᓄᓇᖓ ᑲᑎᓐᖓᓂᖓ. ᐊᖏᓂᖓ ᓯᐊᓐᑕᒦᑕᒃᑰᖅᑐᑦ. ᐃᓱᐃᑦᑐᖅ, ᕿᑭᒻᑖᓗᒃ ᓄᓇᕗᑦ ᐊᖏᓂᖓ ᐊᖏᔾᓕᕙᓪᓕᐊᓂᖓ ᓯᐊᓐᑕᒦᑕᐃᑦ, ᐃᓱᐃᑦᑐᖅ, ᕿᑭᖅᑖᓗᒃ, ᓄᓇᕗᑦ. ᐊᔾᔨᓕᐅᕆᔪᖅ T. Chadwick. 2015-128

ᓄᓇᙳᐊᓕᕆᓂᕐᒧᑦ ᖃᐅᔨᓴᖅᐹᑦ ᑲᓇᑕᒥ ᑐᙵᓱᒃᑎᑦᑎᔪᑦ ᐋᕿᒋᐊᕈᑎᓂᑦ ᐃᓚᒋᐊᕈᑎᓂᒡᓘᓐᓅᑦ ᑐᑭᓯᒋᐊᒃᑲᓐᓂᕈᑎᓂ ᐊᑐᕐᑲᑦᑕᖅᑐᓄᑦ.

ᑐᑭᓯᒋᐊᕈᑎᖏᑦ ᐱᖃᓯᐅᔾᔨᔪᓐᓇᖅᑐᑦ ᑕᑯᔭᐅᒃᑲᓂᖅᑐᓂᑦ ᑕᑯᔅᓴᐅᑎᑕᐅᖏᑦᑐᓂᑦ ᓄᓇᙳᐊᕐᒥᑦ.
ᑕᑯᓗᒍ ᑎᑎᕋᖅᓯᒪᔪᑦ ᐃᓚᓕᐅᔾᔭᐅᓯᒪᔪᑦ ᑖᒃᑯᓇᓂ ᑲᑎᕐᓱᕐᓂ.
ᓇᓗᓇᐃᔭᖅᓯᒪᒃᑲᓂᕐᓂᖏᑦ ᑎᑎᕋᖅᓯᒪᔪᑦ, ᖃᐅᔨᒋᐊᕐᕖᑦ, ᐊᒻᒪ ᐊᔾᔨᓐᖑᐊᑦ ᓄᓇᖑᐊᒦᑦᑐᖅ ᑐᑭᓯᒋᐊᕈᑎᖏᓐᓂᑦ ᑎᑎᕋᖅᓯᒪᔪᓂᑦ.

ᑖᓐᓇ ᓴᖅᑭᖅᑎᑕᐅᔪᖅ ᐊᑭᕐᑲᖏᑦᑐᑦ ᖃᕋᓴᐅᔭᒃᑯᑦ ᐊᑐᐃᓐᓇᐅᔪᑦ ᐅᑯᑎᒎᓇ
GEOSCAN (http://geoscan.nrcan.gc.ca/)
ᑲᓇᑕ ᓄᓇᕗᒻᒥᓗ ᐅᔭᖅᑲᓂᑦ ᖃᐅᔨᓴᖅᑏᑦ ᑎᑎᕋᕝᕕᖓ (http://cngo.ca/).

ᓴᖅᑭᑎᑕᐅᑭᐊᕐᖓᖅᓯᒪᔪᑦ ᑖᒃᑯᓂᖓ ᖃᐅᔨᓴᖅᑎᓄᑦ ᐋᖅᑭᒋᐊᖅᑕᐅᓯᒪᖏᑦᑐᑦ.

ᓄᓇᖑᐊᓂᑦ ᕿᒥᕐᕈᓂᕐᒧᑦ ᑎᑎᕋᖅᓯᒪᔪᑦ

ᓴᖅᑭᖅᑎᑕᐅᓯᒪᔪᖅ ᓄᓇᖑᐊᖅ ᑐᓂᐅᖅᑲᖅᑕᐅᔪᑦ ᖃᕋᓴᐅᔭᑎᒍᑦ ᕿᒥᕐᕈᔭᔅᓴᐅᓪᓗᓂ Portable Document File (PDF)−ᖑᓪᓗᓂ, ᐊᒻᒪ ᐃᓗᓕᖅᑲᕈᓐᓇᖅᑐᑦ ᓄᓇᒥᑦ ᖃᐅᔨᓴᓂᕐᒧᑦ ᑐᑭᓯᒋᐊᕈᑎᓕᒫᑦ ᐅᕐᑲᓕᒫᕋᔅᓴᐅᑎᐊᕐᓂᖏᓐᓄᑦ ᐱᔾᔪᑎᒋᓪᓗᒍ ᓴᖅᑭᖅᑎᑕᐅᓂᖓᓄᑦ ᐊᖏᓂᖓᓄᑦ.

ᓄᓇᖑᐊᓕᐅᓂᕐᒧᑦ ᑕᑯᔅᓴᐅᑎᑕᐅᔪᑦ ᐊᑐᖅᑕᐅᔪᑦ ᓄᓇᖑᐊᒥᑦ

ᐅᓇ ᓄᓇᖑᐊᖅ ᐊᑐᕐᑲᑦᑕᖅᑐᖅ ESRI ᓄᓇᖑᐊᓂᑦ ᑕᑯᔅᓴᐅᑎᑦᑎᓂᖏᑦ ᐊᑲᓐᔭᒥᓄᑦ ᐋᖅᑭᒍᓐᓇᓂᐊᕐᒪᒍ ᑕᑯᔅᓴᐅᓂᖓ ᐊᑐᖅᑕᐅᒐᔪᑦᑐᓂᑦ GSC ᓇᓗᓇᐃᒃᑯᑕᐃᑦ ᑕᑯᔅᓴᐅᓂᖓᒍᑦ ᓇᓗᓇᐃᖅᓯᒪᑦᑎᐊᕐᓗᓂ PDF−ᒥᑦ ᓄᓇᖑᐊᑐᐊᕐᒥᑦ. ᖃᕋᓴᐅᔭᒃᑯᑦ ᑐᑭᓯᒋᐊᕈᑏᑦ ᐃᓗᓕᓇᔭᖕᒋᔅᓯᓕ ᓇᓗᓇᐃᒃᑯᑕᓇᒋᐊᖓᓐᖓᖅᓯᒪᔭᖕᒋᓐᓂᑦ ᐊᑐᖅᑕᐅᒐᔪᑦᑐᒥᑦ GSC ᓇᓗᓇᐃᒃᑯᑕᓄᑦ ᐋᖅᑭᔅᓯᒪᔪᑦ. ᐅᑯᐊ ᓇᓗᓇᐃᒃᑯᑕᐅᔪᑦ ᑕᑯᔅᓴᐅᑎᑦᑎᔪᖅ ᓄᓇᖑᐊᓕᐅᓂᕐᒧᑦ ᑕᑯᔅᓴᐅᑎᑕᐅᔪᑦ ᐊᑐᖅᑕᐅᓂᖓ:

Oblique-slip fault, normal, inferred
Antiform, defined
Antiform, overturned, defined

ᐅᔾᖅᑲᓂᑦ ᖃᐅᔨᓴᓂᕐᒧᑦ

ᖃᓄᖅ ᐅᖃᓕᒫᕋᔅᓴᐅᒪᖕᒫᑦ ᓄᓇᙳᐊᖅ

ᑐᖁᒐᓇᔭᕐᒥᑦ ᓄᓇᙳᐊᓕᐅᕐᓂᖅᑯᑦ ᓂᒋᖕᒐᓂ ᖃᑎᐊᓂ ᖃᑭᖅᑖᓗᒃ 2015 ᐱᐅᓯᑎᒋᐊᖅᑕᐅᓗᓂ ᐅᔾᖅᑲᓂᑦ ᖃᐅᔨᓴᓂᕐᒧᑦ ᖃᐅᔨᒪᔭᐅᔪᑦ ᑎᑎᕋᖅᑕᐅᓯᒪᔪᓪᓗ ᑮᓇᐅᔭᓚᐅᕋᓯᐊᕈᑎᔅᓴᐅᔪᓐᓇᖅᑐᓂᑦ ᐃᖃᓗᐃᑦ ᖃᓂᒋᔭᖕᒐᓂᑦ. ᓄᓇᙳᐊᑦ ᑕᑯᔅᓴᐅᑎᑦᑎᔪᑦ ᓇᒦᓐᓂᕐᒥᑦ ᓄᓇᕐᒥᑦ ᖃᓄᐃᓕᖕᒐᓂᕐᒥᑦ, ᐱᖃᓯᐅᑎᓪᓗᑎ ᐊᔾᔨᒌᖕᒋᑦᑐᑦ ᐅᔾᖅᑲᐃᑦ ᐊᒻᒪ ᓄᓇᐃᑦ ᑲᑎᓂᕐᒥᑦ. ᓄᓇᒥᑦ ᖃᐅᔨᓴᕐᓂᖅ ᐊᔾᔨᒌᖕᒋᑐᖕᒋᓐᓇᐅᒐᓗᐊᖅᑎᓪᓗᒋᑦ ᐊᕕᑦᑐᖅᓯᒪᔪᓕᒫᓂᑦ, ᓄᓇᙳᐊᓕᒫᑦ ᐱᑕᖃᖅᑎᑦᑎᔪᑦ ᐊᑐᖅᑕᐅᒐᔪᑦᑐᓂᑦ: ᐊᒥᐊᓖᑦ ᐊᒻᒪ ᑎᑎᖅᑲᕐᒥᑦ ᓇᓗᓇᐃᖅᓯᓪᓗᑎ ᖃᓄᐃᑦᑑᓂᕐᒥᑦ ᐅᔾᖅᑲᐃᑦ ᓄᓇᐅᑉ ᖄᖕᒐᓃᑦᑐᑦ, ᑎᑎᑰᑦᓯᒪᔪᑦ ᑲᑐᔅᓴᐅᑎᑦᑎᓗᑎ ᖃᓄᐃᑦᑑᓂᖕᒐ ᐊᒻᒪ ᓇᒦᓐᓂᖕᒐ ᐊᑦᑐᕝᕕᒋᔭᖕᒐ ᐊᒻᒪ ᓄᓇᐅᑉ ᑭᓪᓕᕐᒥᑦ, ᑎᑎᑲᓪᓚᔅᓯᒪᔪᑦ ᑕᑯᔅᓴᐅᑎᑦᑎᓗᑎᑦ ᓇᒧᑦ ᖁᓕᓅᑦᑐᑦ ᐅᕕᖕᒐᒻᒪᖕᒐᑕ, ᓄᓇᙳᐊᕐᓗ ᓇᓗᓇᐃᒃᑯᑕᐃᑦ ᓇᓗᓇᐃᔭᐃᔪᑦ ᐊᒥᐊᕐᒋᓐᓂᑦ ᐊᒻᒪ ᓇᓗᓇᐃᒃᑯᑕᕐᒥᑦ ᐊᑐᖅᑕᐅᔪᑦ.

ᑕᑯᔅᓴᐅᓂᓇᔭᕐᒥᑦ ᓄᓇᙳᐊᓂᑦ ᐊᒥᐊᕐᒥᑦ. ᐊᑐᓂ ᐊᒥᐊᕐᒥᑦ ᑭᒡᒐᖅᑐᐃᔪᑦ ᐊᔾᔨᒌᖕᒋᑦᑐᓂᑦ ᓄᓇᓂᑦ ᖃᐅᔨᓴᓂᕐᒧᑦ ᐊᕕᑦᑐᖅᓯᒪᔪᑦ ᓄᓇᓂᑦ ᖃᐅᔨᓴᓂᕐᒧᑦ ᐊᕕᑦᑐᖅᓯᒪᔪᑦ ᐊᕐᒋᓂᓇᔭᕐᒐ ᓇᓗᓇᐃᖅᑕᐅᓯᒪᔪᒥᑦ ᐅᔾᖅᑲᐃᑦ ᖃᓄᐃᑦᑑᓂᕐᒥᓐᓄᑦ ᐊᖁᖏᕐᒥᓪᓗ. ᓄᓇᓂᑦ ᖃᐅᔨᓴᓂᕐᒧᑦ ᐊᕕᑦᑐᖅᓯᒪᔪᑦ ᐊᑎᖃᐅᖅᑐᑦ ᐊᒻᒪ ᓇᓗᓇᐃᖅᑕᐅᓯᒪᔪᑦ ᐅᔾᖅᑲᓂᑦ ᖃᐅᔨᓴᖅᑎᓄᑦ ᓄᓇᙳᐊᓕᐅᖅᐸᑦᑐᑦ, ᑐᓐᖓᓂᐊᖅᑐᑎᑦ ᑕᑯᔭᐅᓂᖅᑲᓂᑦ ᐅᔾᖅᑲᐃᑦ ᖃᐅᔨᓴᕝᕕᐅᔪᓂᑦ ᐊᒻᒪ ᖃᐅᔨᓴᖅᑕᐅᓂᖅᑲᓄᒧᑦ ᐅᔾᖅᑲᐃᑦ ᐊᖁᖏᕐᒐᓂᑦ. ᐃᓚᒋᐊᖁᑐᒍ ᐊᒥᐊᓛᓐᓄᑦ, ᐊᑐᓂ ᐊᕕᑦᑐᖅᓯᒪᔪᑦ ᑎᑎᖅᑲᖃᐅᖅᑎᑕᐅᔪᑦ ᐊᔾᔨᐅᕐᒋᑦᑐᓂᑦ ᓄᓇᙳᐊᒥᑦ. ᓇᓄᓇᐃᒃᑯᑕᓚᐅᔪᑦᑕᕐᒥᑦ ᐊᕐᒋᔪᑦ ᑎᑎᖅᑲᐃᑭᖑᓕᓇᓪᓗᓂᒥᑦ ᐊᕐᒋᔫᑎᒃᑲᓐᓃᑦ ᑎᑎᖅᑲᐃᑦ ᒥᑭᔫᑕᐅᓂᖅᓴᐅᓗᑎᓗᓐᓃᑦ. ᓯᕗᓪᓕᖅᐹᖅ ᑎᑎᖅᑲᖅ ᐊᕐᒋᔪᖅ ᑭᒡᒐᖅᑐᐃᔪᖅ ᐊᖁᖏᕐᒐᓂᑦ ᓄᓇᒥ ᖃᐅᔨᓴᓂᕐᒧᑦ ᐊᕕᑦᑐᖅᓯᒪᔪᖅ. ᓄᓇᓂᑦ ᖃᐅᔨᓴᖅᑕᐅᔪᑦ ᐊᑎᖃᐅᖅᑐᑦ ᐊᒻᒪ ᓇᓗᓇᐃᔭᖅᑕᐅᓯᒪᔪᑦ ᐅᔾᖅᑲᓂᑦ ᖃᐅᔨᓴᖅᑎᓄᑦ ᓄᓇᙳᐊᓕᐅᖃᑦᑕᖅᑐᖅ, ᑐᓐᖓᓂᖃᖅᑐᑎᑦ ᐅᔾᖅᑲᓂᑦ ᑕᑯᔭᕐᒥᓂᑦ ᖃᐅᔨᓴᕝᕕᐅᔪᒥᑦ ᖃᐅᔨᓴᖅᑕᐅᓪᓗᑎᓪᓗ ᐊᖁᖏᕐᒥᑦ ᐅᔾᖅᑲᐃᑦ. ᐃᓚᒋᐊᖁᑐᒍ ᐊᒥᐊᕐᒋᓐᓄᑦ, ᖃᐅᔨᓴᕝᕕᐅᔪᑦ ᐊᕕᑦᑐᖅᓯᒪᔪᑦ ᑎᑎᖅᑲᖃᖅᑎᑕᐅᔪᑦ ᐊᔾᔨᐅᕐᒋᑦᑐᒥᑦ ᓄᓇᐃᒃᑯᑦᑎᒃᑯᑦ. ᓇᓄᓇᐃᒃᑯᑕᓚᐅᔪᑦᑕᕐᒥᑦ ᐊᕐᒋᔪᑦ ᑎᑎᖅᑲᐃᑦ ᑭᖑᓂᐊᒍ ᐊᑕᐅᓯᖅ ᒪᕿᓅᖕᓃᒃ ᐊᕐᒋᔪᑦ ᑎᑎᖅᑲᐃᑦ ᒥᑭᓂᖅᓴᐃᓅᖕᓃᑦ ᑎᑎᖅᑲᐃᑦ. ᓯᕗᓪᓕᖅᐹᖅ ᐊᕐᒋᔪᖅ ᑎᑎᖅᑲᖅ ᓇᓗᓇᐃᖅᓯᔪᖅ ᐊᖁᖕᒐᓂ ᐅᔾᖅᑲᓂᑦ ᖃᐅᔨᓴᕝᕕᐅᔪᖅ. ᐅᔾᖅᑲᓂᑦ ᖃᐅᔨᓴᖅᑮᑦᐊᒡᒍᑐᖅᓯᒪᔭᕐᒥᑦ ᓯᓚᕐᔪᐊᖅ ᖃᓄᐃᓅᖅᑲᑦᑕᕐᓂᖓ ᐱᓕᐊᕐᒋᓐᓃᑦᑐᓂᑦ ᐊᕐᒋᔫᕐᒋᓐᓂᑦ. ᓇᓗᓇᐃᒃᑯᑕᓕᒫᑦ ᐊᕐᒋᔪᓂᑦ ᑎᑎᖅᑲᓂᑦ ᐱᒋᐊᕐᓂᖅᑐᑦ ᓇᓗᓇᐃᖅᓯᔪᑦ ᐊᕐᒋᔫᑎᖏᓐᓂᑦ ᐱᓕᐊᕐᒋᓐᓃᑦᑐᓂᑦ: ᐆᑦᑐᑎᒋᓗᒍ Ᵽ (Paleoproterozoic – 2500 ᑎᑭᑦᑐᒍ 1600 ᒥᓕᐊᓐ ᐊᕐᕌᒍᐃᑦ), N (Neoproterozoic – 1000 ᑎᑭᑦᑐᒍ 541 ᒥᓕᐊᓐ ᐊᕐᕌᒍᐃᑦ), ᐅᖓᓯᖕᓂᖅ Q (Quaternary – 2.58 ᒥᓕᐊᓐ ᐊᕐᕌᒍᐃᑦ ᐅᓪᓗᒥᒧᑦ ᑎᑭᑦᑐᒍ). ᐊᕐᒋᔪᑦ ᑎᑎᖅᑲᐃᑦ ᑭᖑᓂᐊᓂᑦᑐᑦ ᓇᓗᓇᐃᖅᓯᔪᑦ ᐊᑎᖓ ᐊᕕᑦᑐᖅᓯᒪᔪᖅ, ᐱᑕᖃᕈᓂ. ᒥᑭᓂᖅᓴᐃᑦ ᑎᑎᖅᑲᐃᑦ ᓇᓗᓇᐃᖅᓯᔪᑦᖃᓄᐃᑦᑑᓂᖕᒋᑦ ᐅᔾᖅᑲᐃᑦ. ᓈᕐᓗ ᐅᔾᖅᑲᐃᑦ ᐊᑎᖅᑲᖅᑐᑦ ᐊᕕᑦᑐᖅᓯᒪᔪᓂᑦ ᖃᐅᔨᓴᖅᑖᓗᒻᒥ metasedimentary ᐅᔾᖅᑲᐅᔪᑦ ᑕᐃᔭᐅᔪᑦ "ᑭᒻᒥᕈᒻᒥ ᐱᓕᕆᔪᑦ". ᑕᐃᒪᐃᓐᓂᖅᓗᑦ ᏢLHq ᓄᓇᙳᐊᒥᑦ

ᓇᓗᓇᐃᒃᑯᑕᐅᒐᓯᖅᑐᖅ ᑭᒪᒥᕈᒪᒧᑦ ᐱᓕᕆᔪᓄᑦ ᐅᓯᖅᑲᖅ quartzite (ᓄᓇᒨᖅᓯᔪᑦ Paleoproterozoic−ᒥᑦ). ᐊᕐᕌᐸᓗᐊᓂᑦ, Nd ᓇᓗᓇᐃᒃᑯᑕᐅᒐᓯᖅᑐᖅ ᐊᑎᖃᖅᑎᑕᐅᖏᑦᑐᓄᑦ ᐊᕙᑦᑐᖅᓯᒪᔪᓄᑦᐅᓯᖅᑲᐃᑦ diabase ᐃᓕᓯᒪᔪᑦ Neoproterozoic−ᖑᑎᓪᓗᒍ.

ᒪᕿᒃ ᐊᕐᕌᒍᖏᑦᑐᑦ ᐅᓯᖅᑲᓖᑦ ᓴᓂᓕᕇᑦᑐᑎᑦ ᑕᐃᔭᐃᔪᑦ ᑲᑎᓐᓂᖓ, ᐊᒻᒪ ᑖᓐᓇ ᓇᓗᓇᐃᖅᑕᐅᔪᖅ ᐊᕐᕌᒋᖏᑕᖏᓐᓂᑦ ᑎᑎᖅᑕᐅᓯᒪᔪᓂᑦᓄᓇᖑᐊᒥᑦ. ᐊᕐᕌᒋᖏᓂᕆᔭᖏᓐᓄᑦᓅᑦᑕᐅᓯᒪᔪᑦ ᓴᓂᑦᑎᐊᖓᓄᑦ ᐃᒻᒥᓂᒃ ᑕᐃᒪᐃᓚᐅᖅᑎᓪᓗᒋᑦ ᑲᑎᓐᓂᖓ ᐊᕙᒃᓯᒪᓂᖓᒍᑦ ᑲᑎᓐᓂᖃᖅᑐᖅ. ᐅᓯᖅᑲᐅᔪᖅ ᐊᓯᐊᓄᑦ ᐊᔭᐅᖅᑕᐅᒍᓂ (ᓲᕐᓗ ᐅᓯᖅᑲᐃᑦ granite ᐊᑦᑐᖃᑦᑕᐅᑎᒋᓪᓗᓂᐅᒃ sedimentary strata) ᐊᑦᑐᕐᓂᕆᔭᖏᑦ ᐊᐅᓚᔾᔭᐃᓂᖃᖅᑐᑦ ᐊᑦᑐᕐᓂᖓ. ᐊᓯᐊᑦᑕᐅᖅ ᑕᑯᓴᐅᑎᑕᐅᔪᑦ ᑐᑭᓕᐊᖅᑐᑦ ᓄᓇᓄᑦ ᓄᓇᖑᐊᑦ ᐱᕆᒍᓐᓇᖅᑐᖅ. ᐃᓚᒋᐊᕐᓗᒍ ᓅᑦᑕᐅᓂᖏᓐᓄᑦ ᑲᑎᓐᓂᖏᓐᓄᑦ, ᓄᓇᓕᕆᓂᕐᒧᑦ ᐊᕙᑦᑐᖅᓯᒪᔪᑦ ᓂᐅᖓᓂᖃᕈᓐᓇᖅᑐᑦ ᓴᖑᖓᓂᖃᒻᒪᕆᓪᓗᑎᑦ. ᑐᑭᓕᐊᖅᑐᑦ ᑎᑎᕋᖅᑕᐅᓯᒪᔪᑦ ᖃᖓᒎᖅᑐᑑᓐᓃᑦᑕᐃᔭᐅᔪᖅ ᐊᑦᑐᕐᕙᖏᑦ. ᑲᑎᙵᓪᓗᐊᕆᔭᖓᓂᑦ, ᑕᑯᔅᓴᐅᑎᑕᐅᔪᖅ ᑎᑎᑯᑖᔅᓯᒪᓪᓗᓂ, ᑭᓯᐊᓂ ᓇᓗᓇᐃᖅᓯᒪᑦᑎᐊᖏᑉᐸᑦ, ᑕᑯᔅᓴᐅᑎᑕᐅᔪᑦ ᑎᑎᖅᑕᐅᑲᐃᓐᓇᖃᑦᑕᖅᑐᓂ ᑐᑭᓕᐊᖅᑐᓂᑦ. ᑎᑎᑯᑖᔅᓯᒪᔪᑦ ᓄᓇᖑᐊᒥᑦ ᐊᓯᔾᔨᖅᑕᐅᔪᓐᓇᖅᑐᖅ ᐊᓯᖏᓐᓄᑦ ᓇᓗᓇᐃᒃᑕᓄᑦ ᑎᑎᑯᑖᔅᓯᒪᔫᒥᑦ (ᐱᖓᓯᓂᑦ ᓴᓂᕋᓚᒃ, ᒥᑭᔪᑦ ᑎᑎᖅᓯᒪᔪᑦ, ᖃᔾᔪᓐᖑᐊᑦ, ᐊᓯᖏᓪᓗ) ᑐᑭᓯᑎᐊᕈᑎᖃᖅᑎᑦᑎᓂᖅᓴᐅᔪᑦ ᑎᑎᑯᑖᔅᓯᒪᔪᒧᑦ. ᐆᑦᑑᑎᒋᓗᒍ, ᑲᑎᓐᓂᖏᑦ ᐱᖓᓱᑦ ᓄᓇᐃᑦ ᑕᑯᔅᓴᐅᑎᑦᑎᔪᖅ ᓴᓂᕋᖓ ᐱᖓᓱᓂᑦ ᓴᓂᕋᓚᓐᓂᑦ ᖁᙱᓇᐊᖅᓯᒪᔪᖅ ᓴᓂᕌᓅᖅᑐᓂ ᐱᖓᓱᓂᑦ ᓴᓂᕋᓚᒻᒨᖏᑦᑐᖅ. ᐊᕐᕌᒍᖏᑦᑐᓕᒫᑦ ᓇᓗᓇᐃᒃᑕᐃᑦ ᑎᑎᖅᓯᒪᔪᓂᑦ ᓇᓗᓇᐃᔭᖅᓯᒪᔪᑦ ᓄᓇᖑᐊᑉ ᓇᓗᓇᐃᒃᑕᖏᑦ. ᐊᑎᖃᖅᑐᑦ ᖁᓕᕇᑦᑐᑦ ᑕᑯᔅᓴᐅᑎᑕᐅᔪᑦ ᓄᓇᖑᐊᒥᑦ ᑎᑎᑲᓪᓚᔅᓯᒪᔪᑦ ᕿᑭᖅᑕᑲᓪᓚᒥᓪᓗ ᓇᓗᓇᐃᒃᑕᖓ. ᓇᓗᓇᐃᒃᑕᐃᑦ ᐱᖓᓲᓕᖅᑲᖓᔪᑦ: ᑎᑎᑯᑖᔅᓯᒪᔪᑦ, ᓇᑦᑐᓂ ᑎᑎᖅᓯᒪᔪᑦ, ᐊᒻᒪᓗ ᓈᓴᐅᑎᖓ. ᑎᑎᑯᑖᔅᓯᒪᔪᑦ ᑕᐃᔭᐃᔪᑦ ᑎᑎᖅᑕᐅᑐᐃᓐᓇᖅᑐᖅ, ᐊᒻᒪ ᑕᑯᔅᓴᐅᑎᑦᑎᔪᑦ ᖁᓕᕇᑦᑐᑦ ᓄᓇᒧᑦ ᓇᓕᒧᓐᓂᖃᖅᑐᑦ. ᓅᔅᓯᒪᔪᓂᑦ ᓄᓇᐅᑉ ᖃᖓᓃᑦᑐᓂᑦ ᑐᕌᕐᓂᖃᖅᑐᖅ ᓄᓇᒧᑦ ᓇᓕᒧᓐᓂᖃᖅᑐᓂ, ᖃᓄᐃᑦᑐᑐᐃᓐᓇᐃᑦ ᐅᕙᖓᔪᓂᑦ ᑎᑎᖅᓯᒪᔪᑦ ᑐᕌᕐᓂᖃᖅᑐᑦ ᓄᓇᒧᑦ ᓇᓕᒧᓐᓂᖃᖅᑐᑎᑦ (ᐃᓱᒪᒋᓐᖑᐊᑲᐃᓐᓇᕈᒃ ᐱᓱᑦᑎᓪᓗᑎᑦ ᖃᖅᑲᔮᐸ ᓴᓂᕌᒍᑦ,ᐅᐸᒐᔅᓴᐅᓂᐊᓴᑐᐃᓐᓇᖅᑐᖅ ᖁᒻᒧᐊᒐᓂ ᐊᒻᒧᐊᒐᓂᓘᓐᓃᑦ, ᑭᓯᐊᓂ ᒪᑭᑕᑦᑎᐊᖅᑐᖅ). ᓇᐃᑦᑐᑦ ᑎᑎᖅᓯᒪᔪᑦ ᑕᐃᔭᐅᔪᑦ ᑎᑎᑲᓪᓚᔅᓯᒪᔪᑦ ᑐᑭᓕᐊᖅᑐᑦ, ᐊᒻᒪ ᑕᑯᔅᓴᐅᑎᑦᑎᔪᑦ ᖁᓕᕇᑦᑐᑦ ᖃᓄᑎᒋ ᓯᕙᖓᒪᖕᒫᑕ. ᓈᓴᐅᑎᖓ ᑕᐃᔭᐃᔪᑦ ᑎᑎᑲᓪᓚᔅᓯᒪᔪᖅ, ᐊᒻᒪ ᑕᑯᔅᓴᐅᑎᑦᑎᔪᑦ ᖁᓕᕇᑦᑐᑦ ᖃᓄᑎᒋ ᓯᕙᖓᒪᖕᒫᑕ, ᑎᓇᔅᑯᑎᒍᑦ, ᒪᓂᕋᑦᑐᒥᑦ. ᖁᑦᑎᓂᖅᓴᐅᑎᓪᓗᒍ ᓈᓴᐅᑎᖓ, ᓯᕙᖓᓂᖅᓴᐅᔪᖅ ᖁᓕᕇᓐᓂᖏᑦ, ᑎᑎᖅᑕᐅᑐᐃᓐᓇᖅᓯᒪᔪᑦ ᓇᓗᓇᐃᒃᑕᐃᑦ ᐋᖅᑭᒋᐊᖅᑕᐅᔪᓐᓇᖅᑐᑦ ᑐᑭᓯᒋᐊᕈᑎᖃᖅᑎᑦᑎᑲᓂᕐᓂᐊᕐᒪᑦ ᓯᕙᖓᔪᒥᑦ ᖁᓕᕇᑦᑐᓂᑦ ᑎᑎᑯᑖᔅᓯᒪᔪᑦ ᑕᐃᒪᐃᒍᓐᓇᑎᓪᓗᒋᑦ, ᐊᒻᒪ ᑖᒃᑯᐊ ᐊᓯᔾᔨᕈᑎᐅᔪᓐ ᓇᓗᓇᐃᔭᖅᓯᒪᔪᑦ ᓄᓇᖑᐊᑉ ᓇᓗᓇᐃᒃᑕᖏᓐᓂ.

ᓄᓇᒧᑦ ᓄᓇᖑᐊᓕᒫᑦ ᑎᑎᕋᖅᓯᒪᔪᖃᕐᕕᐅᖅᑐᑦ ᑕᐃᔭᐅᔪᑦ ᓄᓇᖑᐊᒧᑦ ᓇᓗᓇᐃᒃᑕᐃᑦ , ᓇᓗᓇᐃᒃᑕᖏᓐᓂ, ᐊᒥᓕᒫᖏᑦ ᐊᒻᒪ ᓇᓗᓇᐃᒃᑕᖏᑦ ᑕᑯᔅᓴᐅᑎᑕᐅᔪᑦ ᐊᒻᒪ ᓇᓗᓇᐃᔭᖅᑕᐅᓯᒪᓪᓗᑎᑦ. ᓄᓇᖑᐊᒧᑦ ᓇᓗᓇᐃᒃᑕᐃᑦ ᐱᒋᐊᖅᓯᒪᔪᑦ ᑎᑎᕋᖅᓯᒪᔪᓂᑦ ᑕᑯᔅᓴᐅᑎᑦᑎᔪᑦ ᐊᒥᐊᖓ ᑎᑎᖅᑲᖓᓗ ᐊᑐᓂ ᓄᓇᖑᐊᓕᒫᓂᑦ, ᐱᒋᐊᖅᓯᒪᓪᓗᓂ ᖁᑖᓂ ᐅᓯᖅᑲᖅᑲᕈᕋᑖᕐᓂᖅᐹᖑᔪᑦ, ᐊᑎᖓᑦᑕᐅᑦ ᐃᑳᒃᑰᖓᓂᖓ (ᐱᑕᖅᑲᕈᓂ) ᐊᒻᒪ ᓇᓗᓇᐃᔭᖅᓯᒪᒐᑖᓐᓂᖓᖃᓄᐃᑦᑑᓂᖏᑦ ᐅᓯᖅᑲᐃᑦ ᐊᕙᑦᑐᖅᓯᒪᔪᒥᑦ, ᐊᕐᕌᒍᖏᑦᑐᑦ ᖃᓄᐃᑦᑑᓂᖏᑦᓴᑎᑎᑯᑖᔅᓯᒪᔪᓂᑦ ᓄᓇᖑᐊᒥᑦ ᓇᓗᓇᐃᔭᖅᑕᐅᓯᒪᔪᑦ, ᐊᒻᒪ ᐊᕐᕌᒍᖏᑦᑐᓕᒫᑦ ᑎᑎᑲᓪᓚᔅᓯᒪᔪᑦ ᑐᑭᓕᐊᖅᑐᑎᑦ ᐊᒻᒪ ᑕᖅᓴᐅᔮᖅᑐᑦ ᓇᓗᓇᐃᒃᑕᐃᑦ. ᓄᓇᖑᐊᒧᑦ ᓇᓗᓇᐃᔭᖅᓯᒪᓂᖏᑦ ᓇᓗᓇᐃᔭᐃᓯᒪᓂᐊᕐᒥᔪᑦ ᖃᓄᐃᑦᑐᑐᐃᓐᓇᖅᓯᑦ ᐊᓯᖏᓐᓂᑦ ᓄᓇᒧᑦ

ᓇᓄᓇᐃᒃᑕᐃᑦ ᐊᑐᖅᑕᐅᔪᓂᑦ ᓄᓇᖑᐊᒥᑦ (ᐆᑦᑑᑎᒋᓗᒍ ᓇᒦᓐᓂᕐᒋᑦ ᐅᔭᖅᑲᐃᑦ ᓇᓂᔭᐅᔪᑦ, ᓇᒦᓐᓂᕐᒋᑦ ᓴᕕᕋᔭᑦᑎᐊᕙᐃᑦ, ᐊᒻᒪ ᐊᓯᕐᒋᑦ ᓄᓇᖓᓂᑦ ᑕᑯᔅᓴᐅᑎᑦᑎᔪᑦ ᐱᒻᒪᕆᐅᔪᓐᓇᖅᑐᑦ ᐊᕙᑦᑐᖅᓯᒪᔪᒧᑦ ᑎᑎᕋᖅᑕᐅᓯᒪᔪᑦ ᓄᓇᖑᐊᒥᑦ). ᐱ−ᔪᑎᒋᓪᓗᒍ ᓄᓇᓕᓐᓂᐅᔪᖅ ᐊᕙᑦᑐᖅᓯᒪᔪᓕᒫᓂᑦ ᐊᔾᔩᕐᒋᑦᑐᐃᓐᓇᐃᑦ, ᓄᓇᖑᐊᒧᑦ ᓇᓄᓇᐃᒃᑯᑕᐃᑦᐱᒻᒪᕆᐅᔪᖅ ᑐᑭᓯᑎᐊᕐᓗᒍ ᓄᓇᖑᐊᖅ.

ᖃᐅᔨᒪᕐᓂᐅᔪᖅ ᐊᒻᒪ ᓄᓇᖑᐊᓕᐅᕐᓂᖅ ᓂᒋᖓᓂ−ᕿᑭᐊᓂ ᕿᑭᖅᑖᓗᒃ ᓴᖅᑭᑎᑦᑎᓚᐅᖅᑐᑦ ᓇᒦᓐᓂᕐᒋᓐᓂᑦ metasedimentary ᐅᔭᖅᑲᐃᑦ (ᑭᒻᒥᕈᒻᒥ ᐱᓕᕆᔪᑦ; ᕗᓴᖑᐊᑦ ᐃᓛᒃᑰᖓᔪᑦ ⱣLHq, ⱣLHc, ⱣLHs, ⱣLHp; ᐳᑑᕆᐋᑦ; ᐊᒃᒍᖅᓯᒪᔪᓂᑦ ⱣPL) ᐊᓯᐊᓄᑦ ᐊᑦᑐᐊᓂᖅᑲᕈᓐᓇᖅᑐᖅ ᐅᕝᕙᓘᓐᓃᑦ ᐅᔭᖅᑲᖅᑲᖅᑲᐅᕐᒋᓪᓗᓂ Meta Incognita Peninsula−ᒥᑦ. ᐊᒥᓱᓚᐃᑦ ᑲᑎᙵᐅᖅᑐᑦ magmatic (sills) ᑎᑎᕋᖅᑕᐅᓚᐅᖅᑐᑦ ᐊᒻᒪ ᖃᐅᔮᓴᖅᑕᓪᓚᑐᐊᕆᔭᐅᓂᐊᖅᑐᑦ (ᓄᓇᖑᐊᑦ ᐊᒃᒍᖅᓯᒪᔪᑦ ⱣLHu, ⱣLHm, ⱣLHd). ᑖᒃᑯᐊ ᑮᓇᐅᔭᓕᐅᕐᓯᐊᕈᑎᔅᓴᐅᔪᓐᓇᖅᓂᕐᒋᓐᓄᑦ ᐱᒻᒪᕆᐅᔪᑦ ᐃᓗᓕᖅᑲᐅᕐᒪᑕ ᓴᕕᕋᔭᔅᓴᓖᑦ ᐅᔭᕋᓐᓂᐊᕋᔅᓴᐅᔪᓐᓇᖅᑐᑦ (sulphides), ᐅᒻᒪ ᓴᖅᑭᖅᑲᑦᑕᕐᓂᕐᒋᑦ ᓇᓄᓇᐃᖅᓯᔪᓐᓇᖅᑐᑦ ᐱᑕᖅᑲᕐᓂᐊᓂᑦ ᑮᓇᐅᔭᓕᐅᕐᓯᐊᕈᑎᔅᓴᐅᔪᓐᓇᖅᑐᓂᑦ ᓴᕕ?ᔭᖅᑲᕐᓂᖓᓂᑦ. ᐱᖓᓱᑦ ᐅᔭᖅᑲᐃᑦᐊᔾᔩᕐᒋᑦᑐᓂᑦ ᐃᓗᓕᖅᑲᐅᖅᑐᑦ ᐊᒻᒪ ᒪᖅᕈᐊᑎᖅᓯᒪᔪᖅ ᐆᓇᖅᓯᓂᒥᓂᖓ ᖃᐅᔮᔭᐅᓚᐅᖅᑐᑦ. ᑕᐃᒪᓐᓇᐃᑦᑐᑦ ᑲᑎᖓᓂᖓᒍᑦ ᐊᐅᓚᔾᔭᖅᑲᑦᑕᐅᑎᒍᓐᓇᖅᑐᑦ ᐊᔾᔨᐸᓗᐊᓂᑦ ᓄᓇ ᓴᔪᑉᐱᓚᓐᓂᓕᓚᐅᖅᑕᖓ 1800 ᒥᓕᐊᓐ ᐊᕐᕌᒍᓕᖅᑐᑦ ᐊᒻᒪ ᑎᑎᕋᖅᑕᐅᓯ,ᒪᔪᖅ ᑕᒪᒃᑭᓐᓂ ᐊᓯᐊᓂᑦᑕᐅᖅ ᕿᑭᖅᑖᓗᒻᒥᓘᓐᓃᑦ ᐊᒻᒪ ᐅᐊᓐᓇᖓᓂᑦ ᑯᕋᐃᒃ. ᑖᒃᑯᐊ ᖃᐅᔮᓴᕈᑕᐅᔪᑦ ᐊᑐᖅᑕᐅᓂᐊᖅᑐᑦ ᐊᔾᔩᓐᖑᐊᖅᑎᑕᐅᓗᑎᑦ ᐊᒻᒪ ᐱᐅᓯᑎᐱᐊᖅᑕᐅᓗᓂ ᐊᑐᖅᑕᐅᓂᕐᒋᑦ ᑕᑯᔅᓴᐅᑎᑦᑎᔪᑦ ᐅᐊᑦᑎᐊᕈᒻᒪᓇᐊᓗᓂᑦ ᓄᓇᖓ ᐊᓯᔾᔨᐸᓪᓕᐊᓂᖓ ᓄᓇᕗᑦ.

ᓇᓄᓇᐃᔭᖅᓯᒪᓂᖏᑦ ᖃᐅᔨᒪᔭᐅᔭᕆᐊᓖᑦ

ᐱᒋᐊᕐᓂᖓ

ᓄᓇᖑᐊᓕᐅᕐᓂᖅ ᐊᐅᓚᔭᓐᓴᐅᑎᓕᓐᓂᒃᑯᓐᓄᑦ ᐅᔭᕋᓐᓂᐊᕋᓱᓐᓄᓪᓗ (GEM) ᐱᓕᕆᐊᖅ ᑐᕌᓚᐅᖅᑐᑦ ᓂᒋᖓᓂ−ᕿᑭᐊᓂ ᕿᑭᖅᑖᓗᒃ ᐊᑐᖅᑕᐅᓂᐊᖅᓯᒪᔪᓂᑦ, ᖁᓚᓛᑰᓕᒃᑯᑦ ᐃᑲᔪᖅᑕᐅᔪᑦ ᖁᐊᖑᐃᓐᓇᖅᑐᒥᑦ ᓄᓇᖑᐊᓕᐅᕐᓂᖅ 2015−ᒥᑦ (ᐊᐅᐸᖅᑐᖅ ᐱᖓᓯᓂᑦ ᐅᖓᑖᓂᓪᓘᓐᓃᑦ ᓴᓐᓂᕋᓖᑦ ᓇᓕᒧᑦᑐᐊᑐᐃᓐᓇᐅᑦᑐᑎᑦ, ᐊᔾᔨᓐᖑᐊᖅ 1). GEM ᐱᓕᕆᐊᖅ ᐱᑕᖅᑲᖅᑎᑦᑎᔪᖅ ᐅᓪᓗᒥᒨᖑᔪᓂᑦ, ᑭᒃᑯᐃᓐᓇᕐᓄᑦ ᐊᑐᐃᓐᓇᐅᔪᑦ, ᐊᕙᑦᑐᖅᓯᒪᔪᑎᒍᑦᐅᔭᖅᑲᓂᑦ ᖃᐅᔨᓴᓂᕐᒧᑦ ᖃᐅᔨᒪᔭᐅᔪᑦ ᑲᓇᑕᐅᑉ ᐅᑭᐅᑕᖅᑐᖑᓂ, ᐃᑲᔪᖅᑐᐃᔪᓂᑦ ᖃᐅᔨᔭᐅᓯᒪᔪᓂᑦ ᕿᓂᖅᑎᓪᓗᒋᑦ ᓄᑖᓄᑦ ᐊᐅᓚᔭᓐᓇᐅᑎᓄᑦ ᐅᔭᕋᓐᓂᐊᕋᓱᐊᖅᑐᓂᓪᓗ ᓄᓇᓕᒻᒥᐅᑕᓂᓪᓗ ᐅᑭᐅᑕᖅᑐᒥᑦ ᐃᓱᒪᓕᐅᕈᓐᓇᖅᑐᑦ ᖃᐅᔨᒪᔭᐅᑎᑕᐅᑦᑎᐊᕐᓗᑎ ᓄᓇᖕᒋᑕ ᒥᔅᓵᓃᖓᔪᓂ, ᑮᓇᐅᔭᓕᐅᕐᓂᕐᒧᑦ, ᐊᒻᒪ ᐃᓅᖃᑎᒌᓐᓂᕐᒧᑦ. 2015−ᒥ ᖃᐅᔨᓴᕐᓂᐅᔪᖅ ᐱᓗᐊᖅᑐᒥᑦ ᐱᒻᒪᕆᐅᓚᐅᖅᑐᖅ ᐅᓪᓗᒥᒨᖓᓕᖅᑎᑕᐅᒻᒪᑕ ᐊᕙᑦᑐᖅᓯᒪᔪᒥᑦ ᖁᐊᖑᐃᓐᓇᖅᑐᒥᑦ ᓄᓇᖑᐊᓕᐅᓂᕐᒥᑦ ᓂᒋᖓᓂ ᓇᑉᐸᖓᓂ ᕿᑭᖅᑖᓗᒃ (ᓂᒋᐊᓂ ᓄᓇᖑᐊᑎᒍᑦ 70°N), ᐊᑯᑭᓐᓇᑎᑦᑎᐊᖅ ᓄᑖᒥᑦ, ᐅᔭᖅᑲᓂᑦ ᖃᐅᔨᓴᓂᕐᒧᑦ ᖃᐅᔨᒪᔭᐅᔪᓂᑦ ᐊᕙᑦᑐᖅᓯᒪᔪᒧᑦ. ᖃᐅᔨᓴᕐᕕᐅᔪᖅ ᐊᕙᑦᑐᖅᓯᒪᔪᑦ (ᐃᓚᖕᒋᑦ NTS ᐊᕙᑦᑐᖅᓯᒪᔪᑦ NTS 26-B, -C, -F, -G, -J and -K) ᑐᑭᒧᐊᖅᑎᑕᐅᓚᐅᖅᑐᑯᑦ ᑲᓇᑕᒥ ᐅ.ᖅᑲᓂᑦ ᖃᐅᔨᓴᓂᕐᒧᑦ ᖃᐅᔨᓴᕐᓂᖅ (GSC) ᐱᓕᕆᖃᑎᖃᖅᑐᑎᑦ ᑲᓇᑕ ᓄᓇᕗᓪᓗ ᐅᔭᖅᑲᓂᑦ ᖃᐅᔨᓴᖅᑏᑦ

ᑎᑎᕋᖅᕕᖓ (CNGO), ᐃᓚᐅᖃᑕᐅᔪᓕᕐᓗ ᓄᓇᕗᒻᒥ ᓯᓚᑦᑐᓴᖅᕕᒃ, ᑲᐅᑕᓐ ᓯᓚᑦᑐᓴᖅᕕᒃᔪᐊᖅ, ᓯᓚᑦᑐᓴᖅᕕᒃᔪᐊᖓ ᐋᒃᓴᕗᑦ, ᐊᒻᒪ ᓄᓇᕗᑦ ᒐᕙᒪᒃᑯᑦ.

ᖃᐅᔨᓴᖃᑦᑕᕐᓂᐅᔪᖅ ᓄᓇᓕᕆᓂᕐᒥ ᕿᑭᖅᑖᓘᑉ ᓂᒋᐊᓂ ᓴᓂᒧᑦ 66°N ᐱᓕᕆᐊᖑᓚᐅᖅᓯᒪᕗᖅ 1949-ᒥᑦ 1965-ᒧᑦ, ᑕᒪᒃᑯᐊ ᖃᐅᔨᔭᐅᕙᓪᓕᐊᔪᑦ ᑲᑎᑕᐅᕙᓪᓕᐊᓪᓗᑎᒃ ᐊᒻᒪ ᐋᖅᑭᒃᑕᐅᓕᖅᑯᓂ ᐅᔭᕋᐃᑦ ᓇᓗᓇᐃᔭᖅᑕᐅᓯᒪᓪᓗᑎᒃ 18-ᓂ 1:250 000 NTS ᓄᓇᙳᐊᓕᐊᓂ ᐊᑐᖅᑯᑎᒃ (ᐸᓖᑲᑐᐊ, 1967 (Blackadar, 1967)). ᑖᒃᑯᐊ ᑭᖑᓂᐊᒍᑦ ᖁᓕᒥᒎᓕᒃᑯᑦ ᐱᓕᕆᖃᑕᒃᑯᑎᒃ ᕿᑭᖅᑖᓘᑉ ᕿᑎᐊᓂᑦ (ᓷᖅᓗ, Henderson, 1985). ᖃᓂᓐᓂᖅᓱᑯᓪᓚ, ᒫᓐᓇᓕᓴᐅᓕᖅᑐᓂᑦ ᓄᓇᒥ ᖃᐅᔨᓴᖅᑐᓕᕆᓂᕐᒧᑦ ᖃᐅᔨᒪᔭᐅᓯᒪᔪᓂ ᑐᓴᖅᑎᑕᐅᓯᒪᕗᑦ ᓄᓇᒥ ᖃᐅᔨᓴᕈᑎᐅᔪᒧᑦ ᖁᓕᒦᓕᖕᒥ ᐊᑐᖅᐸᒃᑯᑎᒃ ᓄᓇᒥ ᐱᓱᑲᑕᒃᐸᒃᑯᑎᒃ ᒦᓂ: ᓂᕆᖅᐸᓯᐊᓂᑦ ᕿᑭᖅᑖᓘᑉ (1995-1997; ᐆᔭᐅᔭᐅᓪᓗᓂ, ᐊᔾᔨᖑᐊᖅ 1), ᕿᑭᖅᑖᓘᑉ ᓂᒋᐊᓂ ᐱᖓᓐᓇᖅᐸᓯᐊᓂ (2006; ᖁᖅᓱᖅᑎᕐᓯᒪᔪᖅ, ᐊᔾᔨᖑᐊᖅ 1), ᑎᓄᔾᔭᖅᕕᒃ (Cumberland Peninsula) (2009–2011; ᑲᔪᒐᓚᐅᓪᓗᑎᒃ, ᐊᔾᔨᖑᐊᖅ 1), Hᐋᓪ ᐸᓂᓐᓯᓚ (2012-2013; ᑐᖑᔪᖅᑐᖅ, ᐊᔾᔨᖑᐊᖅ 1), ᐊᒻᒪ ᒥᑕ ᐃᓐᑲᓪᓃᑕ ᐸᓂᓐᓯᓚ (2014 ᐳᐆᓪᓗᓂ, ᐊᔾᔨᖑᐊᖅ 1). 2015 ᐊᐅᔭᖓᑕ ᓯᕗᓂᐊᓂᑦ, ᐊᑕᐅᓯᑐᐊᖅ ᐱᐊᓂᒃᑕᐅᔭᕆᐊᖃᓕᓚᐅᖅᑐᖅ ᓄᑖᖑᕆᐊᖅᓯᒪᔪᖅ ᑕᒪᕐᒥ ᕿᑭᖅᑖᓘᑉ ᓂᒋᖓ ᓴᓂᒧᑦ 70°N: ᓂᒋᕐᒥᑦ-ᕿᑎᖅᐸᓯᐊᓂᑦ ᕿᑭᖅᑖᓗ ᐅᕙᓂ ᓯᐅᕕᐊ ᒍᕆᓄᓪ ᑕᓯᖅ-ᑭᓕᐅᕗᐊᑐ ᑲᖏᖅᑯ ᒥᒃᓵᓂᑦ (ᐊᐅᐸᖅᑐᑦ, ᐊᔾᔨᖑᐊᖅ 1).

ᓂᖏᕐᒥᑦ-ᕿᑎᖅᐸᓯᐊᓂᑦ ᕿᑭᖅᑖᓗ ᓄᓇᖓ ᐃᓚᖃᖅᐳᖅ ᐅᐊᖕᓇᖅᐸᓯᖕᒥᑦ (ᑯᐸᐃᒃ-ᕿᑭᖅᑖᓗᒃ) ᓄᓇᐅᑉ ᐃᓚᒋᓪᓗᓂᐅᒃ ᑕᐅᔭᐅᔪᖅ Trans-Hudson Orogen (THO), ᑕᒪᓐᓇᓕ ᐃᒪᐅᑉ ᐊᑖᒨᖓᔪᖅ ᐊᖏᔪᐊᓘᓪᓗᓂ ᓴᖑᖓᓂᖃᖅᑯᓂ ᐅᐊᖕᓇᖅᐸᓯᕐᒥᑦ ᑲᓇᖕᓇᕐᒥ ᒪᐅᖓ ᓂᒋᖅᐸᓯᐊᓄᑦ ᕿᑎᖓᓂ ᓄᐊᑦ ᐊᒥᐊᓕᑲᐅ (Hoffman, 1988). ᐅᓇ THO ᐋᖅᑭᖕᓂᑯᕕᓂᖅ ᑭᖑᓪᓕᖅᐹᒥ ᐅᓇ ᐱᕋᖅᐸᓪᓕᐊᑎᓪᓗᒍ Nuna supercontinent, ᐊᒻᒪᓗ *sensu lato* ᑎᑎᕋᐅᓯᖃᖅᓯᒪᔪᖅ ᒪᑐᓂᕕᓂᖓᓂᑦ ᐅᓇ Manikewan Ocean ᕿᑎᐊᓃᑦᑐᖅ ᒦᓂ ᐊᑦᑎᖕᓂᖅᓱᒥ ᓴᐱᐅᓇᔪᒥᑦ ᐊᒻᒪ ᖁᑦᑎᖕᓂᖅᓱᒥ ᓷᓯᐅᐸ ᓄᓇᖏᓐᓂᑦ ᒫᙵᑦ 1.92-ᒥᑦ 1.80-ᒧᑦ Ga. ᓇᓗᓇᐃᔭᐃᓯᒪᔪᑎᒍᑦ, THO ᓄᓇᐅᕗᖅ ᑐᓗᖅᓯᒪᓂᑰᓪᓗᓂ ᐊᔾᔩᖏᑦᑑᑎᒃᑯᑦ ᓇᐃᓈᕐᓯᒪᔪᑎᒍ ᖃᓄᐃᑉᐸᓪᓕᐊᓂᕕᓂᖏ ᐊᖏᔫᑕᐅᓂᖅᓱᓂ 120 Myr ᑕᒪᓐᓇ ᐃᒪᐅᑉ ᐃᓂᖓ ᒪᑐᕙᓪᓕᐊᓂᖓᓂᑦ ᒫᓐᓇ ca 1920 ᐅᓄᖓ 1800 Ma (Corrigan et al., 2009; St-Onge et al., 2009). ᕿᑭᖅᑖᓘᑉ ᓂᒋᐊᓂ ᑲᓇᖕᓇᖅᐸᓯᐊᓂᑦ, ᑎᓴᒪᑦ ᓄᓇᕕᓃᑦ ᖁᓕᓃᓕᖅᓯᒪᔪᑦ ᓇᓗᓇᐃᖅᑕᐅᓯᒪᕗᑦ (ᐊᔾᔨᖑᐊᖅ 2). ᐊᑦᑎᖕᓂᖅᐹᖓᓂ ᖁᑦᑎᖕᓂᖅᐹᒧ ᐋᖅᑭᒃᐸᓪᓕᐊᓂᓄ, ᐃᒪᐃᓕᖓᕙᓪᓕᐊᕗᖅ:

1) ᓄᓇᕕᓂᑐᖃᐃᑦ ᐱᕆᐊᖅᕕᖏ ᓴᓂᒨᖓᔪᑦ, ᑐᑭᓕᐅᓇᔭᐅᓯᒪᔪᑦ ᐅᑭᐅᖅᑕᖅᑐᖅᒥᑦ ᑲᔪᓯᕙᓪᓕᐊᓂᖓᓂ ᐅᓇ Superior ᐱᕆᐊᖅᕕᒋᓯᒪᔭᖓᓂᑦ, ᐊᒻᒪᓗ ᕿᑎᐊᓃᑦᑐᖅ ᐃᒪᐃᑦᑐᖃᖅᑯᓂ Paleoproterozoic supracrustal ᖄᖓᒍᑦ (Povungnituk Group; St-Onge et al., 1996;

2) ᕿᑎᐊᓃᑦᑐᑦ ᐅᔭᕋᐃᑦ Paleoproterozoic ᐃᒪᐃᑦᑑᓂᖅᓱᐅᓪᓗᑎᒃ monzogranitic ᐊᒻᒪ granodioritic orthogneiss, ᑐᑭᓕᐅᓇᔭᐅᓯᒪᔪᖅ ᐋᖅᑭᑦᑎᐊᖅᓯᒪᑦᑎᐊᖏᓐᓂᖓᓂᑦ arc-magmatic terrane (Narsajuaq arc; Scott, 1997; St-Onge et al., 2009), ᐅᕝᕙᓘᓐᓃᑦ ᐃᒪᓐᓇ ᓇᖅᓯᔪᐊᖅᑐᑦ-ᐊᑯᓂᐅᑎᕆᔪᖅ ᐱᖓᔪᕆᓕᖅᑕᖓᓂ ᖁᓕᓃᒃᑑᑎᓂᑦ (Corrigan et al., 2009);

3) ᓄᓇᕕᓂᑐᖃᐃᑦ ᐱᒋᐊᕐᕕᖕᒋ ᓴᓂᒨᖕᖓᔪᑦ ᐊᒻᒪ ᕿᑎᐊᓃᑦᑐᖅ Paleoproterozoic supracrustal ᖄᖕᖓᒍᑦ (Lake Harbour Group), ᑲᑎᓯᒪᓪᓗᑎ ᑕᐃᔭᐅᓯᒪᔪᑦ 'Meta Incognita microcontinent' ᐆᒪᙵᑦ St-Onge et al. (2000a), ᑕᒪᒃᑯᐊᓗ ᓇᓗᓇᐃᖅᓯᓯᒪᔪᑦ ᒪᑯᓂᖕᖓ crust rifted ᐅᕙᙵ the Rae ᐅᕝᕙᓘᓐᓃᑦ Superior craton, ᐅᕝᕙᓘᓐᓃᑦ ᑕᒪᐃᓐᓄᑦ ᐊᑐᖅᑕᐅᓯᒪᖕᒋᓐᓂᑰᕗᑦ: ᐊᒻᒪ

4) ᓄᓇᕕᓂᑐᖃᐃᑦ ᐱᒋᐊᕐᕕᖕᒋ ᓴᓂᒨᖕᖓᔪᑦ, ᑐᑭᓕᐅᕆᔭᐅᓯᒪᔪᖅ ᓂᒋᖅᒥ ᑲᔪᓯᓯᒪᓂᖕᖓᓂ ᐅᓇ Rae craton, ᐊᒻᒪ ᐅᓇ ᕿᑎᐊᓃᑦᑐᖅ Paleoproterozoic supracrustal ᖄᖕᖓᓂ (Piling Group; Wodicka et al., 2014), ᐅᔭᕋᐃ ᐱᕈᕐᕕᐅᕙᓪᓕᐊᔪᓐᓇᖅᑐᑦ ᐊᔾᔨᒋᔭᖕᒋᓐ ᐅᑯᓄᖕᖓ Hoare Bay Group ᐅᕙᓂ Cumberland Peninsula.

ᖁᕝᕙᓯᓐᓂᖕᒋᑦ 3 ᐊᒻᒪ 4 ᓈᒻᒪᒍᓐᓃᖅᑎᑦᑎᓯᒪᓗᐊᒧ ᐆᒧᖕᖓ Cumberland batholith, ᑖᓐᓇ ᐊᔾᔨᒌᖕᒋᑦᑑᑎᓂ ᐅᔭᕋᐅᔭᐅᖂᔨᔪᓂ ᓴᖅᑭᑉᐸᓪᓕᐊᓯᒪᔪᓂ ᐱᑕᖃᖅᐳᑦ ca. 1865–1845 Ma (Whalen et al., 2010). ᐅᓇ Cumberland batholith ᑐᑭᓕᐅᕆᔭᐅᓯᒪᔪᖅ ᐃᒪᓐᓇ Andean-type batholith (St-Onge et al., 2009), ᐅᕝᕙᓘᓐᓃ ᐱᔾᔪᑎᖃᖅᖢᓂ ᑲᑎᖃᑎᒌᖕᓂᑰᓂᖕᒋᓐᓂᑦ ᐅᑯᐊ lithospheric delamination ᐊᒻᒪ ᓄᓇᐅᑉ ᕿᑎᐊᓃᑦᑐᖅ (Whalen et al., 2010). ᑕᒪᐃᓐᓂ ᖁᓖᕇᒃᐸᓪᓕᐊᔪᑦ ᐅᕘᓇ ca. 720 Ma basaltic 'Franklin' ᓵᐳᓕᑎᐅᔪᓂ, ᑭᓯᐊᓂᓕ ᐊᑭᓕᕇᒍᑎᑦᑎᐊᙱᑦᑐᑦ ᐅᕘᓇ Ordovician limestone strata (Blackadar, 1967).

ᑎᓴᒪᑦ ᓄᓇᐅᑉ ᖄᖕᒋ ᐱᒋᐊᖅᓯᒪᕗ ᓂᒋᖅᒥ ᐅᐊᕐᓇᕐᒍᖕᖓᐅᕙᓪᓕᐊᔪᓂᑦ ᐋᖅᑭᑉᐸᓪᓕᐊᓪᓗᑎ ᐆᒧᖕᖓ THO. ᓄᑕᐅᖕᒋᓐᓂᖅᐹᖅ ᓄᓇᕕᓂᖅᓂᑦ, ᖁᓕᕇᒃᑐᓂᑦ 3–4 'ᕿᑭᖅᑖᓗᒃ ᐅᔭᖅᑲᖓ', ᐃᓱᒪᒋᔭᐅᓯᒪᕗᖅ ᐱᒋᐊᕈᑎᖅᑲᖅᓯᒪᔭᕆᐊᒃᓴᖕᖓᓂᑦ ᐋᖅᑭᒃᐸᓪᓕᐊᓂᖅᒧᑦ ᐅᓇ Meta Incognita microcontinent ᐅᕗᖕᖓ Rae craton ᐊᖅᕌᒍᐃᑦ ᐊᑯᓐᓂᖕᖓᓂ ᐅᑯᐊ ca. 1880-ᒥᑦ 1865-ᒧᑦ Ma (St-Onge et al., 2006). ᐅᓇ ᓄᓇ ᐋᖅᑭᒃᐸᓪᓕᐊᓂᖕᖓ ᐅᔾᔨᖅᓇᓗᐊᖅᓯᒪᙱᑦᑐᖅ ᐱᔾᔪᑎᖅᑲᖅᖢᓂ ᓴᖅᑭᑉᐸᓪᓕᐊᓂᖕᖓᑕ ᓂᐱᖅᓇᖅᑐᖅᑲᖅᓂᖕᖓᓂ ᓴᖅᑭᒍᑎᒋᓗᐊᙱᖅᖢᓂᐅᒃ, ᑭᓯᐊᓂᓕ ᐱᑕᖅᑲᖅᖢᓂ ᒥᑭᑦᑐᓂᑦ ᓄᓇᐅᑉ ᐱᕈᖅᐸᓪᓕᐊᓯᒪᓂᖕᖓᓂᑦ (ᒪᓕᒃᖢᑎᒃ ᑕᒫᓂ ᐊᓯᙳᖅᐸᓪᓕᐊᓂᐅᔪᓂᑦ) ᑕᒫᓂ (St-Onge et al, 2009). ᐅᐊᖕᓇᖕᖓᓂᑦ ᓄᓇᓕᕆᕝᐅᓂᐊᖅᑑᑉ ᐅᓇᐅᕗᖅ ᓂᒋᖅᒧᑦ ᓵᖕᖓᓂ Piling Group, ᑖᓐᓇᓕ ᐃᓱᖅᑲᖅᕕᖅᑲᖅᑰᔨᔪᑦ, ᐃᒃᑲᑦᑐᓂ ᐃᒪᖅᑲᖅᕕᐅᓂᑰᓪᓂ ᐅᔭᕋᓚᐃᓪᓗ ᓱᖅᑲᒃᑎᖅᐸᓪᓕᐊᓯᒪᓪᓗᑎᒃ, ᐊᑖᓃᖢᑎᒃ ᓄᓇᐅᑉ ᓱᐳᓂᑯᕕᓂᖕᒋᓐᓂᑦ ᑖᒃᑯᐊᓗ ᐃᓚᖅᑲᖅᖢᑎᒃ ᓴᕕᖃᔭᒃᓴᖕᒎᖅᐸᓪᓕᐊᔪᓂᑦ. ᓂᒋᐊᓄᓪᓕ ᐱᓕᕆᕝᕕᐅᔪᒪᔫᑉ ᐅᓇᐅᕗᖅ ᐅᐊᖕᓇᖅᒧᑦ ᓵᖕᖓᔪᖅ Lake Harbour Group, ᑖᓐᓇᑦᑕᐅᖅ ᐅᔭᕋᐅᔭᖅᑲᐅᓂᓪᓗᓂ ᐃᓄᐊᓂᓱᖕᖓᖅ ᑕᒫᓂ, ᑭᓯᐊᓂᓕ ᐅᔾᔨᖅᓇᖅᑐᖅᑕᖅᑲᐅᓚᐅᖅᐳᖅ ᒪᑯᓂᖕᖓ ᐱᑕᖅᑲᐅᖅᓂᖕᒋᓐᓂᑦᑕᐅᖅ basal orthoquartzite ᐊᒻᒪ ᐃᒪᐃᑦᑐᓂ ᐱᑕᖅᑲᖕᒋᓗᓂ iron-formation ᐊᒻᒪ metagreywacke. ᑕᒪᓐᓇ ᓄᓇ ᐅᔾᔨᖅᓇᖅᑐᖅᑲᓚᐅᖅᒥᔪᖅ ᐊᑖᒍᑦ ᐃᓚᐅᖅᓯᒪᓚᐅᖅᓂᖕᒋᓐᓂᑦ ᖁᓕᕆᓕᖅᓯᒪᓂᒃᑯᑦ ᐱᖕᖓᔪᖕᖓᓐᓂᑦ (level 3) ᓯᕗᓂᐊᓂᑦ ᓴᖅᑭᑦᑐᕕᓃ ᐅᕙᓃᑦᑐᓂᑦ Cumberland batholith (St-Onge et al., 2007). 2015-ᒥ ᖃᐅᔨᓴᖅᓂᐅᔪᖅ ᕿᑭᖅᑖᓗᖕᒥ ᐱᓕᕆᐊᕆᔭᐅᓚᐅᔪᓂᑦ, ᐊᑕᐅᓯᖅ ᐊᖕᒋᓂᖅᐹᖕᖑᖅᑲᑕᐅᔪᖅᑕ ᐱᓕᕆᐊᕆᔪᒪᓂᖅᒧᑦ ᖃᐅᔨᒋᐊᒃᑲᓐᓂᖅᓗᑎ ᑕᒪᑐᒥᖕᖓ ᓄᓇᐅᑉ ᖃᓄᐃᑦᑑᓂᖕᖓᓂᑦ.

ᖁᕝᕙᓯᓐᓂᖕᒋᑦ 2–3 'ᓴᖅᐸ ᑰᒃ' (Soper River) ᓄᓇᖕᖓ ᑎᑎᕋᐅᓯᐅᓯᒪᕗᖅ ᐊᖕᒋᒡᓕᕙᓪᓕᐊᓂᖕᖓᓂᑦ ᓇᖅᓴᖅᔪᐊᖅ ᐊᖅᑭᓐᓂᕆᔭᖕᖓ (magmatic arc) ᒪᐅᖕᖓ Rae-Meta Incognita ᐃᓂᒋᔭᖕᖓᑎᒍᑦ. ᑕᒪᓐᓇ ᐋᖅᑭᒃᐸᓪᓕᐊᓯᒪᓇᓱᒋᔭᐅᔪᖅ ᕿᑎᐊᓂᑦ 1845 Ma, ᑖᓐᓇ ᐅᑭᐅᑎᒍᑦ ᐱᒋᐊᓕᓵᖅᓯᒪᓃᑯᓪᓗᓂ ᑕᒫᓂ ᐊᖅᑭᓐᓂᐅᔪᒥᑦ (Dunphy and Ludden, 1998), ᐊᒻᒪ

ca. 1842 Ma, ᑖᓐᓇᓕ ᐅᑭᐅᕆᔭᐅᓇᓱᒋᔪᖅ ᓄᑖᐅᙱᒋᓛᒥ oldest Andean-type phase (Scott, 1997). ᐋᖅᑭᒃᑎᐊᖅᓯᒪᓐᒋᓐᓂᐅᔪᖅ ᓴᕿ ᑰᓐᒥ ᐊᓐᒋᔫᕗᖅ ᐊᒻᒪ ᐃᓗᐊᓄᐊᕐᓇᖅᓗᓂ, ᐊᒻᒪᓗ ᒪᑯᓂᖓ ᐅᔭᕐᖃᐅᖅᓗᓂ ᐊᓯᖑᖅᐸᓪᓕᐊᔪᓂᑦ syn-metamorphic amphibolite-facies ᒪᐅᖓ granulite-facies metamorphic foliation (St-Onge et al., 2007).

ᖁᖏᕙᓯᓐᓂᖏᑦ 1–2 ‘Bergeron’ ᓄᓇ ᐋᖅᑭᒃᐸᓪᓕᐊᓂᑯ ᑐᓗᓚᐅᖅᑎᓪᓗᒍ ᐅᓇ Superior craton ᒪᑯᓂᖓ ᐃᓚᐅᖅᓯᒪᔪᓂᑦ ᐊᔾᔨᒌᖏᑦᑑᑎᓂᑦ ᖁᓛᓃᓐᓂᕐᓴᓃᑦᑐᓂᑦ (ᑲᑎᓯᒪᓪᓗᑎᒃ Churchill plate, ᐅᖃᕘᓐᓃᑦ peri-Churchill collage), ᐊᒻᒪᓗ ᐃᓱᒪᒋᔭᐅᔪᖅ ᑕᐃᒪᐃᓐᓂᑰᔭᕆᐊᒃᓴᖓᓂᑦ ᐊᑯᓐᓂᖓᓂᑦ 1820 Ma, ᐅᑭᐅᐅᕆᔭᐅᔪᖅ ᓄᑖᖑᓛᒧᑦ ᓴᕿᑦᑐᓂᑦ ᓴᓂᕌᓂᑦ ᖃᖅᑲᐅᑉ (Scott and Wodicka, 1998), ᐊᒻᒪ 1795 Ma, ᐊᕿᒍᒋᔭᐅᔪᕐᓕ ᐃᓗᑐᓂᐅᔻᑉ ᐊᖅᑯᓵᖅᓯᒪᔪᖅ ᓄᓇᒥᑦ (Wodicka and Scott, 1997). ᐅᓇ ᖃᓄᐃᓕᐅᕐᓂᐅᔪᖅ ᓴᕿᑎᑦᑎᔾᔪᑎᐅᓚᐅᖅᐳᖅ retrograde amphibolite-facies metamorphism ᒪᑯᓂᖓ ᐅᔭᕋᓐᓂ granulite-facies rocks ᖁᓪᓕᐅᓂᖅᓴᒦᑦᑐᓂ ᑐᓗᖅᑕᐅᕙᕙᓂᕐᒥ ᕿᑭᖅᑖᓘᑉ ᓂᒋᐊᓂ ᒪᐅᓇ ᓴᕿᐅᑉ ᐃᓂᒋᔭᖓᑕ ᐊᒻᒪᓗ ᐃᒪᐅᑉ ᐃᓂᒋᕙᒃᑕᕐᒋᓐᓂᑦ (St-Onge et al., 2000b).

TECTONOSTRATIGRAPHIC ᐃᓛᒃᑰᖓᔪᐃ

ᐅᔭᕋᐃᑦ ᓄᓇᙳᐊᓕᐅᖅᑕᐅᔪᑦ ᐅᕙᓂ Sylvia Grinnell Lake–Clearwater Fiord ᓄᓇᖓᓂ ᐱᐊᓂᒃᑕᐅᓚᐅᖅᐳᖅ ᐱᓇᓱᐊᕈᓯᕐᓂ 8-ᓂ ᐱᓕᕆᑲᑕᖓᓂᒃᑯᑦ, ᖁᓕᒥᒎᓕᖕᒥ ᐊᑯᑲᑕᒃᓗᑎᒃ 2015 ᐊᐅᔭᖓᓂᑦ Archean crystalline ᑐᙵᕕᐅᔪᑦ ᑲᓇᖕᓇᖅᐸᓯᐊᓂ ᓄᓇᙳᐊᑉ ᐃᓚᖃᖅᐳᖅ ᒪᑯᓂᖓ tonalite ᐊᒻᒪ granodiorite gneiss ᑕᒫᙵ ᐃᓚᔭᐅᕙᓪᓕᐊᓪᓗᓂ monzogranite, ᑕᒪᓐᓇᓗ ᑕᒫᓂ ᓴᕿᓐᓂᑰᓪᓗᑎᒃ K-feldspar porphyritic.

Paleoproterozoic metasedimentary ᖃᓕᓅᒃᑑᑎᑦ ᐅᔭᕋᐃᑦ ᐃᓚᖃᖅᓗᑎᒃ ᒪᑯᓂᖓ quartzite, semipelite, pelite, marble, ᐊᒻᒪ greywacke ᓴᕿᖃᑦᑕᖅᑐᑦ ᐊᓂᖓᔪᑎᑐᑦ, enclaves, screens, ᐊᒻᒪ panels ᑕᒫᓂ ᐊᒻᒪ ᕿᑎᐊᓂ ᐊᔾᔨᒌᖏᑦᑑᑎᓂ ᓄᓇᐃᑦ ᐃᓂᖏᓐᓂᑦ. Mafic-ultramafic ᑎᒥᖏᑦ ᓴᕿᔾᔮᖅᐳᑦ ᑐᖓᕕᐅᕝᑳᔅᓪᓗᑎᒃ ᒪᑯᐊ ᐃᓗᐊᓂ metasedimentary strata.

ᑕᒫᓂ ᐅᔭᕋᐅᑉ ᐃᓂᖏᑦ ᐱᑕᖃᕐᓂᖅᓴᐅᕗᑦ ᐃᒪᐃᑦᑐᓂᑦ Paleoproterozoic metaplutonic ᐊᔾᔨᒌᖏᑦᑑᑎᐅᓪᓗᑎᒃ ᐃᒪᐃᑦᑐᓂᑦ gabbro ᐃᒪᐃᑦᑐᓄᑦ syenogranite. ᐊᖅᑰᓵᖅᓯᑲᑕᖓᓂᖅ ᑐᑭᖃᖅᐳᖅ ᐊᔾᔨᒌᖏᑦᑑᑎᑦ ᐋᖅᑭᒃᐸᓪᓕᐊᓯᒪᓂᖏᓐᓂᑦ ᐊᕿᒍᑦ ᐊᔾᔨᒌᖏᑦᑐᒃᑯᑦ, ᐊᒻᒪᓗ ᑕᒪᓐᓇ ᐃᓱᒪᖕᓇᖅᐳᖅ ᐊᓯᖑᖅᐸᓪᓕᐊᓂᕐᒥᑦ ᐃᒪᐃᑦᑐᒥᑦ mafic-ᒥ ᐃᒪᐃᑑᓂᖅᓴᐅᓕᖅᓗᑎᒃ silicic compositions. ᐊᔾᔨᒌᖏᑦᑑᑎᑦ ᐅᔭᕋᐃᑦ ᐋᖅᑭᒃᐸᓪᓕᐊᓂᖏ ᓇᓗᓇᐃᔭᖅᑕᐅᓯᒪᕗᑦ ᐊᕿᒍᖏᑦᑎᒍᑦ ᐊᑖᒍᑦ, ᓴᕿᔾᔮᖅᑎᑦᑎᓪᓗᑎᒃ ᓄᐊᑕᐅᔪᕕᓂᕐᓂᑦ ᐆᒨᖓ U-Pb ᐅᑭᐅᖏᑦᑎᒍᑦ ᖃᐅᔾᔨᓇᓱᒃᓗᑎᒃ ᐱᓕᕆᕖᖕᒥ ᐊᖁᓵᕐᓂᐅᖃᑦᑕᖅᑐᓂᑦ, ᐊᒻᒪᓗ ᑲᑎᑐᐃᓐᓇᕆᐊᖃᖅᑐᓂᑦ ᐆᒨᖓ Cumberland batholith.

ᑭᖑᓕᖅᐹᕿᓕ, ᒥᑭᑦᑐᑯᓗᐃᑦ ᐊᑰᓴᕐᓂᐅᔪᑦ ᐅᕖᓇ mafic dykes ᐊᒻᒪ ᖁᓛᓃᑦᑐᑦ ᐅᔭᕋᐃ Ordovician limestone ᓄᓇᙳᐊᕐᒥ ᐋᖅᑭᒃᓱᖅᑕᐅᖕᒥᔪᑦ ᒫᓂ Sylvia Grinnell Lake–Clearwater Fiord area.

Archean crystalline basement (ᐃᓛᒃᑰᖓᔪᐃ Āt–Āmm)

ᑕᒪᓐᓇ ᓄᓇ ᐊᓯᖑᖅᐸᓪᓚᐊᓂᖓ ᓴᕿᑎᑦᑎᓯᒪᕗᖅ ᐅᔭᕋᖕᓂ ᖃᐅᔨᓴᕐᓂᕐᒥᑦ ᐅᕙᓂ Hall Peninsula ᐊᒻᒪᓗ ᑲᓇᖕᓇᖅᐸᓯᐊᓂ Sylvia Grinnell Lake–Clearwater Fiord ᓄᓇᙳᐊᓕᐅᕐᕕᖕᒥᑦ. ᐅᔭᕋᐅᔭᐃᑦ ᕿᓪᓚᑲᓚᒃᑐᑦ ᐊᔾᔨᒌᖕᒋᑦᑑᑎᓂᑦ ᒪᐅᖓ ᐅᖃᐅᔭᐅᓕᖅᑰᔨᓯᒪᔪᓂᑦ, ᓯᐅᕋᑦᑐᐊᕖᓗᖕᒥ ᐊᖏᔫᑎᐅᓂᕐᓴᓄᑦ biotite±hornblende tonalite ᒪᐅᖓ granodiorite ᐃᓚᖃᒡᒍᔪᑦ ᖁᓕᓅᒃᑑᑎᓂᑦ diorite ᒪᐅᖓ quartz diorite. ᐊᖏᓪᓗᓂ ᐱᕈᖅᐸᓪᓚᐊᓂᐊᕐᓂᖓ, ᓯᐅᕋᐃᑦ ᐊᖏᓂᕐᓴᑦ biotite±magnetite monzogranite, locally K-feldspar porphyritic, ᐊᖅᑰᓵᖅᓯᒪᓂᐅᔪᑦ ᒪᑯᓂᖓ pegmatitic syenogranite veins.

Paleoproterozoic metasedimentary (ᐃᓛᒃᑰᖓᔪᐃ ⱣLHq–ⱣPL)

Quartzite, semipelite ᐊᒻᒪ pelite, psammite (ᐃᓛᒃᑰᖓᔪᐃ ⱣLHq–ⱣLHp)

ᖁᓕᓅᓕᑦᑎᐊᖅᓯᒪᔪᑦ ᐊᒻᒪ ᖃᑯᖅᑕᐃᑦ ᐅᖁᓕᕐᓯᒪᔪᑦ ᓯᓚᒧᑦ quartzite ᓴᕿᖃᑦᑕᖅᐳᑦ ᐃᒪᐃᑦᑐᑎᑐᑦ panels ᐃᔾᔪᓂᖃᓕᖅᐸᒃᓗᑎᒡᓘᓐᓃᑦ 100 ᒦᑕᓂᑦ ᑕᒃᑯᓇᓂᑦ monzogranite (ᐊᔾᔨᖑᐊᖅ 3a, b), ᐊᒻᒪᓗ ᐃᓚᖏᒍᑦ ᖄᖓᓃᑐᖃᕆᕗᖅ ᒪᑯᓂᖓ interbedded psammite, semipelite, ᐊᒻᒪ/ᐅᕝᕙᓘᓐᓃᑦ pelite (ᐊᔾᔨᖑᐊᖅ 3b). ᒪᑯᐊ Quartzite ᖁᓕᓅᒃᑑᑎᑦ ᐃᒪᓐᓇᐃᑑᖃᑎᒋᕗᑦ ᒫᙵᑦ orthoquartzite ᒪᐅᖓ feldspathic quartzite, ᖄᖏᒍᑦ ᐃᓚᐅᒃᑲᓐᓂᖅᓯᒪᕗᑦ ᐊᒻᒪᓗ ᐃᓛᓐᓂᒃᑯᑦ ᐃᓚᖃᖅᓗᑎᒃ garnet-ᒥᑦ. Pelite horizons ᐃᓚᖃᖅᑐᐃᑦ assemblage biotite-garnet-sillimanite-K-feldspar-melt (ᐊᔾᔨᖑᐊᖅ 3c), ᐊᒻᒪᓗ ᓴᕿᒡᒍᓪᓗᑎᒃ ᖁᓕᓅᒃᑑᑎᓂᑦ ᑭᓱᖃᙱᓐᓂᖅᓴᐅᔪᓂᑦ ᐅᑯᑎᒎᓇᖅ biotite±garnet psammitic ᐅᕝᕙᓘᓐᓃᑦ biotite±garnet±sillimanite semipelitic migmatite. ᐱᒋᐊᕈᑎᐅᓯᒪᔪᑦ ᑲᑎᑉᐸᓪᓕᐅᓂᐅᔪᓂ ᐃᓚᖃᖅᓯᒪᕗᑦ 20 vol. % ᐊᖏᔫᑎᐅᓂᖅᓴᓂ ᓯᐅᕋᕐᓂᑦ leucosome, ᐃᒪᐃᑑᓂᕋᖅᑕᐅᔪᓂᑦ crystallised melt, ᐃᓚᖃᖅᓗᓂ patch to stromatic metatexite textures, ᐊᒻᒪᓗ ᒪᑯᓂᖓ ᐱᑕᖃᖏᓗᑎᒃ muscovite, ᐃᓚᖃᖅᓗᑎᒃ ᒪᑯᓂᖓ peak metamorphic conditions ᒪᑯᓂᖓ ᐊᒥᓲᓂᓴᐅᓪᓗᑎᒃ muscovite-dehydration (St-Onge et al., 2007; Dyck and St-Onge, 2014). Cordierite ᐱᑕᖃᙱᒻᒥᔪᖅ ᐅᑯᓈᙶᑦ metasedimentary assemblages ᑲᑎᓯᒪᐅᖅᑐᓂᑦ, ᐃᒪᐃᑦᑐᖃᕐᓂᖅᓴᐅᓇᓱᒋᔭᐅᓪᓗᓂ paleopressures ᐅᖓᑖᓃᑦᑐᓂᑦ 6 kbar. Gossanous horizons ᐱᑕᖃᒡᒍᕗᑦ ᒪᑯᓇᓂᑦ siliciclastic units, ᑖᒃᑯᐊᓕ ᐃᓂᒋᔭᐅᓂᖅᓴᐅᕙᒃᓗᑎᒃ ᒪᑯᓂᖓ chalcopyrite, graphite, ᐊᒻᒪ pyrite. ᑕᑯᔭᐅᔪᓐᓇᑐᐃᓐᓇᕋᓗᐊᖅᑎᓪᓗᒍ ᐊᑐᐃᓐᓇᐅᙳᑦᑐᓂ ᐃᖓᓛᓂᑦ, ᒪᑯᐊ the siliciclastic ᐃᓂᖏᑦ ᖃᐅᔨᓴᖅᑕᐅᕙᓪᓚᐊᔦᑦᑐᑦ ᐋᕿᒃᓯᒪᓂᖏᑦ ᐊᔾᔨᒋᔭᖃᖅᐳᑦ ᐅᑯᓄᖓ metasedimentary strata ᒫᓂ ᐊᒃᑐᐊᐅᕗᓂᑦ Lake Harbour Group ᐃᓂᖃᖅᕕᐅᓂᖏᑦᑎᑐᑦ (St-Onge et al., 1996, 1998; Scott et al., 1997).

Marble and calc-silicate (ᐃᓛᒃᑰᖓᔪᖅ ⱣLHc)

ᐅᔭᕋᐃᑦ ᐊᕿᑦᑐᑦ ᐊᑭᓐᓇᑎᑑᓕᖅᑲᑦᑕᖅᐳᑦ ᐃᔾᔪᖅᑎᕈᓐᓇᖅᓗᑎᒃ 100 ᒦᑕᓂ ᒪᑯᓇᓂ monzogranite, ᐊᒻᒪᓗ ᐊᖏᓂᖅᑲᖅᓯᒪᓪᓗᑎᒃ 10 ᑭᓚᒦᑕᓂᑦ ᑕᒫᓂ (ᐊᔾᔨᖑᐊᖅ 3d). ᐅᔭᕋᐃᑦ ᓯᐅᕋᐅᓂᖏᑦ ᐊᖏᓂᖅᓴᐅᔪᑦ ᐊᒻᒪ ᐊᖏᓂᖅᓴᐅᒃᑲᓐᓂᖅᓗᑎᒃ ᐊᒻᒪ ᑕᒫᓃᓗᑎᒃ ᖃᓕᓅᒃᑎᓯᒪᔪᑎᓐᓂ ᓇᓗᓇᖏᓗᓂ ᖃᓄᐃᑦᑑᕙᓪᓚᐊᓂᖏᑦ ᐅᑯᓂᖓ apatite, calcite, diopside, humite, forsterite, magnetite, phlogopite, scapolite, spodumene, titanite, ᐊᒻᒪ tremolite (ᐊᔾᔨᖑᐊᖅ 3e). ᑕᒃᑯᐊ ᐊᕿᒡᓕᔭᑦᑐᑦ ᐅᔭᕋᐃ ᐃᓱᒪᒋᔭᐅᔪᑦ ᐃᒪᐃᑦᑐᖃᕐᓂᖅᓴᐅᔭᕆᐊᒃᓴᖓᓂᑦ

tectonostratigraphically ᖁᑦᑎᖕᓂᕐᓴᒥ ᐅᕙᓂ Lake Harbour Group ᒪᑯᓇᙱᑦᑐᓂᖕᒋᓐᓂᒃ siliciclastic units ᖁᓛᑐᑦ ᓇᓗᓇᐃᖅᑕᐅᓯᒪᔪᓂᑦ.

Metagreywacke (ᐃᓛᒃᑰᖓᔪᕐᒃ ᑭᑭᒪ)

Metagreywacke ᑎᑎᕋᐅᓯᐅᓯᒪᔪᖅ ᐅᐊᖕᓇᖕᖓᓂ ᑲᓇᖕᓇᖅᐸᓯᐊᓂ ᖃᐅᔨᓴᖅᑕᐅᕕᐅᔪᒥᑦ, ᓴᖕᒍᖕᖓᔪᑎᑐᑦ ᐅᑯᐊ ᐃᓗᐊᒍᑦ biotite monzogranite (ᐊᔾᔨᖕᒍᐊᖅ 3f). ᖁᓛᑐᑦ ᑎᑎᕋᖅᑕᐅᓯᒪᔪᑎᑐᑦ, greywacke ᐱᑕᖃᙱᑦᑐᖅ ᐅᕙᓂ Lake Harbour Group ᐅᔭᕋᐃᑦ ᖃᓄᐃᑦᑑᓂᖕᒋᓐᓂᑦ, ᑭᓯᐊᓂᓕ ᐱᑕᖃᕐᓂᖅᓴᐅᓪᓗᓂ ᐅᕙᓂ Longstaff Bluff ᐋᕿᒃᓯᖅᓯᒪᓂᖕᖓᓂ ᐅᕙᓂ Piling Group ᓄᓇᙳᐊᒦᑦᑐᑦ ᐅᐊᓈᖕᖓᓂ (Wodicka et al., 2014), ᐊᓯᔾᔨᖅᐸᓪᓕᐊᓂᕆᔭᖕᖓᓂᑦ granitoid-ᒥ ᐅᔭᕋᖕᓂᑦ.

Paleoproterozoic mafic-ultramafic sills (ᐃᓛᒃᑰᖓᔪᐃ ᑭᒪHu–ᑭᒪHd)

ᐅᔭᕋᐃᑦ ᓵᑦᑑᑎᐅᔪᑦ ᒪᑯᓇᙱᑦ ᓯᐅᕋᕐᓂ ᐊᖕᒋᓂᖅᓵᕐᔪᖕᓂ ᐊᖕᒋᔫᑎᓅᖕᖓᔪᓄᑦ ᐃᒪᐃᓕᖅᑲᑦᑕᖅᐳᑦ, mafic-ᒥᑦ ᐅᕗᖕᖓ ultramafic rocks ᐅᔭᕋᖕᓄᑦ ᐅᕙᓂ ᕗᐹᐱᓯ ᐃᓂᒋᔭᖕᖓᓂᑦ (Liikane et al., 2015) ᑕᐃᒪᐃᐸᒃᑯᑎᒡᓗ ᒪᐅᓇᓕᒫᖅ siliciclastic strata ᕿᑭᖅᑖᑑᐸ ᓂᒋᐊᓂ ᕿᑎᐸᓗᐊᓂᑦ. ᐃᒻᒥᒃᑰᖓᔪᑦ ᐃᔾᔪᓂᖅᑲᑦᑕᖅᐳᑦ 10-20 ᒦᑕᓴᓂᑦ, ᐃᓚᖕᒋᓪᓕ ᐊᖕᒋᒡᓕᔪᓐᓇᖅᑯᑎᒃ 100 ᒦᑕᓴᓂ ᐃᔾᔪᓂᖅᑲᓕᕐᑯᑎᒃ, ᐊᒻᒪᓗ ᖁᒻᒧ ᑭᓛᒥᑕᓴᖓᓕᖕᓂ ᖁᑦᑎᒃᓯᓯᒪᔪᓐᓇᖅᑯᑎᒃ. ᒪᑯᐊ mafic ᐊᒻᒪ ultramafic rocks ᐃᐱᒃᑑᑎᐅᕗᑦ ᓴᕿᔾᔭᖅᑲᑎᖅᑲᖅᑯᑎᒃ ᐅᑯᓂᖕᖓ their host metasedimentary units, ᐊᒻᒪᓗ ᐃᓯᒪᖕᓇᖅᑯᑎᒃ ᑐᙱᕕᐅᔭᕆᐊᒃᓴᖕᒋᓐᓂᑦ. ᐊᖕᒋᓂᕐᓴᐃᑦ ᐅᔭᕋᐃᑦ ᖁᓕᕇᒃᑐᑕᐅᕗᑦ, ᐊᔾᔨᒌᖕᒋᑦᑑᑎᐅᓪᓗᑎ ᐃᒪᓐᓇ ᑲᑎᓯᒪᐅᖅᑐᓂᑦ clinopyroxene-orthopyroxene±hornblende metapyroxenite ᑐᙱᕕᖕᖓᓂᑦ (ᐊᔾᔨᖕᒍᐊᖅ 4a), ᑮᖕᒍᓂᐊᒍᑦ ᐃᒪᓕᖕᖓᓪᓗᑎᒃ olivine-clinopyroxene-orthopyroxene metaperidotite ᐊᒻᒪ metagabbro ᒪᐅᖓ metaleucogabbro up section (ᐊᔾᔨᖕᒍᐊᖅ 4b). ᐃᓕᑭᕙᕗᑦ, ᓖᑲᓂ, ᐱᓕᕆᓕᒪᓂᖅᓴᖅ ᐃᓕᓐᓂᐊᖅᑎᐅᔪᖅ ᖃᐅᔨᓴᖅᑎᓂᑦ ᐃᑲᔪᖅᑎ ᐱᓕᕆᐊᖅᑲᖅᐳᖅ ᐆᒥᖓ MSc thesis ᑎᑎᕋᐅᓯᖅᑲᖅᓂᐊᖅᓗᓂ ᒪᑯᓂᖓ petrology, geochemistry, ᐊᒻᒪ geochronology ᒪᑯᓂᖓ ᖁᓕᕇᒃᑎᓯᒪᔪᓂᑦ ᐅᔭᕋᖕᓂᑦ ᑯᐸᐃᒃ ᑕᕋᖕᖓᓂᑦ ᐊᒃᑐᐊᓂᖅᑲᖅᑯᑎᒃ ᐅᑯᓂᖓ Raglan Ni-Cu deposit (ᐊᔾᔨᖕᒍᐊᖅ 2). ᐅᖃᐅᓯᖅᑲᒃᑲᓐᓂᖅᓯᒪᔪᑦ ᐆᒥᖓ mafic-ultramafic ᐅᔭᕋᖕᓂ ᐅᕙᓃᑉᐳᑦ Liikane et al. (2015).

Paleoproterozoic metaplutonic suite (ᐃᓛᒃᑰᖓᔪᐃ ᑭg–ᑭsb)

Gabbro (ᐃᓛᒃᑰᖓᔪᖅ ᑭg)

ᖃᔅᓯᒐᓴᐃᑦ ᓯᐅᕋᐅᖁᔾᔪᑦ ᐃᒪᐃᑦᑐᓂ pegmatitic, kilometre-scale, layered biotite-clinopyroxene-magnetite±hornblende gabbro plutons ᐱᑕᖃᖅᐳᑦ ᐱᖓᖕᓇᖅᐸᓯᐊᓂ Sylvia Grinnell Lake–Clearwater Fiord ᐃᓂᒋᔭᖕᖓᑕ. ᐃᓚᖕᒋᑦᑎᒍᑦ, ᑕᒪᒃᑯᐊ plutons ᐃᒪᖅᑯᑦ ᒪᑯᓂᖓ clinopyroxene-bearing anorthosite.

Quartz diorite (ᐃᓛᒃᑰᖓᔪᖅ ᑭd)

Quartz diorite ᓴᖅᑭᖅᑲᑦᑕᖅᑐᑦ ᒪᓂᕋᑦᑐᑎᑦ, ᕿᓐᓂᖅᑐᑎᑦ, ᐊᖕᒋᔫᒪᕇᑦ ᑕᑯᓵᐅᖕᒋᑎᑕᐅᔪᑦ ᐃᓛᒃᑰᖓᔪᒥᑦ ᐃᓗᓕᖅᑲᖅᑐᖅ ᑲᑎᓐᖓᔪᓂᑦ biotite-clinopyroxene-orthopyroxene±hornblende. ᑕᑯᓵᐅᔪᑦ ᑕᑯᓵᐅᑎᐊᕐᓇᑎ ᐅᔭᖅᑲᓂᑦ plutons iᐱᖕᖓᓐᓇᖕᖓᓂ ᐃᓚᖕᖓᓂᑦ ᖃᐅᔨᓴᕐᕕᐅᔪᒥᑦ, ᐊᒻᒪᓗ ᐊᔾᔨᖕᒋᑕᖕᒋᑦ ᓴᓂᐊᓃᑦᑐᓂᑦ ᐃᓗᐊᓂ ᐃᓛᒃᑰᖓᔪᓕᒫᓂᑦ ᑲᓇᓐᓇᒧᑦ (ᐊᔾᔨᓐᖕᒍᐊᖅ 5a).

ᓄᓇᖑᐊᖅ–ᐊᖏᓂᖓ ᓴᓇᓯᒪᓂᖓ ᓇᓗᓇᐃᖅᓯᔪᖅ ᐃᓛᒃᑰᖓᔪᖅ ᓴᖅᑭᖃᑦᑕᖅᑐᑦ ᖃᓂᒋᔭᖏᓐᓂ ᖁᓕᕇᑦᑐᓂᑦ ᐅᔾᖃᓂᑦ ᑐᓐᖓᕕᖓ metaplutonic.

Biotite granodiorite (ᐃᓛᒃᑰᖓᔪᖅ Ᵽgo)

ᐊᖏᔫᖏᑦᑐᖅ, ᐊᖏᒨᐋᓚᔪᑦᑐᖅ, biotite±hornblende±magnetite granodiorite ᑎᑎᕋᖅᑕᐅᓯᒪᔪᑦ ᐅᐊᓐᓇᖓ ᐱᖓᓐᓇᖓᓂ ᖃᐅᓵᓴᕝᕕᐅᔪᒥᑦ. ᕿᓐᓂᕋᔪᑦᑐᑦ ᐊᒻᒪᕿᑎᐊᓃᑦᑐᓂ ᒫᓐᓂᖓ.

K-feldspar megacrystic biotite monzogranite (ᐃᓛᒃᑰᖓᔪᐃ Ᵽmo, Ᵽms, Ᵽmh)

ᐊᐅᐸᔾᖓᔪᖅ ᐊᐅᐸᕈᔪᑦᑐᒧᑦ ᓯᓇᖓᓄᒃ, ᕿᑎᐊᓂ ᑎᑭᑦᑐᒍ ᒫᓐᓂᖓ, ᐊᖏᔪᕐᔪᐊᒥᑦ ᔮᑦᑑᑕᓄᑦ biotite±orthopyroxene±magnetite±garnet monzogranite ᓇᓗᓇᕋᑎ K-feldspar megacrysts ᓴᖅᑭᖃᑦᑕᖅᑐᑦ ᐊᖏᔪᒥᑦ ᐃᓚᖏᓐᓂᑦ ᓂᒋᐊᓂ ᕿᑎᐊᓂᓗ ᕿᑭᖅᑖᓗᒃ. K-feldspar phenocrysts ᐃᔨᑎᑐᑦ ᐊᖏᓂᖃᖅᑐᑦ ᑎᑭᓯᒪᔪᑦ 10 cm ᓴᓂᒧᑦ, ᓄᓇᓕᒻᒥ ᑕᑯᔅᓴᐅᑎᑕᐅᔪᑦ rapakivi ᖃᓄᐃᑦᑑᓂᖏᑦ (ovoid alkali feldspar ᑕᕐᓇᑕᐅᓯᒪᔪᑦ plagioclase feldspar; ᐊᔾᔨᖑᐊᖅ 5b). ᐃᓛᒃᑰᖓᔪᖅ ᐃᖅᑲᓇᐃᔾᔪᒃᑲᓂᖅᑐᖅ ᑭᓚᒦᑕᑎᑐᑦ ᐊᖏᓂᖃᖅᑐᓂ ᐅᐊᓐᓇᒨᖓᔪ ᐊᕕᑦᑐᖅᓯᒪᔪᖅᐅᐊᓐᓇᖅᐸᓯᖓᓂᑦ ᐃᓚᖓᓂᑦ ᖃᐅᔨᓴᕝᕕᐅᔪᒥᑦ, ᐃᓚᒋᓪᓗᓂᐅᒃ σ-porphyroclasts ᐅᑯᓇᓂ ᓇᓗᓇᐃᔭᐃᔪᖅ ᖁᓛᓂ ᓂᒋᐊᓂ.

Biotite monzogranite (ᐃᓛᒃᑰᖓᔪᖅ Ᵽmb)

ᐅᖃᐅᔭᖃᐅᖅᑐᐃᑦ biotite±orthopyroxene±magnetite±hornblende±garnet monzogranite ᓄᓇᐅᑉ ᐊᑖᓃᑦᑑᑎᐅᕗᑦ ᕿᑭᖅᑖᓘᑉ ᓂᒋᐊᑕ ᕿᑎᐊᓂᑦ. ᐃᓂᖓᓪᓕ ᓯᐅᕋᖃᕐᓂᖅᓴᖅ ᐊᖏᔩᑎᐅᓂᔅᓴᓂᑦ, ᖃᑯᕈᔫᒡᒍᑎᒃ ᐊᐅᐸᔪᕈᔫᒡᒍᑎᒡᒍ ᓯᓚᒧᑦ. ᑕᒪᒃᑯᐊ ᐃᓂᖏᔭᐅᕙᒃᑐᑦ ᐊᔾᔨᕿᑲᑦᑕᖏᑦᑐᑦ ᒫᙵᑦ magnetite-rich ᐊᒻᒪ magnetite-free ᐃᓂᒋᔭᐅᔪᓂᑦ, ᐊᒻᒪ ᐃᓚᖃᖅᑐᑎᒃ ᒪᑯᓂᖓ hornblende ᐅᐊᖕᓇᖓᑕ ᐱᖓᖕᓇᖅᐸᓯᐊᓂ ᑕᒫᓂ ᖃᐅᔨᓴᕝᕕᐅᔪᒥᑦ. ᐃᓚᖏᓐᓂᑦ, ᐱᕈᖅᑐᐃᑦ ᑕᑯᔭᐅᓯᒪᕗᑦ ᐃᒪᓐᓇ axial planar-ᒥᑦ ᐊᑕᐅᓯᕐᒨᖅᐸᓪᓕᐊᔪᓂᑦ ᐃᓂᖏᓐᓂᑦ (ᐊᔾᔨᖑᐊᖅ 5c), ᓇᓗᓇᕈᓐᓃᖅᓯᒪᓪᓗᓂ ᐊᒥᓱᒪᓇᐅᓂᖏᓐᓂᑦ ᒥᒃᓵᒋᐊᕐᓂᐅᔪᑦ ᑕᒫᓂ.

Garnet-biotite monzogranite (ᐃᓛᒃᑰᖓᔪᖅ Ᵽmg)

ᖃᑯᖅᓯᓯᒪᓕᖅᑐᑦ ᓯᓚᒧᑦ, ᐊᖏᔫᒪᓅᑦ ᐱᕈᕕᐅᔪᓐᓇᖅᑐᑦ, ᓯᐅᕋᑦᑎᐊᕚᖑᒥ ᐊᖏᓂᕝᓴᕐᔪᖕᓄᑦ ᐅᔭᕋᐃᑦ garnet-biotite±magnetite monzogranite ᓴᕿᖃᑦᑕᖅᓯᒪᕗᑦ ᖃᐅᔨᓴᕝᕕᐅᔫᑉ ᑲᓇᖕᓇᖅᐸᓯᐊᓂᑦ. ᑕᒪᓇ ᐃᓂᖃᕝᕕᐅᔪᖅ ᓴᕿᔮᖅᐳᖅ ᐃᓗᑐᓂᖅᑎᑐᑦ ᐊᒻᒪ ᑐᖓᕕᒃᑎᑐᑦ ᒫᓂ K-feldspar megacrystic monzogranite (ᐊᔾᔨᖑᐊᖅ 3d), ᐋᕿᒍᑎᐅᓪᓗᓂ ᒪᑯᓂᖓ plutons-ᓂ ᐃᓚᓕᐅᑎᔭᑦᑐᓂᑦ ᒪᑯᓂᖓ biotite monzogranite. Garnet ᐱᑕᖃᖅᑐᐃᑦ ᐃᒪᓐᓇᐅᓕᖓᓪᓗᑎᒃ 2–30 mm burgundy coloured phenocrysts, ᑕᒪᒃᑯᐊᓗ ᐱᖃᑎᖃᒃᒍᓐᓪᓗᑎᒃ ᒪᑯᓂᖓ (ᐃᓗᐊᓃᓐᓂᕐᓴᖅ, ᐊᔾᔨᖑᐊᖅ 5d).

Garnet-sillimanite leucogranite (ᐃᓛᒃᑰᖓᔪᖅ ᏢLHw)

Garnet-sillimanite leucogranite ᓴᖅᑭᖃᑦᑕᖅᐸᑦ ᐃᒪᓐᓇ ᐃᓗᑐᔪᓂ ᐊᐳᖃᑎᖃᖅᐸᒃᓗᑎᒃ ᒪᑯᓂᖓ garnet-biotite monzogranite ᐅᕙᓘᓐᓃᑦ ᓄᓇᙳᐊᑦ ᓇᓗᓇᐃᒃᑎᖏᑦᑎᒍᑦ plutons ᐊᒃᑐᐃᓂᖃᖅᓯᒪᔪᑦ ᒪᑯᓂᖓ garnet-biotite monzogranite ᑲᓇᖕᓇᖅᐸᓯᐊᓂᑦ ᖃᐅᔨᓴᖅᑕᐅᔫᑉ. ᐃᓂᒋᔭᐅᕚᒃᑐᖅ ᓯᐅᕋᑦᑎᐊᕚᐅᓂᖅᓴᐅᖃᑦᑕᖅᐸᑦ, ᐃᓚᖃᖅᑐᑎᒃ 1–5 mm ᐆᔭᐅᔭᕈᔪᖏᒥ

ᑕᖅᓴᖅᑲᖅᑐᓂᑦ garnet phenocrysts ᐊᒻᒪ ᒪᑯᐊ sillimanite (ᐊᔾᔨᖑᐊᖅ 5e). ᐱᑕᖅᑲᖅᓂᐅᔪᖅ ᒪᑯᓂᖓ sillimanite ᐃᓱᒪᖕᓇᖅᐳᖅ ᒪᑯᐊ leucogranite ᓴᕿᓐᓂᑰᔭᕆᐊᒃᓴᖏᓐᓂᑦ ᒪᑯᓇᙵᑦ muscovite-dehydration ᐊᐅᒃᐸᓪᓕᐊᕙᓪᓕᐊᓂᖏᓐᓄᑦ ᒪᑯᓂᖓ metasedimentary units ᑎᑎᕋᖅᑕᐅᓯᒪᓂᖏᑦᑎᒍᑦ ᐊᓱᐊᒍᑦ ᕿᑭᖅᑖᕐᓗᑉ ᓂᕿᐊᓅᖓᔪᓂᑦ (ᓱᒃᑯ, Dyck and St-Onge, 2014), ᐃᒪᓐᓇᐅᙱᖔᖅᑐᖅ ᐃᓚᕿᑎᑕᐅᔭᕆᐊᒃᓴᖓᓂᑦ ᒪᑐᒧᖓ plutonic suite.

Biotite syenogranite (ᐃᓛᒃᑰᖓᔪᖅ Psb)

ᓯᐅᕋᐃᑦ ᐊᖏᔫᑎᐅᓂᖒᖅᔪᑦ ᐃᒪᐃᑦᑐᙳᖅᑐᑦ pegmatitic, ᐊᐅᐸᔪᖑᖅᓯᒪᓪᓗᑎᒃ ᓯᓚᒧᑦ biotite syenogranite ᐃᒪᐃᑦᑐᖑᖅᑎᑦᑎᓯᒪᕗᑦ anastomosing dykes ᐃᓚᖏᓐᓂᑦ ᐃᓂᕿᔭᐅᔪᓂᑦ (ᐊᔾᔨᖑᐊᖅ 5f). ᐃᓚᖏᓐᓂᑦ ᐃᓂᕿᔭᐅᔪᓂᑦ ᒪᑯᐊ syenogranite ᐱᕈᖅᕕᐅᓯᒪᔪᑦ, ᑭᓯᐊᓂᓕ ᐃᓂᕿᔭᐅᔪᑦ ᐃᓕᖅᑯᓯᖏᓐᓃᑦᑐᓐᓃᖅᑲᑦᑕᖅᑐᑦ ᐊᒻᒪ ᐊᐳᖅᕕᖅᑲᓕᖅᓗᑎᒃ ᐱᕈᖅᑐᓂᑦ (ᐊᔾᔨᖑᐊᖅ 5a). ᖃᑯᑎᒃᑯᓪᓕ ᑕᒪᒃᑯᐊ ᐃᓗᑐᓂᐅᔪᑦ ᐱᑕᖅᑲᖅᑲᑦᑕᖅᐳᑦ ᒪᑯᓂᖓ phenocrysts of garnet ᐊᒻᒪ tourmaline.

ᐊᓯᖏᑦ ᐃᓛᒃᑰᖓᔪᓂᑦ

Basaltic dykes (ᐃᓛᒃᑰᖓᔪᐃ Mcd, Nd)

ᒪᕿᒃ ᐃᓂᕿᔭᐅᔫ ᒥᑭᑦᑐᓂᑦ 1–20 m ᓯᓕᖕᓂᖅᑲᖅᑐᓂᑦ ᐅᕕᖓᓪᓗᑎᒃ ᓯᐅᕋᑦᑎᐊᕙᐅᕗᑦ ᐊᖏᓂᖅᓴᐅᓪᓗᑎᒃ ᐃᓚᖏᑦ basaltic dykes containing 1–2 mm plagioclase phenocrysts ᐱᑕᖅᑲᕆᕗᑦ ᕿᑭᖅᑖᕐᓗᑉ ᓂᕿᐊᑕ ᕿᑎᖅᐸᓯᐊᓂᑦ (ᐊᔾᔨᖑᐊᖅ 4c). ᑕᒪᒃᑯᐊ ᐃᓗᑐᔫᑏᑦ ᓂᐱᓐᓇᖅᑐᖅᑲᖅᐳᑦ ᐊᒻᒪᓗ ᑕᐃᒪᐃᓯᒪᓪᓗᑎᒃ ᒫᓂ 110–120° (Tschirhart et al., 2015), ᐅᕝᕙᓘᓐᓃ ᒫᓂᐸᓗᒃ ᐅᐊᖕᓇᖓᓂᑦ ᐅᐊᖕᓇᖓᑕ ᑲᓇᖕᓇᖅᐸᓯᐊᓂᑦ. ᓯᕗᓪᓕᐅᔪᑦ ᒫᓃᓐᓂᖅᓴᐅᕗᑦ Neoproterozoic (ca. 720 Ma) Franklin dyke suite (Heaman et al., 1992), ᑕᒪᒃᑯᐊᓕ ᐊᐃᑉᐸᖏᑦ ᑲᑎᓯᒪᐅᖅᓯᒪᕗᑦ ᐱᐅᓗᐊᙱᑦᑐᓂᑦ Mesoproterozoic–Cenozoic Kekertaluk swarm of Buchan and Ernst (2013).

Limestone (ᐃᓛᒃᑰᖓᔪᖅ OA)

ᐃᒃᑲᑦᑐᒦᑦᑐᑦ (<10°) limestone (Blackadar, 1967) ᒫᓐᓃᑦᑐᑦ ᕿᑎᐊᓂᑦ Ordovician Amadjuak Formation ᐱᑕᖅᑲᓕᖅᑲᑦᑕᖅᐳᑦ ᓄᓇ ᐊᐅᓚᔾᔭᒃᐸᓪᓕᐊᓂᖓᓂᑦ ᒫᓂ ᓂᕿᖅᐸᓯᐊᓂᑦ ᐱᖓᖕᓇᖓᓂᑦ ᐃᓚᖓᓂ ᐆᒪ Sylvia Grinnell Lake–Clearwater Fiord area (ᐊᔾᔨᖑᐊᖅ 2). ᐃᓚᖏᓐᓂᑦ ᓄᓇᓂ, ᒪᑯᐊ limestone ᓴᓂᓕᖅᑲᖅᑲᑦᑕᖅᐳᑦ ᒪᑯᓂᖓ plutonic suite ᐃᒪᓐᓇ ᐅᐊᖕᓇᕿ ᐱᖓᖕᓇᖅᐸᓯᖕᒥ ᖃᓄᐃᓕᐅᕈᓗᔭᓕᕚᖓᑕ, ᑕᐃᒪᐃᓐᓂᖅᓴᐅᓂᑰᓪᓗᑎ Paleocene rifting ᐊᑐᖅᑎᓪᓗᒍ ᒫᓂ Davis Strait (Clarke et al., 1989). ᒪᑯᐊ limestone ᒪᑯᓂᖓ ᐱᕆᐊᕈᑎᖅᑲᖅᑲᑦᑕᖅᑐᑦ medium grey lime ᒪᕋᕿ, ᐊᒻᒪᓗ ᓂᖅᔪᑎᑦᕕᓂᕐᓄᑦ ᐃᓂᖅᑲᖅᕕᐅᓂᑰᓂᖏᓐᓂ ᓇᓗᓇᙱᕐᓗᑎᒃ, ᐊᔾᔨᖏᑦᑑᑎᓂ ᐃᓚᐅᖁᓯᒪᓂᖏᓐᓂᑦ ᐃᓚᖅᑲᖅᑐᓂᑦ ᒪᑯᓂᖓ maclurites, gastropods, cephalopods, brachiopods, coral fragments, ᐊᒻᒪ crinoid stems (ᐊᔾᔨᖑᐊᖅ 4d).

EQUILIBRIUM PHASE DIAGRAMS

Phase equilibria modelling ᖃᐅᔨᔾᔪᑎᐅᓇᔭᖅᑐᓂ ᒪᑯᓂᖓ monzogranite ᕿᑭᖅᑑᕐᓗᑉ ᓂᕿᐊᓂᑦ ᐱᓕᕆᐊᖑᓚᐅᖅᓯᒪᕗᑦ ᖃᐅᔨᓴᕋᐅᒃᑯᑎᒃ ᖃᓄᐃᖅᑲᑦᑕᕆᐊᒃᓴᖏᓐᓂᑦ ᐃᖏᕋᕙᓪᓕᐊᔪᑦ ᓄᓇᐃᑦ, ᐆᓇᖅᓂᖏᓪᓗ ᐊᒻᒪ ᖃᓄᐃᓕᖓᓂᖏᑦ. (P, T, and X) ᒫᓂ metamorphic mineral assemblage in felsic granitoid units (Weller et al., 2015). ᑕᒪᒃᑯᐊ ᖃᓄᐃᑦᑑᓂᖏᑦᑎᒍᑦ ᐊᔾᔨᒌᒍᑎᖏ ᖃᐅᔨᓴᖅᑕᐅᓯᒪᔪᑦ ᒫᓂ P-T space, ᕿᑎᐊᓃᓯᒪᓪᓗᓂ ᑎᑎᕋᐅᓯᐅᓯᒪᔪᑦ ᑕᒫᓂ metamorphic conditions of 6–8 kbar ᐊᒻᒪ 700–800°C (St-Onge et al., 2007), ᐃᓱᒪᒋᔭᖃᖅᖢᑎᒃ ᐅᖓᓯᒌᒃᑑᑎᐅᓂᖏᓐᓂᑦ ᑎᑎᕋᖅᑕᐅᓯᒪᔪ ᒪᑯᓄᖓ metagranitoid units, ᐃᒪᓐᓇᐅᖏᖔᖅᑐᖅ ᐋᕿᒋᐊᖅᓯᒃᑲᓐᓂᖏᖢᑎᒃ P-T ᐃᓱᒪᒋᔭᐅᓯᒪᔪᑦ. ᑕᒪᐃᓐᓂ P-T ᐊᒻᒪ T-X phase-ᒧᑦ ᑎᑎᕋᐅᔭᖅᓯᒪᔪᑦ ᐋᕿᒃᓱᖅᑕᐅᓯᒪᓂᑯᑦ ᐃᒪᐃᑦᑐᒥ ᐊᑐᖅᖢᑎᒃ THERMOCALC v3.40 ᐊᒻᒪᓗ ᓄᐊᑕᐅᕙᓪᓕᐊᖏᓐᓇᖅᑐᓄᑦ dataset tc-ds55 (Holland and Powell, 1998; ᐋᕿᒋᐊᖅᑕᐅᓂᑯᑦ ᐋᒐᓯ 2004-ᒧᑦ). ᓇᓗᓇᐃᒃᑯᑎᖃᕈᑎᖃᓚᐅᖅᑐᑦ 11-ᐅᔪᓂ ᐱᓕᕆᐊᖑᔪᓂᑦ $MnO-Na_2O-CaO-K_2O-FeO-MgO-Al_2O_3-SiO_2-H_2O-TiO_2-Fe_2O_3$ ᐊᑐᖅᓯᒪᓪᓗᑎᒃ ᐆᓇᒻᒪᕆᒃᑐᓂ ᐊᑐᕐᓂᒃᑯᑦ, ᐃᓱᒪᒋᔭᐅᓯᒪᓂᑯ ᐅᕙᓂ Weller et al. (2016). ᖃᓄᑎᒋ ᓴᖏᓂᖃᓇᐊᒃᓴᖏᓐᓂᑦ ᐋᕿᒃᓱᖅᓯᒪᐅᖅᑐᐃᑦ ᐃᒪᓐᓇᐅᓪᓗᐊᖅᐸᑦ ±1 kbar at the 2σ level (Powell and Holland, 2008; Palin et al., 2015). ᐊᖏᔪᑦ ᐅᔭᕋᐃᑦ ᖃᐅᔨᓴᖅᑕᐅᓚᐅᖅᑐᑦ ᓄᑖᖑᕆᐊᖅᑎᑦᑎᓪᓗᑎᒃ ᐅᔭᕋᖕᒥ ᐊᔾᔨᓕᐅᕆᔭᓐᓇᖅᑐᒧᑦ ᓄᐊᑕᐅᓯᒪᔪᓂᑦ ᐆᒪ ᓴᕿᓐᓂᑯᖏᑦ Thériault et al. (2001) ᐅᔭᕋᐅᔭᕐᓂ ᓄᐊᑕᕕᓂᖏᓐᓂᑦ ᕿᑭᖅᑖᓘᑉ ᓂᒋᐊᓂᑦ (95-D078B), ᒪᓕᓚᐅᖅᑎᓪᓗᒋ ᖃᓄᐃᓕᐅᕈᓯᐅᓂᑯᒥᑦ ᐆᒪ Weller et al. (2013).

A P-T ᑎᑎᕋᐅᔭᖅᓯᒪᔪᖅ ᐋᕿᒃᑕᐅᓂᑯ ᓴᕿᔮᖅᑎᑦᑎᔾᔪᑎᐅᓇᓱᒃᖢᓂ ᒪᑯᓂᖓ monzogranite sample (sample 95-D078B from Thériault et al., 2001; Figure 6a) ᓴᕿᑎᑦᑎᓯᒪᕗᖅ ᖃᔅᓯᐊᕐᔪᑯᓗᖕᓂ ᖃᓄᐃᓕᒍᑎᐅᔪᓂᑦ ᒪᑯᓇᙵ high variance assemblages ᐊᖏᕈᓘᔭᖅᑐᒥᑦ ᓄᓇᒥ P-T space, ᐃᒪᓐᓇ ᐅᔭᕋᐅᓂᖏᓐᓂᑦ metagranitoid rocks, ᒪᑯᐊᑐᐊᖅ magnetite (ᑐᖑᔪᖅᑐᑦ ᑐᑭᓕᐊᕆᓯᒪᔪᑦ) ᐊᒻᒪᓗ orthopyroxene (ᐆᔭᐅᔭᖅ ᑐᑭᓕᐊᕆᓯᒪᔪᑦ) ᐋᕿᒃᑕᐅᓯᒪᕗ ᑕᐃᒪᓐᓇ ᐊᔪᕐᓇᕐᓂᖅᓴᐅᓂᖓᓂᑦ ᐃᒪᓐᓇ ᐊᑐᖔᕐᓂᕐᒥᑦ sub-solidus conditions. ᑎᑎᕋᖅᑕᐅᓯᒪᔪᒃᑯᑦ, ᑕᒪᐃᓐᓂ orthopyroxene ᐊᒻᒪ magnetite ᐱᑕᖃᑦᑎᐊᕐᓂᖏ ᐃᓱᖃᖅᓯᒪᕗᑦ ᒫᓂ P-T range ᐊᑑᑎᖃᕐᓂᖅᓴᓂᑦ ᕿᑭᖅᑖᓘᑉ ᓂᒋᐊᓂᑦ ᕿᑎᖅᐸᓯᐊᓂᑦ (ᖃᑯᖅᑕᑦ ᑐᓯᓕᐅᕆᓯᒪᔪᑦ ᓇᐃᓈᕐᓯᒪᓪᓗᑎᒃ), ᐃᓚᖃᖅᖢᑎᒃ ᖃᐅᔨᓴᕈᑎᕕᓂᕐᓂᑦ ᐱᓯᑲᑕᖕᓂᒃᑯ ᐱᓕᕆᐊᖑᔪᓐᓃᖅᓯᒪᔪᕕᓂᕐᓂᑦ ᑕᒪᐃᑎᒍᑦ ᐱᓕᕆᐊᓂ ᑕᒫᓂ.

ᖃᐅᔨᓴᕐᓂᐊᕐᓗᓂ ᐊᒃᑐᐃᒍᑎᐅᔪᓂ ᐃᒪᐅ (H_2O) ᑕᒫᓃᑦᑐᒥᑦ, T-MH_2O ᑎᑎᕋᐅᔭᖅᓯᒪᔪᑦ ᕿᑎᐊᓃᖢᓂ ᓴᖏᓂᖓᓂᑦ (7 kbar), with MH_2O varying from 0 to 1 mol. % (ᐊᔾᔨᖑᐊᖅ 6b). ᐅᓇ ᑎᑎᕋᐅᔭᖅᓯᒪᔪᖅ ᓴᕿᑎᑦᑎᓯᒪᕗᖅ ᐊᖏᓪᓕᕙᓪᓕᐊᑎᓪᓗᒍ ᐃᒪᖃᕐᓂᖓ H_2O content, ᐆᓇᕐᓂᖓ ᐅᑯᐊ orthopyroxene-in (ᐆᔭᐅᔭᖅ ᑐᑭᓕᐊᖅᓯᒪᔪᖅ) ᓱᒃᑲᔪᒥᑦ ᐆᓇᖅᓯᕙᓪᓕᐊᖃᑦᑕᖅᐸᖅ ᒫᙵᐸᓗᒃ 640°C -ᒥᑦ ᒪᐅᖓ 810°C-ᒧᑦ, ᐊᒻᒪᓗ ᑎᓯᓂᕆᔭᖓ ᐅᓇᕈᓐᓃᖅᐹᓪᓕᖃᑦᑕᖅᐸᖅ ᒫᙵ 810°C-ᒥᑦ ᒪᐅᖓ 640°C-ᒧᑦ. ᐆᓇᕐᓂᕆᓂᖅᓴᐅᖃᑦᑕᖅᑕᖓ ᐃᓱᒪᒋᓪᓗᒍ 600–800°C, ᐱᑕᖃᕐᓂᐅᔪᖅ ᐅᑯᓂᖓ orthopyroxene ᐊᒻᒪ ᐱᑕᖃᙱᓐᓂᐅᔪᖅ ᐊᐅᒃᐸᓪᓕᐊᓂᑯᓂ ᑕᒫᓂ metagranitoid rocks ᓴᕿᑎᑦᑎᓯᒪᕗᖅ ᐱᑕᖃᑐᐃᓐᓇᕆᐊᖃᕐᓂᖓᓂ ᐊᖏᔪᒥᑦ (anhydrous bulk composition (0.1 mol. % H_2O; orange line, Figure 6b) ᓈᒻᒪᒃᓂᖅᓴᐅᓇᔭᖅᐸᖅ. ᑕᐃᒪᐃᔾᔪᑎᒋᔭᖓᓕ ᐱᑕᖃᖅᓯᒪᓂᖓᓂᑦ ᐃᒪᐃᑦᑐᓂᑦ rapakivi textures ᑕᒫᓂ ᖃᐅᔨᓴᖅᑕᐅᔪᒥᑦ (ᐊᔾᔨᖑᐊᖅ 5b), ᑕᒪᓐᓇᓗ ᐃᓱᒪᒋᔭᐅᓚᐅᖅᑐᖅ ᐱᑕᖃᕆᐊᖃᕐᓂᖓᓂᑦ ᒪᑯᓂᖓ H_2O-undersatured conditions ᓴᕿᑉᐸᓪᓕᐊᓗᑎᒃ (Nekvasil, 1991). ᑭᓯᐊᓂᓕ, ᑎᑎᕋᐅᔭᖅᓯᒪᔪᖅ ᓴᕿᑎᑦᑎᓯᒪᒋᕗᖅ ᒪᑯᓄᖓᓕ moderately anhydrous bulk ᐅᔭᕋᒐᓚᖕᓄᑦ (<0.2 mol. % H_2O), ᒪᑯᐊ silicate ᐊᐅᖕᓂᑯᕕᓃᑦ ᑎᓯᓕᕈᓐᓇᕋᔭᙱᒻᒪ ᒫᓂ <800°C, ᑕᒪᐃᓐᓂ

orthopyroxene ᐊᒻᒪ magnetite (ᑐᖑᔪᖅᑐᖅ ᑐᑭᓕᐊᖅᓯᒪᔪᖅ) ᐊᒃᑐᖅᑕᐅᑲᐅᖅᑐᔾᑐᑦ ᐃᒪᐃᑦᑐᓘᑦ MH_2O. ᑕᐃᒪᐃᓐᓂᖓᓄᑦ, ᐊᒻᒪᑦᑕᐅᖅ ᐊᒃᑐᐃᓂᐊᕐᓗᓂ ᐊᕙᒃᑐᖅᓯᒪᓂᒃᑯᑦ ᒪᑯᐊ P-T ᐊᔾᔨᒌᖕᖏᓐᓂᐅᔪᑦ ᐅᖃᐅᓯᐅᓯᒪᔪᑦ ᖁᕐᒍᑦ, ᐃᒪᐅᑉ ᐊᓯᖑᑳᓪᓚᖕᓂᖓ ᒫᓂ typical granitoid composition ᐊᑕᐅᑦᑎᒃᑯᑦᑕᐃᓐᓇ P-T ᖃᓄᐃᑦᑑᓂᖓᒍᑦ ᐊᒻᒪ ᐊᒃᑐᐃᒍᑎᐅᓯᒪᙵᖅ ᑕᒪᐃᓐᓄᑦ ᐱᓕᕆᐊᖑᓂᑯᓄᑦ.

ᑕᒪᒃᑯᐊ ᐃᓱᒪᒋᓂᐊᕐᓗᒋᑦ ᐊᒃᑐᐃᓂᑰᒍᑎᐅᕚᒃᑐᑦ ᐆᓘᖓ XFe^{3+} ᑲᑎᖕᖓᐅᖅᑐᓂᑦ, ᐃᒪᐃᑦᑐᒥ T-XFe^{3+} ᑎᑎᕋᐅᔭᖅᓯᒪᔪᒥᑦ ᓴᓇᓚᐅᖅᐳᑦ ᑕᒪᐅᓇᑦᑕᐃᓐᓇᖅ ᓴᖏᓂᖅᑲᖅᑎᑕᐅᓪᓗᓂ (7 kbar), with XFe^{3+} varying from 0.0 to 0.5 (ᐊᔾᔨᖑᐊᖅ 6c). ᐅᓇ ᑎᑎᕋᐅᔭᖅᓯᒪᔪᖅ ᓴᕿᑎᑦᑎᓯᒪᙵᖅ ᑕᒪᐃᓐᓂ magnetite (ᑐᖑᔪᖅᑐᖅ ᑐᑭᓕᐊᓇᓯᒪᔪᖅ) ᐊᒻᒪ orthopyroxene (ᐆᔭᐅᔭᕐᒥ ᑐᑭᓕᐊᓇᓯᒪᔪᖅ) ᓴᖏᖕᓂᖅᑲᖅᐳᑦ ᐅᕝᕙ XFe^{3+}, ᐃᒪᓐᓇᐅᕙᓵᖅᓗᓂ ᐊᔾᔨᒌᖕᖏᔾᔪᑎᐅᔪᑦ ᐅᕙᓂ XFe^{3+} ᐃᓚᒍᑎᐅᓕᖅᓯᒪᑐᐃᓐᓇᓇᐊᖃᖅᐳᖅ ᓈᒻᒪᖕᒋᓕᐅᕈᑎᓂᑦ ᓄᓇᙳᐊᕐᒥᑦ ᑕᒪᐃᓐᓂ ᐱᓕᕆᐊᓂ. ᐊᖏᔪᖅ ᖃᓄᐃᓕᓂᐅᕚᒃᑐᖅ ᐅᑯᓄᖓ magnetite- ᐊᒻᒪ orthopyroxene-bearing metagranitoid ᐅᔭᕋᖕᓂ ᑕᐃᒪᐃᑦᑐᖃᖅᑐᓂᑦ ᓴᕿᑎᑦᑎᓯᒪᙵᖅ ᒪᑯᐊ ᓇᓗᓇᐃᒃᑯᑏ XFe^{3+} = 0.05–0.25 ᓈᒻᒪᓛᖑᓂᖏᓐᓂᑦ (ᓄᓇ ᐃᓚᖃᖅᓯᒪᔪᖅ ᐆᒥᖓ assumed value of 0.1; ᐊᐅᐸᙶᖅᑐᓂ ᑐᑭᓕᐊᓇᓯᒪᔪᓂᕐ) ᑕᒪᐃᓐᓂ ᐱᓕᕆᐊᖑᔪᑦ ᐋᕿᒃᑕᐅᓕᑕᐃᓐᓇᕋᔭᖅᐳᑦ ᐃᓱᒪᒋᔭᐅᔪᒥᑦ ᐆᓐᓇᕐᓂᐅᓇᔭᖅᑐᒥᑦ.

ᐊᕙᒃᑐᖅᓯᒪᓂᒃᑯᑦ ᒪᑯᐊ aeromagnetic ᑎᑎᖃᑦ ᓄᐊᑕᐅᕙᓪᓕᐊᔪᑦ ᓴᕿᑎᑦᑎᓯᒪᙳᑦ ᐊᔾᔨᒌᖕᖏᑦᑑᑎᒻᒪᓇᖕᓂ ᓂᐱᓐᓇᖅᑐᖅᑲᖅᑐᓂᑦ ᑕᒫᓂ ᐅᔭᕋᓚᖕᓂ ᐱᓕᕆᖃᕙᐅᔪᒥᑦ (ᓲᕐᓗ, ᐊᔾᔨᖑᐊᖅ 6d; Kiss and Tschirhart, 2015a–r). ᓄᓇᒥ ᖃᐅᔨᓴᕈᑎᕗᓃᑦ ᓴᕿᑎᑦᑎᓯᒪᙳᑦ ᐱᔾᔪᑎᐅᓗᐊᕋᓱᒋᔭᐅᓪᓗᓂ ᐊᔾᔨᒌᖕᖏᑦᑑᓂᐅᓂᕐᒥᑦ ᒪᑯᓄᖓ ᐊᔾᔨᒌᖕᖏᑦᑐᓄᑦ ᓂᐱᓐᓇᖅᑐᖅᑲᖅᑐᓄᑦ magnetite, ᒫᓃᓐᓂᖅᓴᐅᕚᒃᓗᑎᒃ homogeneous plutons (Tschirhart et al., 2015). ᖃᐅᔨᔭᐅᕙᓪᓕᐊᔪᑦ ᑕᒪᑐᒥᖓ ᒪᓕᒃᓯᒪᑲᑕᒃᐳᑦ, ᓴᕿᔮᖅᑎᑦᑎᓂᖏᓐᓂᑦ ᐊᓯᖑᕈᑎᕙᓂᕐᓂᑦ ᐅᕙᓂ P, T, ᐊᒻᒪ X-ᒥ ᖃᐅᔨᒪᔭᐅᔾᔪᑎᐅᓂᐊᖅᑐᓂᑦ ᐅᔭᕋᖕᓄᑦ (ᐊᒻᒪᓗ orthopyroxene) ᐃᓂᖏᔭᐅᖄᑎᒋᔪᑦ, ᐱᓕᕆᓂᒃᓴᐃᑦ ᓱᓕ ᓱᕐᑯᓯᓗᐊᖅᓯᒪᑎᓐᓇᒋᑦ.

ᖃᓄᐃᓕᖕᒐᓂᖏᑦ ᐊᓯᔾᔨᐸᓪᓕᐊᓂᖏᑦ ᐊᒻᒪ ᐊᓯᔾᔨᕐᓂᖏᑦ ᖃᓄᐃᓕᖕᒐᓂᖏᑦ ᐅᔭᖅᑲᐃᑦ

D_1 ᖃᓄᐃᓕᖕᒐᓂᖏᑦ ᐊᓯᔾᔨᖅᐸᓪᓕᐊᓂᖏᑦ ᐊᒻᒪ M_1 ᐊᓯᔾᔨᕐᓂᖏᑦ ᖃᓄᐃᓕᖕᒐᓂᖏᑦ ᐅᔭᖅᑲᐃᑦ

Paleoproterozoic tectonostratigraphic ᐃᓛᒃᑰᖓᔪᑦ ᓇᑐᓴᐃᔭᖅᓯᒪᔪᑦ ᖁᓛᓂ ᓇᑐᓴᐃᖅᑕᐅᓯᒪᒐᔪᑦᑐᑦ ᐱᕙᓪᓕᐊᑎᑕᐅᓂᖓᓄᑦ ᓯᐊᒻᒪᐸᓪᓕᖓᓂᖓ ᒥᓕᒦᑕᒥᑦ ᓯᐊᓐᑕᒦᑕᓄᑦ ᐃᓗᓕᖕᒋᑦ ᖁᓕᓇᓐᓂᖕᒋᑦ (S_1) ᐃᒃᑳᑦᓗᓂ ᑯᑐᖅᑐᖅ, ᐊᒻᒪ ᓇᓕᒧᐃᓐᓇᖅᑐᓂ ᐅᔭᖅᑲᐃᑦ ᑲᑎᓐᓂᓇᔭᖕᒋᓐᓂᑦ ᐊᑯᓐᓂᖕᒋᓐᓂ supracrustal ᐊᒻᒪ plutonic ᐃᓛᒃᑰᖓᔪᑦ. metasedimentary strata,−ᒥᑦ S_1 ᓇᑐᓇᐃᖅᑕᐅᔪᖅ ᖁᓕᓇᓐᓂᖕᒋᓐᓄᑦ ᓇᓕᒧᑦᑐᓂᑦ M_1 biotite, sillimanite, ᐊᒻᒪ garnet, ᖁᓕᓇᒃᑲᓐᓂᖃᑦᑕᖅᑐᑦ ᐱᓗᐊᖅᑐᓂ plagioclase, K-feldspar ᐊᒻᒪ quartz. garnet ᐅᔭᕋᑦᑎᐊᕙᐃᑦ ᒥᓕᒦᑕᖕᒋᓐᓃᒍᓐᓇᖅᑐᑦ ᐊᖏᓂᖕᒋᑦ ᐊᒻᒪ ᑕᑯᔅᓴᐅᓂᖃᖅᑐᑎᑦ poikiloblastic. metasedimentary ᐃᓛᒃᑰᖓᔪᓂᑦ, S_1 ᓇᑐᓇᐃᖅᑕᐅᔪᖅ ᐅᔭᖅᑲᐃᓄᑦ ᐊᓯᔾᔨᓇᐊᕈᑎᖕᒋᑦ ᐱᓗᐊᖅᑐᒥᑦ ᓄᓴᐅᑉ ᐃᑭᖓᓂ (S_0). foliated mafic−ᒥᑦ ᐊᒻᒪ felsic plutonic −ᓂᑦ, S_1 ᓇᑐᓇᐃᖅᑕᐅᔪᖅ ᓇᒧᓐᖓᖃᑦᑕᑲᓐᓂᕐᓂᖕᒋᓐᓄᑦ ᐱᓗᐊᖅᑐᒥᑦ ferromagnesian-rich ᖁᓕᓃᑦᑐᑦ ᐃᓗᓕᓈᓪᓗᓂᒋᑦ granoblastic, ᒥᓕᒦᑕᓂᑦ ᐊᖏᓂᓕᒃ. M_1 orthopyroxene, biotite, magnetite, clinopyroxene, hornblende, ᐊᒻᒪ/ᐅᕝᕙᓘᓐᓃᑦ garnet, ᐊᒻᒪ ᖁᓕᓃᑦᑐᑦ ᐃᓗᓕᖅᑲᖅᑐᑦ

ᐱᓗᐊᖅᑐᒥᑦ plagioclase ᐊᒻᒪ quartz±K-feldspar. ᓇᓕᒨᓂᕆᔾᔪᑎ orthopyroxene, biotite, clinopyroxene, ᐊᒻᒪ hornblende ᓇᓗᓇᐃᖅᓯᔪᑦ S_1 ᓵᑦᑐᓂᑦ metaplutonic ᐃᓛᒃᑰᖓᔪᓂᑦ ᐱᑕᖃᖅᑎᓪᓗᒋᑦ. S_1 ᓵᑦᑐᑦ ᑕᑯᓐᓇᖅᑕᐅᔪᑦ axial-planar ᑎᑭᑦᑐᒍ ~100 m ᐊᖏᓂᖓ isoclinal ᐱᕆᓐᓂᖏᑦ ᐃᒃᑲᑦᑐᒥᑦ ᐅᐊᓐᓇᖓᓂ ᐊᓂᖏᓂ ᐊᒻᒧᐊᐸᓪᓕᖓᔪᑦᐱᕆᓐᓂᖏᑦ (Dyck and St-Onge, 2014).

ᐅᔭᕋᐅᔭᒐᓚᐅᑦ ᒪᑯᐊ granulite-facies M_1 metamorphism ᒫᓃᑦᑐᑦ ᑭᒻᒥᕈᒻᒥ ᕿᓂᖅᑐᓂᑦ ᒥᑕ ᐃᓐᑲᒡᓃᑕ ᐸᓂᓐᓯᓚᐅᑉ ᐱᖓᓐᓇᖅᐸᓯᐊᓃᑦᑐᖅ ᐅᕙᓂ ca. 1.84 Ga by St-Onge et al (2007). ᓄᓇᐅᐸ ᖃᓄᐃᓕᖓᓂᖓᒍᑦ ᐊᒻᒪ ᑭᓯᑕᖃᕐᓂᖓᒍᑦ ᖃᐅᔨᓴᕐᓂᖅᑕᖃᕐᓂᐊᕐᑐᖅ ᑕᒪᒃᑯᐊᑦᑕᐃᓐᓇᖅ ᐅᔭᕋᔭᐃᑦ ᐱᑕᖃᕐᒪᖔᑕ ᒫᓐᓇ ᓄᓇᙳᐊᓕᐅᕝᕕᒥᑦ.

D_2 ᖃᓄᐃᓕᖓᓂᖏᑦ ᐊᓯᔾᔨᖅᐸᓪᓕᐊᓂᖏᑦ

Ptarmigan Fiord−ᒥᑦ, D_2 ᓯᓚᑎᖓ ᐃᔾᔪᔪᖅ ᐱᖃᓯᐅᔾᔨᔪᖅ ᐊᕿᒍᒐᓵᓗᓐᓂᑦ ᑐᓐᖓᕝᕙ ᐅᔭᖅᑲᐃᑦ orthogneiss ᐊᒻᒪ Paleoproterozoic supracrustal ᐅᔭᖅᑲᐃᑦ (Chadwick et al., 2015). ᑕᒪᒃᑷᓐᓂᒃᐃᓗᐊᓂ ᐊᒻᒪ ᓯᓚᑖᓂ ᐊᔭᐅᖅᓯᓂᖅ ᓴᖅᑭᖃᑦᑕᖅᑐᖅ. D_2 ᐊᔭᐅᖅᓯᓂᖓ ᖁᓕᕇᖃᑦᑕᐅᑎᔪᑦ ᓇᓗᓇᐃᖅᑕᐅᔪᑦ ᖁᕚᓯᑦᑐᒥᑦ mylonitic ᐊᑦᑐᖅᑕᐅᔪᑦ ᐊᑯᓐᓂᖏᓐᓂ supracrustal ᐅᔭᖅᑲᐃᑦ ᐊᒻᒪ ᐋᖅᑭᔅᓯᒪᓂᖓ ᖁᓛᓃᑦᑐᑦ ᐊᑖᓂ. L_2 ᐅᔭᕋᓐᓂᐊᕋᔅᓴᐅᔪᓐᓇᖅᑐᓂᑦ ᑐᑭᓕᐊᕐᓂᖓ, ᐊᒻᒪᓗ S_2 ᖃᓪᓗᓈᖅᑕᔭᐅᔮᖅᑐᑦ ᓇᓕᒨᓂᖃᖅᑐᑦ ᐊᔭᐅᖅᑕᐅᒧᒧᑦ ᓴᓇᓯᒪᑦᑎᐊᖅᑐᑦ. ᐃᔾᔪᓂᖏᑦ ᐃᒻᒥᑰᖅᑐᑦ ᐋᖅᑭᔅᓯᒪᔪᑦ ᖁᓕᕇᑦᑐᑎᑦ ᐱᒋᐊᖅᑐᓂ ~100 ᑎᑭᑦᑐᒍ 800 m ᐊᒻᒪ ᑕᑭᓛᕆᔪᓐᓇᖅᑕᖓ ᐃᒻᒥᑰᖅᑐᑦ ᖁᓕᕇᖃᑦᑕᐅᑎᔪᑦ ᐋᖅᑭᔅᓯᒪᔪᕖᑦᑐᖅ ~25 km.

D_1 ᑭᓱᕈᓘᔭᐃᑦ (ᐃᓚᐅᓪᓗᑎᒃ ᐅᓇ S_1 foliation) ᐊᒻᒪ D_2 ᖁᓕᕇᖁᐋᓯᒪᓪᓗᑎ ᐊᒻᒪ ᐋᕿᒋᐊᒃᑲᓐᓂᕐᓯᒪᓪᓗᑎᒃ ᐅᐊᓐᓇᕐᒧ ᐅᐊᓐᓇᐅ ᐱᖓᓐᓇᖓᓄᖓᐅᕙᓪᓕᐊᓂᐅᔪᒥᑦ ᐆᒧᖓ D_2 ᐃᒧᓯᒪᓂᖓᓄᑦ. ᐅᓇ D_2 ᐃᒧᓯᒪᓂᐅᔪᖅ ᓇᓗᓇᐃᖅᑕᐅᓯᒪᔪᖅ ᓄᓇᙳᐊᑎᒍᑦ ᐊᒻᒪ ᓴᕿᔮᖅᑎᑦᑎᓪᓗᓂ ᒪᑭᑕᔪᓂ ᑲᓇᓐᓇᖅᐸᓯᒧᐊᖓᔪᓂᑦ ᖁᓕᕇᒄᑎᓂᑦ. ᐃᒪᐃᑦᑐᓂ mesoscopic ᐱᑕᖃᕆᑦᑐᖅ ᐊᒃᑐᐊᔪᓂᑦ ᐆᒥᖓ D_2 ᖃᓕᕇᓕᖅᓯᒪᓂᖏᓐᓂᑦ ᑎᑎᕋᐅᓯᐅᓯᒪᔪᑦ.

ᐅᐊᓐᓴᖓᓂ ᑯᐸᐃᒃ, ᓄᓇᐅᐸ ᖄᖓᓂ−ᐊᖏᓂᖓᓄᑦ D_2 ᐱᕆᖃᑦᑕᖅᑐᑦ ᓴᓇᓯᒪᓂᖓ ᖁᕚᓯᓐᓂᖓ 1 ᐊᒻᒪ 2 ᑭᓪᓕᖃᖅᑎᑕᐅᔪᖅ ca. 1.76 Ga (Lucas and St-Onge, 1992). Lucas and Byrne (1992) ᐱᔪᒪᓚᐅᖅᑐᑦ orogen-ᓇᓕᒨᓂᖓ ᐱᕆᔾᔪᑎᖃᖅᓯᒪᔪᖅ ᑲᔪᓰᓐᓇᖅᑐᓂᑦ ᓄᓇᒧᑦ ᓇᓕᒧᑦᑐᓂᑦ ᓄᓇᐃᑦ ᓯᓚᕐᔪᐊᒥᑦ ᐊᐳᖃᑦᑕᐅᑎᑎᓪᓗᒋᑦ ᓇᐃᓪᓕᒋᐊᖅᓯᒪᔪᖅ ᐅᐊᓐᓇᖓᑕ ᑲᓇᓐᓇᖓᓂ Trans-Hudson Orogen.−ᒥᑦ.

D_3 ᖃᓄᐃᓕᖓᓂᖏᑦ ᐊᓯᔾᔨᖅᐸᓪᓕᐊᓂᖏᑦ

ᒪᑭᑕᓪᓗᐊᖅᑐᑦ ᐱᕆᖃᑦᑕᖅᑐᑦ ᐱᑐᖃᐅᓂᖅᓴᓄᑦ ᐃᓗᓕᕆᔾᔪᑎᖏᓐᓂᑦ ᑲᓇᓐᓇᖓᓂ ᐅᐊᓐᓇᖓᓄ ᑲᓇᓐᓇᖓᓅᖅᐸᓪᓕᐊᔪᖅ D_3 ᐱᕆᓐᓂᖏᑦ ᐱᕆᓐᓂᖓ ᐸᕝᕚᓴᐃᓯᒪᔪᖅ, ᓄᓇᖑᐊᖅ ᑕᑯᔅᓴᐅᓛᖑᔪᖅ ᓂᒋᐊᓂ ᐊᒻᒪ ᑲᓇᓐᓇᖓᓂ Sylvia Grinnell Lake–Clearwater Fiord−ᒧᑦ. ᐸᕝᕚᓴᐃᔪᑦ D_2 ᐊᒻᒪ D_3 ᐱᕆᔅᓯᒪᔪᑦ ᓴᓇᓯᓴᓂᖓ ᖃᐅᔨᓴᕈᓐᓇᑎᑦᑎᓯᒪᔪᖅ ᓄᓇᐅᐸ ᐃᑭᖓᓂ ᓂᒋᐊᓂ ᕿᑭᖅᑖᓗᒃ, ᐱᖃᓯᐅᑎᓪᓗᑎ ᐱᖓᓱᑦ ᓴᓇᓯᒪᓪᓗᐊᑕᕆᔾᔪᑎ ᖁᕚᓯᓐᓂᖏᑦ ᑕᑯᔅᓴᐅᔪᑦ ᐅᓪᓗᒥ ᓄᖑᑎᖅᐸᓪᓕᖓᓂᖓᓄ ᓄᓴᐅᐸ ᖄᖓ (ᐊᔾᔨᙳᐊᖅ 2). D_3 ᐱᕆᓐᓂᖓ ᐅᐊᓐᓇᖓᓂ ᑯᐸᐃᒃ ᕿᑎᐊᓃᑦᑐᖅ 1.76 ᐊᒻᒪ 1.74 Ga (Lucas and St-Onge, 1992).

ᑰᓇᐅᔭᓕᕆᓂᕐᒧᑦ ᐃᓱᒪᒋᔭᐅᔭᕆᐊᓖᑦ

ᐊᒥᓱᒐᓚᐃᑦ ᐅᔭᖅᑲᐃᑦ ᖃᓄᐃᓕᖓᓂᖏᑦ ᐊᑦᑐᐊᓂᓖᑦ ᐊᒻᒪ ᓴᖅᑭᖃᑦᑕᕐᓂᖏᑦᑰᓇᐅᔭᓕᕆᔾᔪᑎᓭᓄᑦ ᐊᑦᑐᐃᓂᕐᑲᕈᓐᓇᖅᑐᑦ ᓇᓗᓇᐃᖅᑕᐅᓚᐅᖅᑐᑦ 2015−ᒥ ᓇᓗᓇᐃᖅᑕᐅᓯ ᒪᔪᓂᑦ ᑐᕌᖅᑕᐅᔪᓂᑉᓗ ᓄᓇᖑᐊᓕᐅᓚᐅᖅᑐ Sylvia Grinnel Lake–Clearwater Sound area. ᖁᓕᓈᑦᑐᑦ mafic-ultramafic sills ᐃᓗᐊᓃᑦᑐᑦ sulphidic siliciclastic ᐅᔭᖅᑲᐃᑦ ᖁᓕᕐᑰᑦᑐᑦ ᐅᔭᖅᑲᐃᑦ ᖃᓄᐃᓕᖓᓂᖏᑦ ᐊᔾᔨᐸᓗᒋᔭᖏᑦ Ni–Cu–platinum-ᐃᓚᖏᑦ ᐃᓗᓕᖏᑦ ᐅᔭᕋᓂᐊᕋᓵᐅᔪᓇᖅᑐᑦ ᐊᓱᖓᓂ Trans-Hudson Orogen (ᓲᕐᓗ Raglan ᐅᔭᖅᑲᐃᑦ ᑲᓇᓐᖓᓂ Cape Smith Belt oᐅᐊᓐᓇᖓᓂ ᑯᐸᐃᒃ; St-Onge and Lucas, 1994; Lesher, 2007). ᖃᐅᔨᓴᕐᕕᐅᔪᒥᑦ ᖃᓄᐃᓕᖓᓂᖏᑦ ᐅᔭᖅᑲᐃᑦ ᓇᓗᓇᐃᔭᖅᑎᓯᑦᑎᐊᓂᖅᓴᐃᑦ ᓖᑲᐃᓐ Liikane et al. (2015). ᐅᒃᑯᓯᔅᓴᕈᖅᓯᒪᔪᑦ ᐅᔭᖅᑲᐃᑦ ᓇᓗᓇᐃᖅᑕᐅᓯᒪᔪᑦ ᐊᒥᓱᒐᓚᓐᓂᑦ ᓇᒦᓐᓂᖏ ᓄᓇᖑᐊᒥᑦ, ᐃᓚᖏᑦ ᓴᓇᖑᐊᒐᔅᓴᐅᒍᓐᓇᑐᐃᓐᓇᕆᐊᓖᑦ ᐊᓱᖏᑦ ᓴᖅᑭᕐᑲᑦᑕᖅᑐᑦ ᐱᔪᒥᓇᖅᑐᑦ sulphide-bearing gossans; ᐊᒻᒪ magnetite ᐊᒻᒪ ᐱᐅᔪᑦ ᐅᔭᕋᓂᐊᕋᓵᐅᔪᓇᖅᑐᑦᑐᓐᓄᔭᐃᑦ, ᐱᕐᑲᓱᐅᑎᑉᓗᑎᐅᔭᕋᑦᑎᐊᕙᐅᔪᓇᖅᑐᑦ apatite ᐊᒻᒪ diopside.

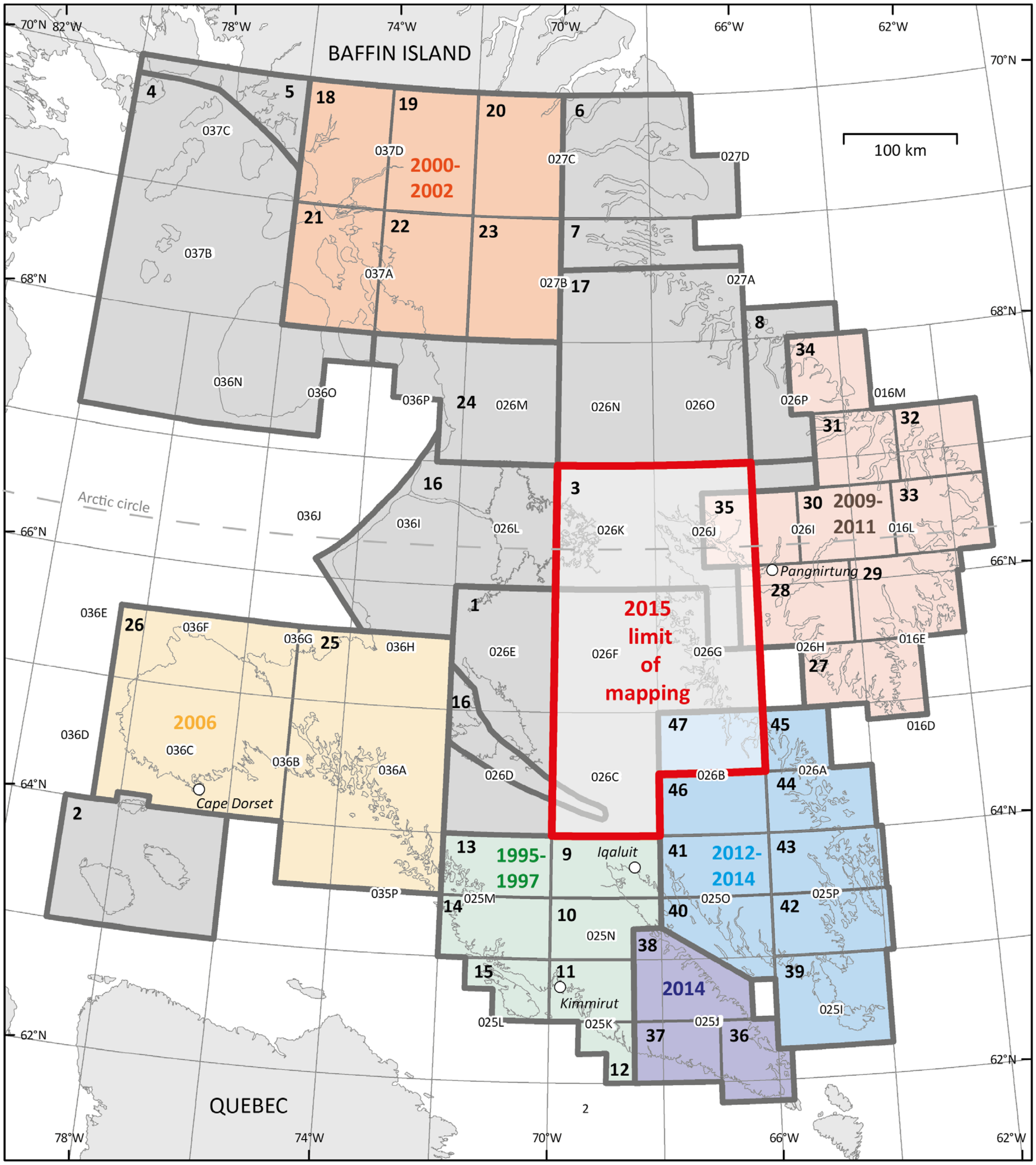

ᐊᔾᔨᖑᐊᖅ 1. ᓇᓄᓇᐃᔭᖅᓯᒪᓂᖏᑦ ᖁᐊᖑᐃᓐᓇᖅᑐᒥᓂᑦ ᓄᓇᖑᐊᓕᐅᕐᓂᖅᐱᓕᕆᐊᖑᔪᑦ ᕿᑭᖅᑖᓗᒃ, ᓄᓇᕗᑦ. ᓇᒦᓐᓂᖓ 2015–ᒥ ᓂᒋᐊᓂ–ᕿᑎᐊᓂ ᕿᑭᖅᑖᓗᒻᒥ ᑕᑯᔅᓴᐅᑎᑕᐅᔪᖅ ᐊᐅᐸᖅᑐᖅ ᑐᑭᓕᐊᖅᑐᑦ ᓴᓂᕋᖏᑦ, ᐱᔭᕇᖅᑕᐅᓪᓗᓂᓗ ᐅᓪᓗᒥᓚᐅᖔᖓᔪᓂᑦ ᓄᓇᖑᐊᓂᑦ ᓂᒋᐊᓂ 70 °N. ᕿᕐᓂᓂᖅᓴᐃᑦ ᓈᓴᐅᑏᑦ ᓇᓄᓇᐃᖅᓯᔪᑦ ᓄᓇᖑᐊᒧᑦ ᖃᐅᔨᒋᐊᕈᑏᑦ ᐋᖅᑭᐅᖅᓯᒪᓪᓗᑎᑦ ᐊᒻᒪ ᑎᑎᕋᖅᓯᒪᔪᑦ ᐊᑖᓂ. ᐊᒥᐊᓖᑦ ᓇᓄᓇᐃᖅᓯᔪᑦ ᓇᒦᓐᓂᖏᑦ ᐊᒻᒪ ᐊᕐᕌᒍ(ᐃᑦ) ᖃᐅᔨᓴᖅᑕᐅᕋᑖᖅᓯᒪᔪᑦ. ᓈᓴᐅᑎᓖᑦ ᑎᑎᖅᑲᖅᑲᖅᑐᑎᑦ ᓇᓄᓇᐃᖅᓯᔪᑦ ᑲᓇᑕᒥ ᓄᓇᖑᐊᓕᐅᓂᕐᒧᑦ ᓄᓇᖑᐊᑦ.

1. Blackadar, R.G., 1967. Geology, Cumberland Sound, District of Franklin; Geological Survey of Canada, Preliminary Map 17-1966, scale 1:506 880. doi:10.4095/108490

2. Blackadar, R.G., 1970. Nottingham, Salisbury, and Mill Islands, District of Franklin; Geological Survey of Canada, Map 1205A, scale 1:250 000. doi:10.4095/109212

3. Jackson, G.D., 1971. Operation Penny Highlands, south-central Baffin Island; *in* Report of Activities, Part A: April to October 1970, Geological Survey of Canada, Paper 71-1, Part A, p. 138–140.

4. Trettin, H.P., 1975. Geology, Lower Paleozoic geology, central and eastern parts of Foxe Basin and Baird Peninsula, Baffin Island, District of Franklin; Geological Survey of Canada, Map 1406A, scale 1:500 000. doi:10.4095/109081

5. Morgan, W.C., 1982. Geology, Koch Island, District of Franklin; Geological Survey of Canada, Map 1535A, scale 1:250 000. doi:10.4095/127056

6. Henderson, J.R., 1985a. Geology, McBeth Fiord-Cape Henry Kater, District of Franklin, Northwest Territories; Geological Survey of Canada, Map 1605A, scale 1:250 000. doi:10.4095/120467

7. Henderson, J.R., 1985b. Geology, Ekalugad Fiord-Home Bay, District of Franklin, Northwest Territories; Geological Survey of Canada, Map 1606A, scale 1:250 000. doi:10.4095/120468

8. Jackson, G.D., 1998. Geology, Okoa Bay-Padloping Island area, District of Franklin, Northwest Territories; Geological Survey of Canada, Open File 3532, scale 1:250 000. doi:10.4095/209911

9. St-Onge, M.R., Scott, D.J., and Wodicka, N., 1999a. Geology, Frobisher Bay, Nunavut; Geological Survey of Canada, Map 1979A, scale 1:100 000. doi:10.4095/210833

10. St-Onge, M.R., Scott, D.J., and Wodicka, N., 1999b. Geology, Hidden Bay, Nunavut; Geological Survey of Canada, Map 1980A, scale 1:100 000. doi:10.4095/210835

11. St-Onge, M.R., Scott, D.J., and Wodicka, N., 1999c. Geology, McKellar Bay, Nunavut; Geological Survey of Canada, Map 1981A, scale 1:100 000. doi:10.4095/210836

12. St-Onge, M.R., Scott, D.J., and Wodicka, N., 1999d. Geology, Wright Inlet, Nunavut; Geological Survey of Canada, Map 1982A, scale 1:100 000. doi:10.4095/210840

13. St-Onge, M.R., Scott, D.J., and Wodicka, N., 1999e. Geology, Blandford Bay, Nunavut; Geological Survey of Canada, Map 1983A, scale 1:100 000. doi:10.4095/210837

14. St-Onge, M.R., Scott, D.J., and Wodicka, N., 1999f. Geology, Crooks Inlet, Nunavut; Geological Survey of Canada, Map 1984A, 1:100 000 scale. doi:10.4095/210838

15. St-Onge, M.R., Scott, D.J., and Wodicka, N., 1999g. Geology, White Strait, Nunavut; Geological Survey of Canada, Map 1985A, scale 1:100 000. doi:10.4095/210839

16. Sanford, B.V. and Grant, A.C., 2000. Geological framework of the Ordovician system in the southeast Arctic platform, Nunavut; *in* Geology and Paleontology of the southeast Arctic Platform and southern Baffin Island, Nunavut; Geological Survey of Canada, Bulletin 557, p. 13–38.

17. Jackson, G.D., 2002. Geology, Isurtuq River-Nedlukseak Fiord, Nunavut; Geological Survey of Canada, Open File 4259, scale 1:250 000. doi:10.4095/213304

18. St-Onge, M.R., Scott, D.J., Corrigan, D., and Wodicka, N., 2005a. Geology, Ikpik Bay, Baffin Island, Nunavut; Geological Survey of Canada, Map 2077A, scale 1:100 000. doi:10.4095/221054

19. St-Onge, M.R., Scott, D.J., Corrigan, D., and Wodicka, N., 2005b. Geology, Flyway Lake, Baffin Island, Nunavut; Geological Survey of Canada, Map 2078A, scale 1:100 000. doi:10.4095/221091

20. St-Onge, M.R., Scott, D.J., Corrigan, D., and Wodicka, N., 2005c. Geology, Clyde River, Baffin Island, Nunavut; Geological Survey of Canada, Map 2079A, scale 1:100 000. doi:10.4095/221092

21. St-Onge, M.R., Scott, D.J., Corrigan, D., and Wodicka, N., 2005d. Geology, Piling Bay, Baffin Island, Nunavut; Geological Survey of Canada, Map 2080A, scale 1:100 000. doi:10.4095/221093

22. St-Onge, M.R., Scott, D.J., Corrigan, D., and Wodicka, N., 2005e. Geology, Straits Bay, Baffin Island, Nunavut; Geological Survey of Canada, Map 2081A, scale 1:100 000. doi:10.4095/221094

23. St-Onge, M.R., Scott, D.J., Corrigan, D., and Wodicka, N., 2005f. Geology, Dewar Lakes, Baffin Island, Nunavut; Geological Survey of Canada, Map 2082A, scale 1:100 000. doi:10.4095/221095

24. Jackson, G.D., 2006. Geology, Hantzsch River area, Baffin Island, Nunavut; Geological Survey of Canada, Open File 4202, scale 1:250 000. doi:10.4095/221809

25. St-Onge, M.R., Sanborn-Barrie, M., and Young, M.D., 2007a. Geology, Mingo Lake, Baffin Island, Nunavut; Geological Survey of Canada, Open File 5433, scale 1:250 000. doi:10.4095/224163

26. St-Onge, M.R., Sanborn-Barrie, M., and Young, M.D., 2007b. Geology, Foxe Peninsula, Baffin Island, Nunavut; Geological Survey of Canada, Open File 5434, scale 1:250 000. doi:10.4095/224222

27. Sanborn-Barrie, M., Young, M., Whalen, J., and James, D., 2011a. Geology, Ujuktuk Fiord, Nunavut; Geological Survey of Canada, Canadian Geoscience Map 1 (2nd edition, preliminary), scale 1:100 000. doi:10.4095/289237

28. Sanborn-Barrie, M., Young, M., and Whalen, J., 2011b. Geology, Kingnait Fiord, Nunavut; Geological Survey of Canada, Canadian Geoscience Map 2 (2nd edition, preliminary), scale 1:100 000. doi:10.4095/289238

29. Sanborn-Barrie, M., Young, M., Whalen, J., James, D., and St-Onge, M.R., 2011c. Geology, Touak Fiord, Nunavut; Geological Survey of Canada, Canadian Geoscience Map 3 (2nd edition, preliminary), scale 1:100 000. doi:10.4095/289239

30. Sanborn-Barrie, M. and Young, M., 2013a. Geology, Circle Lake, Nunavut; Geological Survey of Canada, Canadian Geoscience Map 5 (preliminary), scale 1:100 000. doi:10.4095/288929

31. Sanborn-Barrie, M., Young, M., Keim, R., and Hamilton, B., 2013. Geology, Sunneshine Fiord, Nunavut; Geological Survey of Canada, Canadian Geoscience Map 6 (preliminary), scale 1:100 000. doi:10.4095/288931

32. Sanborn-Barrie, M. and Young, M., 2013b. Geology, Padle Fiord, Nunavut; Geological Survey of Canada, Canadian Geoscience Map 37 (preliminary), scale 1:100 000. doi:10.4095/292014

33. Sanborn-Barrie, M. and Young, M., 2013c. Geology, Durban Harbour, Nunavut; Geological Survey of Canada, Canadian Geoscience Map 38 (preliminary), scale 1:100 000. doi:10.4095/292015

34. Sanborn-Barrie, M. and Young, M., 2013d. Geology, Qikiqtarjuaq, Nunavut; Geological Survey of Canada, Canadian Geoscience Map 39 (preliminary), scale 1:100 000. doi:10.4095/292016

35. Jackson, G.D. and Sanborn-Barrie, M., 2014. Geology, Pangnirtung Fiord, Nunavut; Geological Survey of Canada, Canadian Geoscience Map 4 (preliminary), scale 1:100 000. doi:10.4095/288928

36. St-Onge, M.R., Rayner, N.M., Steenkamp, H.M., and Gilbert, C., 2015a. Geology, Terra Nivea, Baffin Island, Nunavut; Geological Survey of Canada, Canadian Geoscience Map 215E (preliminary); Canada-Nunavut Geoscience Office, Open File Map 2015-02E, scale 1:100 000. doi:10.4095/296104

37. St-Onge, M.R., Rayner, N.M., Steenkamp, H.M., and Gilbert, C., 2015b. Geology, Pritzler Harbour, Baffin Island, Nunavut; Geological Survey of Canada, Canadian Geoscience Map 216E (preliminary); Canada-Nunavut Geoscience Office, Open File Map 2015-03E, scale 1:100 000. doi:10.4095/296109

38. St-Onge, M.R., Rayner, N.M., Steenkamp, H.M., and Gilbert, C., 2015c. Geology, Grinnell Glacier, Baffin Island, Nunavut; Geological Survey of Canada, Canadian Geoscience Map 217E (preliminary); Canada-Nunavut Geoscience Office, Open File Map 2015-04E, scale 1:100 000. doi:10.4095/296111

39. Steenkamp, H., Gilbert, C., and St-Onge, M.R., 2016a. Geology, Loks Land, Baffin Island, Nunavut, NTS 25-I (part); Geological Survey of Canada, Canadian Geoscience Map 264 (preliminary); Canada-Nunavut Geoscience Office, Open File Map 2016-01, scale 1:100 000. doi:10.4095/297344

40. Steenkamp, H., Gilbert, C., and St-Onge, M.R., 2016b. Geology, Ward Inlet (south), Baffin Island, Nunavut, NTS 25-O (south) and NTS 25-J (part); Geological Survey of Canada, Canadian Geoscience Map 266 (preliminary); Canada-Nunavut Geoscience Office, Open File Map 2016-02, scale 1:100 000. doi:10.4095/297349

41. Steenkamp, H., Gilbert, C. and St-Onge, M.R., 2016c. Geology, Ward Inlet (north), Baffin Island, Nunavut, NTS 25-O (north); Geological Survey of Canada, Canadian Geoscience Map 265 (preliminary); Canada-Nunavut Geoscience Office, Open File Map 2016-03, scale 1:100 000. doi:10.4095/297348

42. Steenkamp, H., Gilbert, C., and St-Onge, M.R., in press a. Geology, Beekman Peninsula (south), Baffin Island, Nunavut, NTS 25-P (south) and NTS 15-M (part); Geological Survey of Canada, Canadian Geoscience Map 267 (preliminary); Canada-Nunavut Geoscience Office, Open File Map 2016-04, scale 1:100 000. doi:10.4095/297351

43. Steenkamp, H., Gilbert, C., and St-Onge, M.R., in press b. Geology, Beekman Peninsula (north), Baffin Island, Nunavut, NTS 25-P (north) and NTS 15-M (part); Geological Survey of Canada, Canadian Geoscience Map 268 (preliminary); Canada-Nunavut Geoscience Office, Open File Map 2016-05, scale 1:100 000. doi:10.4095/297352

44. Steenkamp, H., Gilbert, C., and St-Onge, M.R., 2016d. Geology, Leybourne Islands (south), Baffin Island, Nunavut, NTS 26-A (south); Geological Survey of Canada, Canadian Geoscience Map 269 (preliminary); Canada-Nunavut Geoscience Office, Open File Map 2016-06, scale 1:100 000. doi:10.4095/297353

45. Steenkamp, H., Gilbert, C., and St-Onge, M.R., 2016e. Geology, Leybourne Islands (north), Baffin Island, Nunavut, NTS 26-A (north); Geological Survey of Canada, Canadian Geoscience Map 271 (preliminary); Canada-Nunavut Geoscience Office, Open File Map 2016-07, scale 1:100 000. doi:10.4095/297355

46. Steenkamp, H., Gilbert, C., and St-Onge, M.R., in press c. Geology, Chidliak Bay (south), Baffin Island, Nunavut, NTS 26-B (south); Geological Survey of Canada, Canadian Geoscience Map 272 (preliminary); Canada-Nunavut Geoscience Office, Open File Map 2016-08, scale 1:100 000. doi:10.4095/297357

47. Steenkamp, H., Gilbert, C., and St-Onge, M.R., in press d. Geology, Chidliak Bay (north), Baffin Island, Nunavut, NTS 26-B (north); Geological Survey of Canada, Canadian Geoscience Map 270 (preliminary); Canada-Nunavut Geoscience Office, Open File Map 2016-09, scale 1:100 000. doi:10.4095/297354

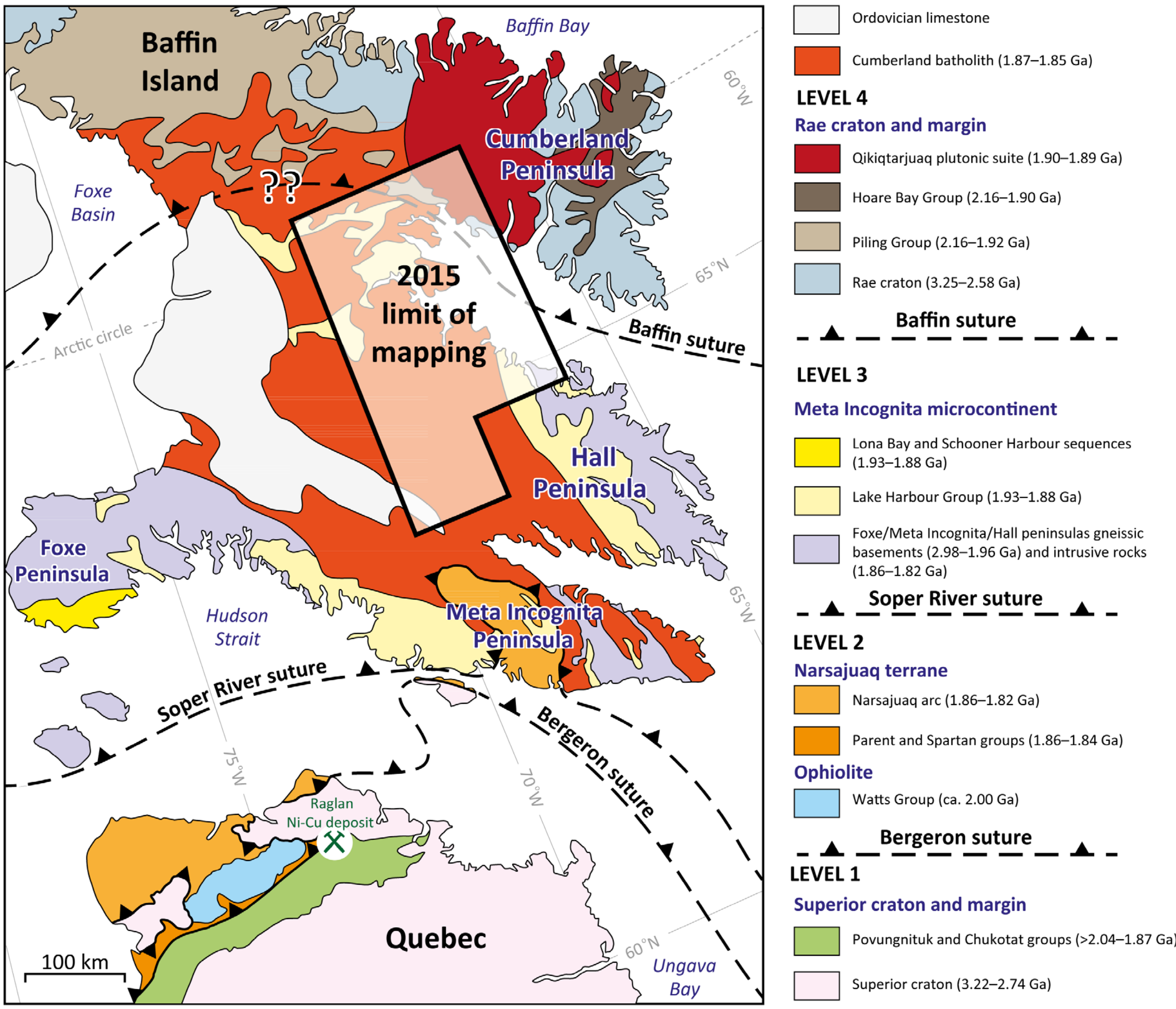

ᐊᔾᔨᖑᐊᖅ 2. ᑐᑭᓯᓇᖅᓯᑎᑕᐅᑦᑎᐊᖅᓯᒪᔪᖅ ᓄᓇᐅᖑᑉ ᓄᓇᖓᓂ ᓄᓇᖑᐊᖅ ᑯᐸᐃᒃ−ᕿᑭᖅᑖᓗᒃ ᐃᓚᒥᔭᖓ Trans-Hudson Orogen (ᐋᖅᑭᒋᐊᖅᑕᐅᓯᒪᔪᖅ ᑭᖑᓂᐊᒍᑦ St-Onge ᐱᓕᕆᖃᑎᖏᑦᑐ., 2007), ᑕᑯᔅᓴᐅᑎᑦᑎᔪᖅᑎᓴᒪᑦ ᐋᖅᑭᔅᓯᒪᓂᖏᑦ ᖁᓕᓃᓐᓂᖏᑦ ᐱᖓᓱᑦ ᓄᓇᐃᑦ ᑲᑎᓐᓂᖏᑦ. ᓄᓇᖑᐊᖅ ᑕᑯᔅᓴᐅᑎᑦᑎᔪᖅ ᐊᕕᑦᑐᖅᓯᒪᔪᓂᑦ ᓄᓇᐃᑦ ᐊᐅᓚᓂᓇᕙᑦᑕᖏᑦ ᓂᒋᐊᓄᑦ−ᕿᑎᐊᓂ ᕿᑭᖅᑖᓗᒃ, ᓇᓄᓇᐃᖅᑕᐅᓯᒪᔪᑦ ᕿᑦᓂᓴᐅᓪᓗᑎ.

ᐊᔾᔨᓐᖑᐊᖅ 3. ᐊᔾᔨᓐᖑᐊᖅ ᑕᑯᔅᓴᐅᑎᑦᑎᔪᖅ ᐃᖅᑲᖓᓃᑦᑐᑦ Sylvia Grinnell Lake–Clearwater Fiord. ᑎᑎᖅᑲᑲᖅᑐᑎᑦ ᓈᓴᐅᑎᓖᑦ ᑕᓕᖅᐱᐊᓂ ᑎᑭᖅᑯᐊᓂ ᐊᑐᓂ ᐊᔾᔨᓐᖑᐊᓂᑦ ᓇᓗᓇᐃᖅᓯᒍᑎᐅᔪᑦ 15SAB-ᖃᐅᔨᓵᕆᕖᒃ. a) 10 m ᑕᑯᔅᓴᖅ ᓯᓚᒦᓐᓂᑯ quartzite ᐅᔭᖅᑲᒃ biotite–ᒦᑦᑐᓂ ᐅᔭᖅᑲᐃᑦ. b) ᖁᓕᓅᑦᑎᐊᖅᑐᑦ quartzite ᐃᓗᐊᓃᑦᑐᑦ ᐃᖅᑲᖓᑕ ᒪᕋᓂ ᐃᓗᐊᓂᔫᓐᓃᑦ. c) ᑕᑯᔅᓴᐅᑎᑦᑎᔪ 1–2 cm ᐊᐅᐸᖅᑐᑦ ᐅᔭᕋᑦᑎᐊᕙᐃᑦᐊᓯᔾᔨᐸᓪᓚᐊᔪᓂᑦ ᐅᔭᖅᑲᓂᑦ ᐃᒍᓯᒪᓪᓗᑎᑦ ᓵᑦᑐᓂᑦ ᐊᒡᒍᖅᓯᒪᔪᑦ ᐃᓗᓕᖅᑲᖅᑐᑦ biotite ᐊᒻᒪ sillimanite. d) ᖃᕕᑦᑐᖅᓯᒪᔪᒥᑦ ᓇᓗᓇᖏᓐᓂᖓ ᑐᓐᓃᔭᐃᑦ ᐅᔭᖅᑲᐃᑦ ᐃᓗᐊᓂ biotite-orthopyroxene monzogranite. e) ᓴᐅᒥᒻᒥ: ᓂᐱᖅᑲᕐᓇᓖᑦ ᑐᓐᓃᔭᐃᑦ ᐅᔭᖅᑲᐃᑦ ᓄᓇᐅᑉ ᖄᒪᒍᑦ ᑐᓐᓃᔭᖅ, ᑕᓕᖅᐱᐊᓂ: ᑲᑎᓐᓂᖅᑲᖅᑐᑦ ᒫᐸᐅᓪ ᐊᔾᔨᑮᖏᔾᔪᑎᖓ ᖃᐅᓯᕐᓂᖓᓄᑦ, diopside ᐊᒻᒪ phlogopite. f) ᓇᓗᓇᐃᖅᓯᒪᓂᖏᑦ metagreywacke ᐃᓗᐊᓂ biotite monzogranite.

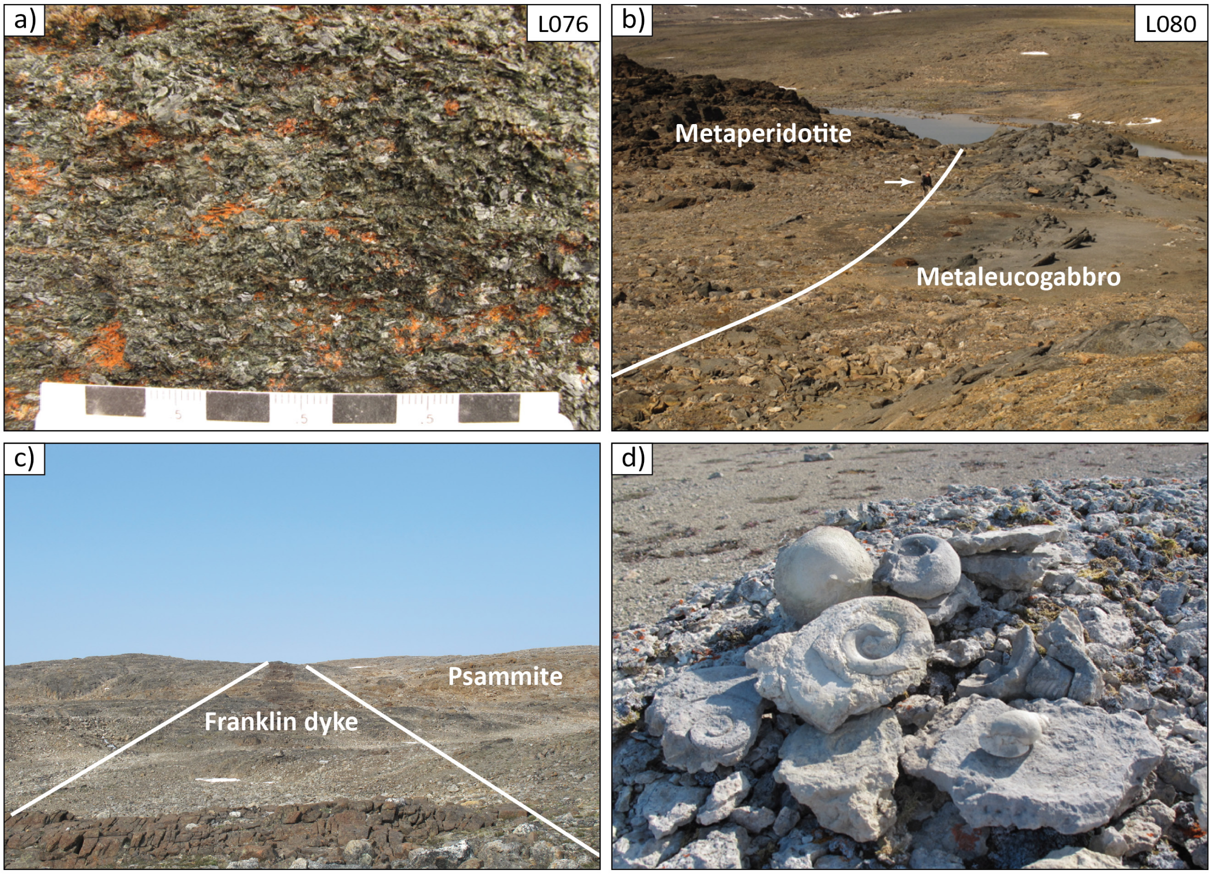

ᐊᔾᔨᓐᖑᐊᖅ 4. ᐊᔾᔨᓐᖑᐊᑦ ᐊᓯᖏᓐᓂᑦ ᐊᕕᑦᑐᖅᓯᒪᔪᓂᑦ Sylvia Grinnel Lake–Clearwater Fiord−ᒥᑦ. ᐊᑦᑐᐊᓂᒃᑲᓐᑎᓪᓗᒍ, ᑎᑎᖅᑲᐃᑦ ᓈᓴᐅᑎᒃᑲᓐᑐᑦ ᑕᓪᓚᖅᐱᒻᒥ ᖁᓛᓂ ᑎᑭᖅᑯᖏᓐᓂ ᐊᑐᓂ ᐊᔾᔨᓐᖑᐊᑦ ᓇᓗᓇᐃᖅᓯᔪᑦ 15SAB- ᖃᐅᔾᔭᕕᒻᒧᑦ. a) ᖃᓂᓈᖅᓯᒪᔪᖅ metaclinopyroxenite ᐊᓪᓚᖅᐹᖓᓂᑦ ᖁᓚᓅᑦᑐᓂᑦ mafic sill. ᕿᓐᓂᓂᖅᓴᐃᑦ ᓇᓗᓇᐃᖅᓯᔪᑦ ᒥᑭᔪᒥᑦ ᖃᓄᐃᓚᖓᓂᓇᓚᐅᖅᑕᖓᓄᑦ ᐅᑎᖅᑎᑕᐅᓂᖓ hornblende−ᒧᑦᖅ. b) ᕿᑎᐊᓂ −ᖁᓛᓂ ᖁᓚᓅᑦᑐᓂᑦ mafic sill, ᑕᑯᔅᓴᐅᑎᑦᑎᔪᖅ ᑲᔪᕈᔪᒻᒥᑦ metaperidotite ᖁᓚᖃᒃᑐᓂ ᑲᔪᕈᔪᒻᒥᑦ metaleucogabbro. ᖃᐅᔾᔭᒃᑏᑦ ᐊᖏᓂᖓᓄᑦ (ᖄᔭᓐᖑᐊᓚᒃ) 1.8 m ᑕᑭᓂᖓ. c) ᑭᒻᒥᕈᒻᒥ ᐱᓚᓇᔪᑦ psammite ᖁᓚᓅᖃᑦᑕᐅᑎᔪᑦ ᐊᕕᔅᓯᒪᓂᖏᑦ Franklin dyke, ᑯᑯᑎᑐᑦ ᑲᔪᕈᔪᖃᓂᖃᒃᑐᖅ ᐊᒻᒪᓗ ᐃᓚᖓ ᑲᑎᑦᑎᑦᑎᔪᑦ ᐅᐊᑦᑎᐊᑬᓂᖅᓴᐅᔪᓂᑦ. ᓯᒥᔅᓯᒪᓂ ᖃᓂᒋᔾᐸᓗᐊᓂ 10m ᓴᓂᒧᑦ. d) ᕿᐱ[ᓯᒪᒪᔪᑦᑐᑦ ᓴᖑᖓᓪᓗᑎ ᓄᓇᐅᑉᖁᓛᓂ0 limestone, ᑕᑯᔅᓴᐅᑎᑦᑎᔪᖅ ᐅᐊᑦᑎᐊᕈᖅᓂᓴᕐᓂᑦ ᓯᐊᒻᒪᖅᓯᒪᓂᖅᓴᒥᑦ ᓄᓇᒥᑦ. ᖃᐅᔾᔭᕕᐅᔪᖅ ᑕᑯᔅᓴᐅᓂᖓ ᓯᕗᓂᐊᓂ 50 cm.

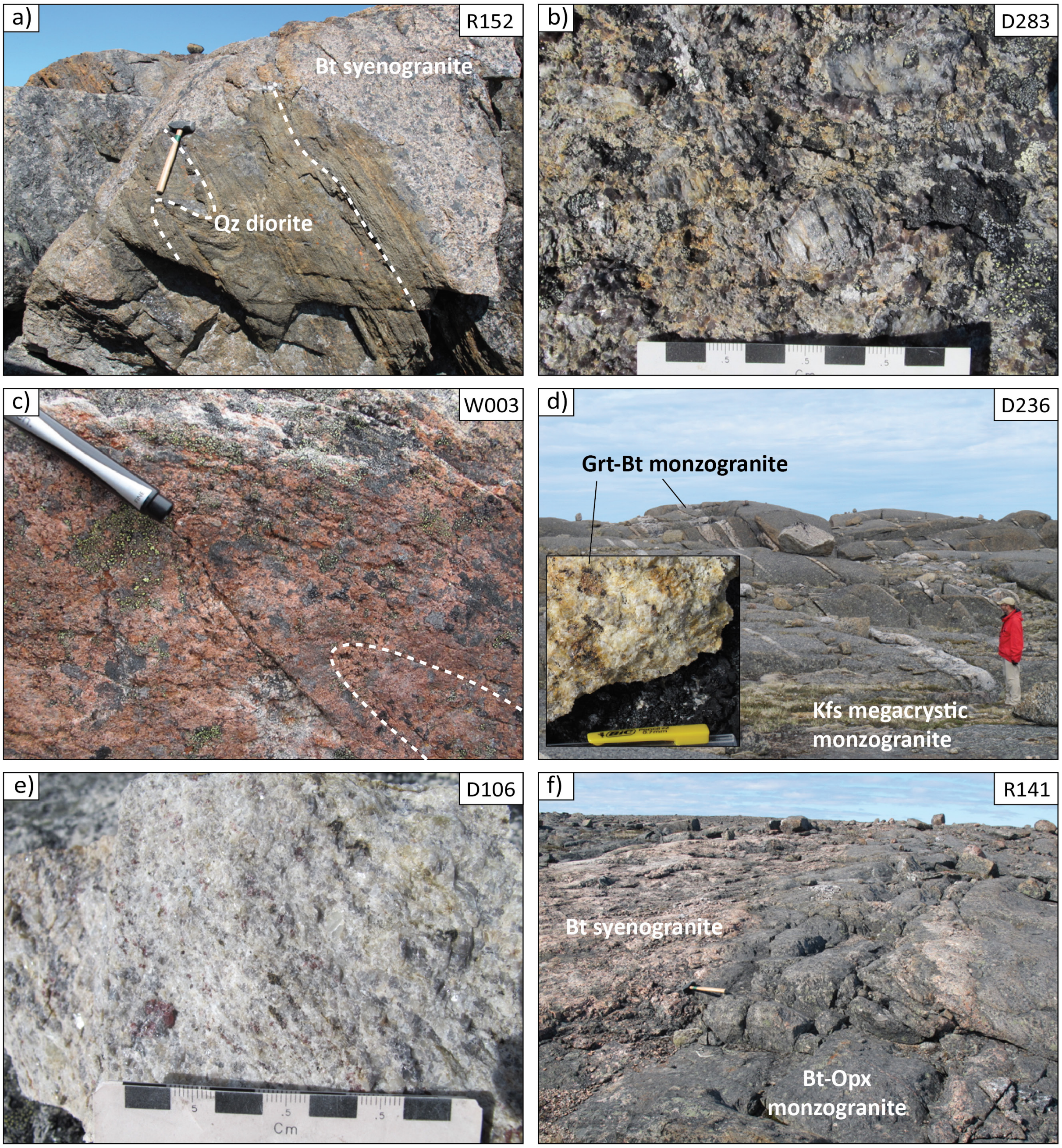

ᐊᔾᔨᖑᐊᖅ 5. ᓇᓄᓇᐃᖅᓯᒪᔪᑦ ᐊᔾᔨᖑᐊᑦ metagranitoid−ᓂᑦ Sylvia Grinnell Lake–Clearwater Fiord−ᒥᑦ. ᑎᑎᖅᑲᑲᖅᑐᑎᑦ ᓈᓴᐅᑎᓖᑦ ᖁᓖᓂ ᑕᓕᖅᐱᐊᓂ ᑎᑭᖅᑯᐊᓂ ᐊᑐᓂ ᐊᔾᔨᖑᐊᓂᑦ ᓇᓄᓇᐃᖅᑕᐅᔪᑦ 15SAB- ᖃᐅᒃᓴᕐᕕᒃ. a) ᓇᓄᓇᐃᔭᖅᓯᒪᔪᑦ ᐱᓇᔅᓯᒪᔪᑦ ᐊᒻᒪ ᐅᔭᒻᑕᐃᑦ quartz diorite ᐊᖏᔪᒻᒪᕆᐅᓪᓗᑎ grained biotite syenogranite. b) ᖃᓂᓘᖅᑐᖅ K-feldspar megacrystic monzogranite ᑕᑯᔅᓴᐅᑎᑦᑎᔪᖅ 3–6 ᓱᐊᓐᑕᒦᑕᐃᑦ ᑕᑯᔅᓴᐅᑎᑦᑎᔾᓂ rapakivi ᖃᓄᐃᓕᖓᓂᖓ. c) ᐊᔾᔨᒌᓂᓕᓐᓂ ᓂᐱᖅᑲᕐᓇᓖᑦ ᐱᓇᓯᒪᔪᑦ biotite-orthopyroxene monzogranite. d) ᐊᖏᔪᒻᒪᕆᒃ K-feldspar megacrystic monzogranite ᑲᑎᔅᓯᒪᔪᑦ ᐊᒥᓱᓚᓐᓄᑦᑯᓕᓃᖅᑦᑕᐅᑎᔪᓂᑦ biotite-garnet monzogranite ᓯᒥᑦᑕᐅᓯᒪᔪᓂᑦ. ᖃᐅᔨᓴᖅᑎᒧᑦ ᐊᖏᓂᖓ ᐅᓇᐅᔪᖅ 1.8 m ᑕᑭᓂᖓ. ᐊᔾᔨᖑᐊᖅ: ᖃᓂᓈᖅᓯᒪᔪᖅ biotite-garnet monzogranite ᖃᐅᔨᓴᕋᓭᖅ, ᑕᑯᔅᓴᐅᑎᑦᑎᔪᖅ 1–3 ᓱᐊᓐᑕᒦᑕᐃᑦᐊᐅᐸᕈᔪᑦᑐᖅ ᐊᒥᐊᖓ garnet phenocrysts ᐊᒻᒪ ᓵᑦᑐᓂᑦ ᐊᒃᒍᕋᔅᓴᐅᓇᓂ ᓇᓄᓇᐃᖅᑕᐅᔪᖅ ᐆᒧᖓ sub-parallel biotite flakes. e) ᖃᓂᓈᖅᓯᒪᔪᖅ garnet-sillimanite leucogranite, ᑕᑯᔅᓴᐅᔪᑦ ᐊᒥᓱᑦ ᒥᖅᑯᑎᐅᑉ ᓄᕗᖓᑎᑐᑦ ᐊᖏᓂᕐᖅᑐᑦᓕᓖᒃ ᐊᒥᐊᓖᑦ ᐅᔭᖅᑕᐃᑦ. f) ᐊᖏᔪᒻᒪᕆᒃ biotite-orthopyroxene monzogranite ᑲᑎᙵᔪᑦ ᐊᒥᓱᓚᓐᓄᑦ ᑲᑎᓐᓂᕐᑲᕐᕕᖏᑦ biotite syenogranite ᓯᒥᑦᑕᐅᓯᒪᔪᑦ. ᐊᖏᓂᖑᐊᖓ ᐅᓇᐅᔪᖅ 35 cm ᑕᑭᓂᖓ.

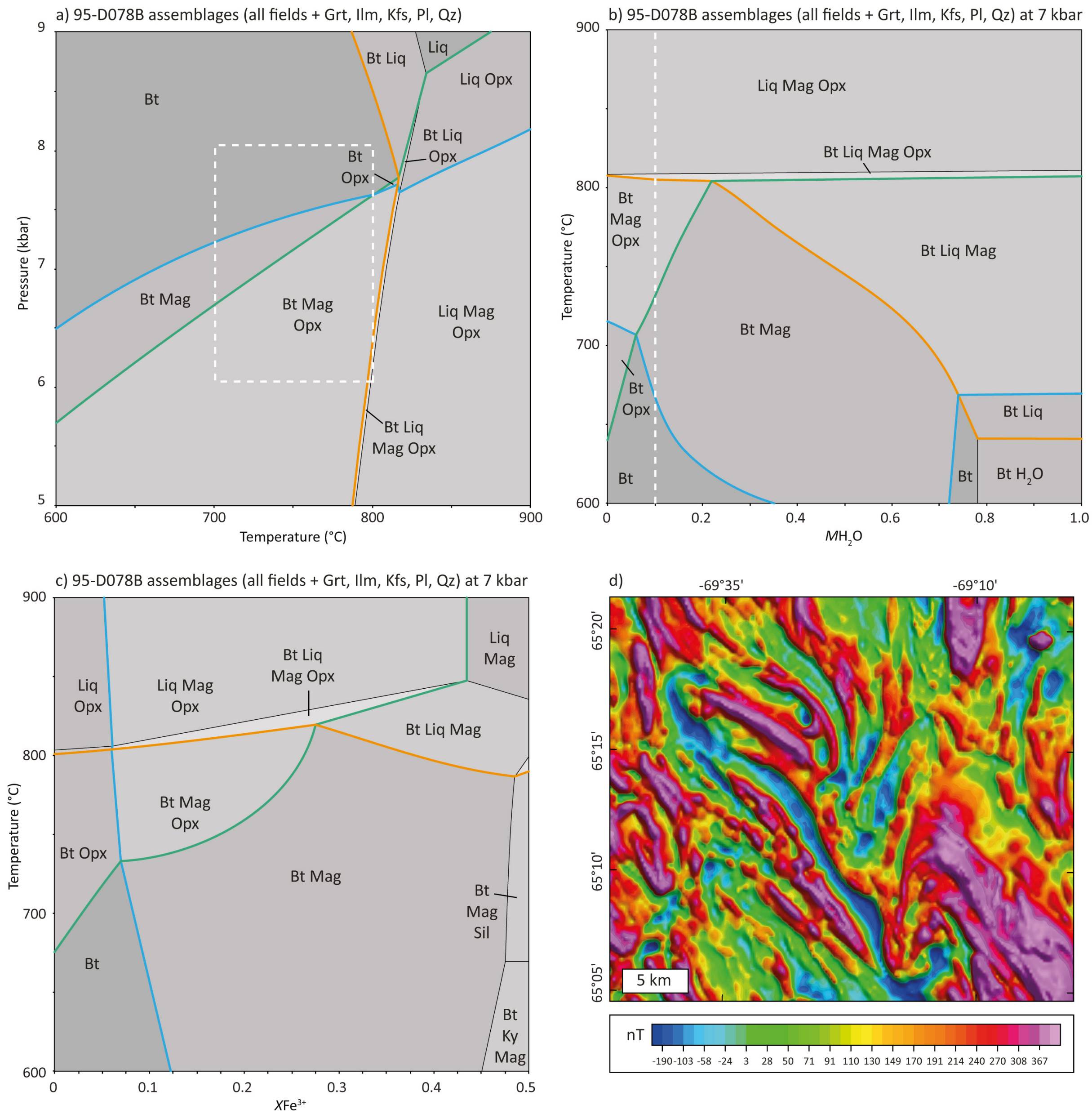

ᐊᔾᔨᓐᖑᐊᖅ 6. ᓇᓕᒧᑦᑎᑦᑎᓂᕐᒥᑦ ᐊᔾᔨᓐᖑᐊᑦ ᑕᑯᔅᓴᐅᑎᑦᑎᔪᑦ ᖃᐅᔨᓴᕋᔅᓴᓂᑦ monzogranite, ᕿᓂᖅᑐᑎᑦ metagranitoid amphibolite-granulite ᓇᒦᓐᓂᖓ ᐊᑦᑐᐊᓂᓖᑦ: a) P-T ᐊᔾᔨᓐᖑᐊᖅ; b) T-MH_2O ᐊᔾᔨᓐᖑᐊᖅ; c) T-XFe^{3+} ᐊᔾᔨᓐᖑᐊᖅ; d) ᑲᑎᑦᑐᒋᑦ ᖃᐅᔨᓴᕐᕕᐅᔪᓂᑦ biotite±magnetite±orthopyroxene monzogranite ᖃᐅᔨᓴᕐᕕᐅᔪᒥᑦ.

ᖃᐅᔨᒋᐊᕐᕕᒃᓴᑦ

Blackadar, R.G., 1967. Geological Reconnaissance, southern Baffin Island, District of Franklin; Geological Survey of Canada, Paper 66-47, 32 p. doi:10.4095/100926

Buchan, K.L. and Ernst, R.E., 2013. Diabase dyke swarms of Nunavut, Northwest Territories and Yukon, Canada; Geological Survey of Canada, Open File 7464. doi:10.4095/293149

Chadwick, T.C., St-Onge, M.R., Weller, O.M., Carr, S.D., and Dyck, B.J., 2015. Ptarmigan Fiord basement–cover thrust imbricates, Baffin Island, Nunavut: summary of fieldwork; *in* Summary of Activities 2015, Canada-Nunavut Geoscience Office, p. 61–72.

Clarke, D.B., Cameron, B.I., Muecke, G.K., and Bates, J.L., 1989. Early Tertiary basalts from the Labrador Sea and Davis Strait region; Canadian Journal of Earth Sciences, v. 26, p. 956–968.

Corrigan, D., Pehrsson, S., Wodicka, N., and de Kemp, E., 2009. The Palaeoproterozoic Trans-Hudson Orogen: a prototype of modern accretionary processes; *in* Ancient Orogens and Modern Analogues, J.B. Murphy, J.D. Keppie, and A.J. Hynes (ed.), The Geological Society, London, Special Publications, v. 327, p. 457–479. doi:10.1144/SP327.19

Dunphy, J.M. and Ludden, J.N., 1998. Petrological and geochemical characteristics of a Paleoproterozoic magmatic arc (Narsajuaq Terrane, Ungava Orogen, Canada) and comparisons to Superior Province granitoids; Precambrian Research, v. 91, p. 109–142.

Dyck, B.J. and St-Onge, M.R., 2014. Dehydration-melting reactions, leucogranite emplacement and the Paleoproterozoic structural evolution of Hall Peninsula, Baffin Island, Nunavut; *in* Summary of Activities 2013, Canada-Nunavut Geoscience Office, p. 73–84.

Heaman, L.M., LeCheminant, A.N., and Rainbird, R.H., 1992. Nature and timing of Franklin igneous events, Canada: implications for a Late Proterozoic mantle plume and the break-up of Laurentia; Earth and Planetary Science Letters, v. 109, p. 117–131.

Henderson, J.R., 1985. Geology, McBeth Fiord-Cape Henry Kater, District of Franklin, Northwest Territories; Geological Survey of Canada, Map 1605A, scale 1:250 000. doi:10.4095/120467

Hoffman, P.F., 1988. United Plates of America, the birth of a craton: Early Proterozoic assembly and growth of Laurentia; Annual Reviews of Earth and Planetary Sciences, v. 16, p. 543–603.

Holland, T.J.B. and Powell, R., 1998. An internally consistent thermodynamic dataset for phases of petrological interest; Journal of Metamorphic Geology, v. 16, p. 309–343.

Kiss, F. and Tschirhart, V., 2015a. Residual total magnetic field, aeromagnetic survey of the Amittok Lake area, Baffin Island, Nunavut, NTS 26-J south; Geological Survey of Canada, Open File 7888, scale 1:100 000. doi:10.4095/296504

Kiss, F. and Tschirhart, V., 2015b. First vertical derivative of the magnetic field, aeromagnetic survey of the Amittok Lake area, Baffin Island, Nunavut, NTS 26-J south; Geological Survey of Canada, Open File 7889, scale 1:100 000. doi:10.4095/296505

Kiss, F. and Tschirhart, V., 2015c. Residual total magnetic field, aeromagnetic survey of the Amittok Lake area, Baffin Island, Nunavut, NTS 26-K south; Geological Survey of Canada, Open File 7890, scale 1:100 000. doi:10.4095/296506

Kiss, F. and Tschirhart, V., 2015d. First vertical derivative of the magnetic field, aeromagnetic survey of the Amittok Lake area, Baffin Island, Nunavut, NTS 26-K south; Geological Survey of Canada, Open File 7891, scale 1:100 000. doi:10.4095/296507

Kiss, F. and Tschirhart, V., 2015e. Residual total magnetic field, aeromagnetic survey of the McKeand River area, part of NTS 26-B/North, Nunavut; Geological Survey of Canada, Open File 7819, scale 1:100 000. doi:10.4095/296382

Kiss, F. and Tschirhart, V., 2015f. First vertical derivative of the magnetic field, aeromagnetic survey of the McKeand River area, part of NTS 26-B/North, Nunavut; Geological Survey of Canada, Open File 7820, scale 1:100 000. doi:10.4095/296383

Kiss, F. and Tschirhart, V., 2015g. Residual total magnetic field, aeromagnetic survey of the McKeand River area, part of NTS 26-C/South, Nunavut; Geological Survey of Canada, Open File 7821, scale 1:100 000. doi:10.4095/296384

Kiss, F. and Tschirhart, V., 2015h. First vertical derivative of the magnetic field, aeromagnetic survey of the McKeand River area, part of NTS 26-C/South, Nunavut; Geological Survey of Canada, Open File 7822, scale 1:100 000. doi:10.4095/296385

Kiss, F. and Tschirhart, V., 2015i. Residual total magnetic field, aeromagnetic survey of the McKeand River area, part of NTS 26-C/North, Nunavut; Geological Survey of Canada, Open File 7823, scale 1:100 000. doi:10.4095/296386

Kiss, F. and Tschirhart, V., 2015j. First vertical derivative of the magnetic field, aeromagnetic survey of the McKeand River area, part of NTS 26-C/North, Nunavut; Geological Survey of Canada, Open File 7824, scale 1:100 000. doi:10.4095/296387

Kiss, F. and Tschirhart, V., 2015k. Residual total magnetic field, aeromagnetic survey of the McKeand River area, part of NTS 26-F/South, Nunavut; Geological Survey of Canada, Open File 7825, scale 1:100 000. doi:10.4095/296388

Kiss, F. and Tschirhart, V., 2015l. First vertical derivative of the magnetic field, aeromagnetic survey of the McKeand River area, part of NTS 26-F/South, Nunavut; Geological Survey of Canada, Open File 7826, scale 1:100 000. doi:10.4095/296389

Kiss, F. and Tschirhart, V., 2015m. Residual total magnetic field, aeromagnetic survey of the McKeand River area, part of NTS 26-F/North, Nunavut; Geological Survey of Canada, Open File 7827, scale 1:100 000. doi:10.4095/296390

Kiss, F. and Tschirhart, V., 2015n. First vertical derivative of the magnetic field, aeromagnetic survey of the McKeand River area, part of NTS 26-F/North, Nunavut; Geological Survey of Canada, Open File 7828, scale 1:100 000. doi:10.4095/296391

Kiss, F. and Tschirhart, V., 2015o. Residual total magnetic field, aeromagnetic survey of the McKeand River area, part of NTS 26-G/South, Nunavut; Geological Survey of Canada, Open File 7829, scale 1:100 000. doi:10.4095/296392

Kiss, F. and Tschirhart, V., 2015p. First vertical derivative of the magnetic field, aeromagnetic survey of the McKeand River area, part of NTS 26-G/South, Nunavut; Geological Survey of Canada, Open File 7830, scale 1:100 000. doi:10.4095/296393

Kiss, F. and Tschirhart, V., 2015q. Residual total magnetic field, aeromagnetic survey of the McKeand River area, part of NTS 26-G/North, Nunavut; Geological Survey of Canada, Open File 7831, scale 1:100 000. doi:10.4095/296394

Kiss, F. and Tschirhart, V., 2015r. First vertical derivative of the magnetic field, aeromagnetic survey of the McKeand River area, part of NTS 26-G/North, Nunavut; Geological Survey of Canada, Open File 7832, scale 1:100 000. doi:10.4095/296395

Lesher, C.M., 2007. Ni-Cu-(PGE) deposits in the Raglan area, Cape Smith Belt, New Quebec; *in* Mineral Deposits of Canada: a Synthesis of Major Deposit Types, District Metallogeny, the Evolution of Geological Provinces and Exploration Methods, W.D. Goodfellow (ed.), Geological Association of Canada, Special Publication, v. 5, p. 351–386.

Liikane, D.A., St-Onge, M.R., Kjarsgaard, B.A., Rayner, N.M., Ernst, R.E., and Kastek, N., 2015. Frobisher suite mafic, ultramafic and layered mafic-ultramfic sills, southern Baffin Island; *in* Summary of Activities 2015, Canada-Nunavut Geoscience Office, p. 21–32.

Lucas, S.B. and Byrne, T., 1992. Footwall involvement during arc-continent collision, Ungava orogen, northern Canada; Journal of the Geological Society of London, v. 149, p. 237–248.

Lucas, S.B. and St-Onge, M.R., 1992. Terrane accretion in the internal zone of the Ungava orogen, northern Quebec. Part 2: Structural and metamorphic history; Canadian Journal of Earth Sciences, v. 29, p. 765–782.

Nekvasil, H., 1991. Ascent of felsic magmas and formation of rapakivi; American Mineralogist, v. 76, p. 1279–1290.

Palin, RM., Weller, O.M., Waters, D.J., and Dyck, B., 2015. Quantifying geological uncertainty in metamorphic phase equilibria modelling; a Monte Carlo assessment and implications for tectonic interpretations; Geoscience Frontiers. doi:10.1016/j.gsf.2015.08.005

Powell, R. and Holland, T.J.B., 2008. On thermobarometry; Journal of Metamorphic Geology, v. 26, p. 155–179.

Scott, D.J., 1997. Geology, U-Pb, and Pb-Pb geochronology of the Lake Harbour area, southern Baffin Island: implications for the Paleoproterozoic tectonic evolution of north-eastern Laurentia; Canadian Journal of Earth Sciences, v. 34, p. 140–155.

Scott, D.J. and Wodicka, N., 1998. A second report on the U-Pb geochronology of southern Baffin Island; Geological Survey of Canada, Current Research 1998-F, p. 47–57.

Scott, D.J., St-Onge, M.R., Wodicka, N., and Hanmer, S., 1997. Geology of the Markham Bay – Crooks Inlet area, southern Baffin Island, Northwest Territories; Geological Survey of Canada, Current Research 1997-C, p. 157–166.

St-Onge, M.R. and Lucas, S.B., 1994. Controls on the regional distribution of iron-nickel-copper-platinum group element sulfide mineralization in the eastern Cape Smith Belt, Quebec; Canadian Journal of Earth Sciences, v. 31, p. 206–218.

St-Onge, M.R., Hanmer, S., and Scott, D.J., 1996. Geology of the Meta Incognita Peninsula, south Baffin Island: tectonostratigraphic units and regional correlations; Geological Survey of Canada, Current Research 1996-C, p. 63–72.

St-Onge, M.R., Scott, D.J. and Lucas, S.B., 2000a. Early partitioning of Quebec: Microcontinent formation in the Paleoproterozoic; Geology, v. 28, p. 323–326.

St-Onge, M.R., Scott, D.J., Wodicka, N., and Lucas, S.B., 1998. Geology of the McKellar Bay – Wight Inlet – Frobisher Bay area, southern Baffin Island, Northwest Territories; Geological Survey of Canada, Current Research 1998-C, p. 43–53.

St-Onge, M.R., Searle, M.P., and Wodicka, N., 2006. Trans-Hudson Orogen of North America and Himalaya-Karakoram-Tibetan Orogen of Asia: Structural and thermal characteristics of the lower and upper plates; Tectonics, v. 25, TC4006, 22p. doi:10.1029/2005TC001907

St-Onge, M.R., Wodicka, N., and Ijewliw, O., 2007. Polymetamorphic evolution of the Trans-Hudson Orogen, Baffin Island, Canada: Integration of petrological, structural and geochronological data; Journal of Petrology, v. 48, p. 271–302. doi:10.1093/petrology/eg1060

St-Onge, M.R., Wodicka, N., and Lucas, S.B., 2000b. Granulite- and amphibolite-facies metamorphism in a convergent plate-margin setting: Synthesis of the Quebec-Baffin segment of Trans-Hudson Orogen. Canadian Mineralogist, v. 38, p. 379–398.

St-Onge, M.R., Van Gool, J.A.M., Garde, A.A., and Scott, D.J., 2009. Correlation of Archaean and Palaeoproterozoic units between northeastern Canada and western Greenland: constraining the pre-collisional upper plate accretionary history of the Trans-Hudson orogen; *in* Earth Accretionary Systems in Space and Time, P.A. Cawood and A. Kroner, The Geological Society, London, Special Publications, v. 318, p. 193–235. doi:10.1144/SP318.7

Thériault, R.J., St-Onge, M.R., and Scott, D.J., 2001. Nd isotopic and geochemical signature of the Paleoproterozoic Trans-Hudson Orogen, southern Baffin Island, Canada: implications for the evolution of eastern Laurentia; Precambrian Research, v. 108, p. 113–138.

Tschirhart, V., St-Onge, M.R., and Weller, O.M., 2015. Preliminary geophysical interpretation of the McKeand River area, Baffin Island, Nunavut: insights from gravity, magnetic and geological data; *in* Summary of Activities 2015, Canada-Nunavut Geoscience Office, p. 49–60.

Weller, O.M., Dyck, B.J., St-Onge, M.R., Rayner, N.M, and Tschirhart, V., 2015. Completing the bedrock mapping of southern Baffin Island, Nunavut: plutonic suites and regional stratigraphy; *in* Summary of Activities 2015, Canada-Nunavut Geoscience Office, p. 33–48.

Weller, O.M., St-Onge, M.R., Rayner, N., Searle, M.P., and Waters, D.J., 2016. Miocene magmatism in the Western Nyainqentanglha mountains of southern Tibet: an exhumed bright spot?; Lithos, doi:10.1016/j.lithos.2015.06.024

Weller, O.M., St-Onge, M.R., Searle, M.P., Rayner, N., Waters, D.J., Chung, S.L., Palin, R.M., Lee, Y.H., and Xu, X.W., 2013. Quantifying Barrovian metamorphism in the Danba Structural Culmination of eastern Tibet; Journal of Metamorphic Geology, v. 31, p. 909–935. doi: 10.1111/jmg.12050

Whalen, J.B., Wodicka, N., Taylor, B.E., and Jackson, G.D., 2010. Cumberland batholith, Trans-Hudson Orogen, Canada: Petrogenesis and implications for Paleoproterozoic crustal and orogenic processes; Lithos, v. 117, p. 99–118. doi:10.1016/j.lithos.2010.02.008

Wodicka, N. and Scott, D.J., 1997. A preliminary report on the U-Pb geochronology of the Meta Incognita Peninsula, southern Baffin Island, Northwest Territories; Geological Survey of Canada, Current Research 1997-C, p. 167–178.

Wodicka, N, St-Onge, M.R., Corrigan, D., Scott, D.J., and Whalen, J.B., 2014. Did a proto-ocean basin form along the southeastern Rae cratonic margin? Evidence from U-Pb geochronology, geochemistry (Sm-Nd and whole rock), and stratigraphy of the Paleoproteorozoic Piling Group, northern Canada; GSA Bulletin, v. 126, p. 1625–1653. doi: 10.1130/B31028.1

ᐊᓯᖏᑦ ᑐᓴᐅᒪᔾᐅᔾᓇᐊᕐᑲᖅᑐᑦ

ᑐᓴᒃᓴᒃᑲᓐᓂᐅᑎᑕᐅᔪᑦ ᐅᕙᓂ ᖃᕋᓴᐅᔾᑯᖓᔪᑦ ᓄᓇᐅᑉ ᖃᓄᐃᓕᖓᓂᖓᓂᑦ ᓇᓗᓇᐃᔾᐃᒃᑲᓂᕐᓯᒪᔪ ᓴᕿᔾᖏᑦᑐᓂᑦ PDF-ᒥ ᓄᓇᙳᐊᕐᒧᑦ, ᐃᓚᐅᑎᑕᐅᖏᑦᑐᑦ ᐅᕙᓂ ᓄᓇᙳᐊᕐᒧᑦ ᑎᑎᕋᖅᑕᐅᓯᒪᔪᓂᑦ, ᐅᕝᕙᓘᓐᓃᑦ ᐃᓚᐅᑎᑕᐅᓯᒪᖏᑐᓂ ᓄᓇᙳᐊᓕᕆᓂᒃᑯᑦ ᓄᐊᑦᑎᕝᕕᖕᒥᑦ. ᑐᓴᒃᓴᒃᑲᓐᓂᐅᑎᑕᐅᔪᖅ ᑎᑎᕋᕐᓯᒪᓂᖓᓄᑦ Excel® ᑎᑎᕋᕐᕕᒃᓴᖏᓐᓂᑦ ᓄᓇᙳᐊᑉ ᖃᓄᐃᓕᖓᓂᖓᓂᑦ.

ᑎᑎᕋᖅᑐᖅ ᖃᐅᓕᒋᐊᕐᕕᖓ

ᐊᐱᖅᑯᑏᓪᓚ ᐅᕐᑲᖅᑕᐅᔪᑦ, ᐊᒻᒪ ᐅᕐᑲᐅᓯᔅᓴᐃᑦ ᐱᔾᔪᑎᕐᑲᖅᑐᑦᓄᓇᓂᑦ ᖃᐅᔨᓴᓂᕐᒧᑦ ᑐᑭᓯᒋᐊᖓᕈᑎᖏᑦ ᐃᓗᐊᓃᑦᑐᑦ ᑐᕌᖓᑎᑕᐅᔾᓇᐊᓖᑦ ᐅᕗᖓ:

M.R. St-Onge
Geological Survey of Canada
601 Booth Street
Ottawa ON
K1A 0E8
marc.st-onge@canada.ca

ᓇᒦᓐᓂᖏᓐᓄᑦ ᐊᑐᖅᑕᐅᔪᑦ

ᑕᑯᔅᓴᐅᑎᑦᑎᔪᑦ: Universal Transverse Mercator
ᐊᑐᖅᑕᐅᔪᑦ: ᒦᑕᐃᑦ
ᐊᕕᑦᑐᖅᓯᒪᓂᖓ: 19
ᓴᓂᒧᑦ ᐱᒋᐊᕐᕕᖓ: NAD83
ᑐᑭᒧᑦ ᐱᒋᐊᕐᕕᖓ: ᑐᑭᕐᑲᖅᑐᖅ ᐃᒪᕐᒧᑦ ᓇᓕᒧᓐᓂᖓ

ᓯᕗᒧᐊᒋᐊᖅᑐᑦ ᓇᒦᓐᓂᖏᑦ

ᐱᖓᓐᓇᖓᓂ ᑐᑭᒧᑦ: 68°00’00”W
ᑲᓇᓐᓇᖓᓂ ᑐᑭᒧᑦ: 66°00’00”W
ᐅᐊᓐᓇᖓᓂ ᓴᓂᒧᑦ: 67°00’00”N
ᓂᒋᖓᓂ ᓴᓂᒧᑦ: 66°30’00”N

ᖃᕋᓴᐅᔾᒧᑦ ᐃᓚᒃᓵᖅᓯᒪᔪᖅ

ᓄᐊᑕᐅᓯᒪᔪᑦ ᐋᕿᓱᖅᓯᒪᓚᐅᖅᓯᒪᔪᑦ ᐊᑐᖅᑕᐅᔪᓐᓇᖅᑑᑎᒃ ᐃᒪᐃᑦᑐᒃᑯᑦ ArcGIS™ ᑭᐳᒥᐅᑕᓅᖓᔪᓄ 10.1 ᐋᕿᒃᑕᐅᓂᑯᑦ ESRI®.

ᑐᑭᓯᒋᐊᕈᑏᑦ ᐊᑐᖅᑕᐅᔪᑦ ᑐᑭᓯᒋᐊᕈᑎᓄᑦ

ᓄᓇᓂᑦ ᖃᐅᔮᓴᓂᕐᒧᑦ ᑐᑭᓯᒋᐊᕈᑏᑦ ᐊᔾᔩᖏᑦᑐᓂᑦ ᐃᓗᓕᖅᑲᐅᖅᑐᑦ ᐱᖃᓯᐅᑎᓯᒪᔪᑦ ᑕᕝᕙᓂ ᓴᖅᑭᖅᑎᑕᐅᔪᓂᑦ ᒪᓕᓐᓂᖅᑲᖅᑐᖅ GSC−ᑯᑦᐱᓕᕆᐊᖅ ᖁᐊᙳᐃᓐᓇᖅᑐᒥᑦ ᐸᕐᓇᑕᐅᓯᒪᔪᑦ (ᓴᖅᑭᖅᑎᑕᐅᓚᐅᖅᑎᓐᓇᒥᑦ 2.6). ᑎᑎᕋᖅᓯᒪᔪᖅ ᓇᓗᓇᐃᔾᐃᓪᓗᓂ ᖃᓄᐃᑦᑑᓂᖓᒍᑦ ᐋᕿᒃᑕᐅᓯᒪᙱᓚᑦ ᐃᓂᖏᓐᓂᓪᓗ ᐊᑐᐃᓐᓇᐅᓂᖓᓂ ᐅᕙᓂ…\Data\DataModelInfo.

ᓴᓇᓯᒪᓂᖓ XML ᐃᖅᑲᓇᐃᔭᕐᕕᒃ ᐊᑕᖏᓐᓇᓂ ᒪᓕᒃᓂᖃᖏᑦᑐᖅ ᑕᐃᒃᑯᓂᖓ ᖃᓄᐃᓕᖓᓂᖏᓐᓂᑦ. ᐊᑐᒐᓇᕐᓂᐊᖏᓪᓗᓂ, ᖃᓄᐃᑦᑑᓂᖏᑦ ᑎᑎᕋᖅᓯᒪᔪᑦ ᐱᔭᐅᖃᑦᑕᖅᑐᑦ ᖁᐊᖑᐃᓐᓇᖅᑐᓂᑦ ᑐᑭᓯᒋᐊᕈᑎᖏᓐᓂᑦ ᖃᓄᐃᑦᑑᓂᖏᑎᒍᑦ.

ᓚᐃᓴᓯ ᐊᑐᐃᓐᓇᐅᔪᖅ ᖃᓪᓗᓈᑎᑐᑦ ᐅᕝᕙᓘᓐᓃᑦ ᐅᐃᕕᖅᑎᑐᑦ